UNIVERSIDAD SAN FRANCISCO DE QUITO USFQ

Colegio de Ciencias e Ingenierías

Caffeine Removal through the use of a Dynamic Filter with *Moringa oleifera* Lam. and common filtering beds

Proyecto de investigación

.

Israel Sornoza Merino

Ingeniería Química

Trabajo de titulación presentado como requisito
para la obtención del título de
Ingeniero Químico

Quito, 21 de diciembre de 2017

UNIVERSIDAD SAN FRANCISCO DE QUITO USFQ

Colegio de Ciencias e Ingenierías

HOJA DE CALIFICACIÓN
DE TRABAJO DE TITULACIÓN

Caffeine Removal through the use of a Dynamic Filter with *Moringa oleifera* Lam. and common filtering beds

Israel Sornoza Merino

Calificación:

Nombre del profesor, Título académico   Andrea Landázuri , Ph.D.

Firma del profesor

_____

Quito, 21 de diciembre de 2017

Derechos de Autor

Por medio del presente documento certifico que he leído todas las Políticas y Manuales de la Universidad San Francisco de Quito USFQ, incluyendo la Política de Propiedad Intelectual USFQ, y estoy de acuerdo con su contenido, por lo que los derechos de propiedad intelectual del presente trabajo quedan sujetos a lo dispuesto en esas Políticas.

Asimismo, autorizo a la USFQ para que realice la digitalización y publicación de este trabajo en el repositorio virtual, de conformidad a lo dispuesto en el Art. 144 de la Ley Orgánica de Educación Superior.

Firma del estudiante: _____

Nombres y apellidos: Israel Sornoza Merino

Código: 00110689

Cédula de Identidad: 1723529119

Lugar y fecha: Quito, 21 de diciembre de 2017

Resumen

El estudio de contaminantes emergentes tiene una importancia trascendental para los humanos y animales; estos pueden alterar sus funciones reproductivas como también incrementar el riesgo de enfermedades para la salud. Muchas de estas especies se infiltran en el ambiente y consecuentemente en animales a través de las descargas de aguas residuales, razón por la cual es requerido un sistema efectivo que permita su remoción. La filtración lenta de arena es considerada no solo como la tecnología más barata, sino la más eficiente en el tratamiento de aguas según la Organización Mundial de la Salud. En esta investigación la cafeína es escogida como un modelo polar orgánico de contaminantes emergentes, siendo esta la más abundante y representativa en las descargas del Distrito Metropolitano de Quito (DMQ). Se llevó a cabo un análisis dinámico de la filtración de cafeína a escala de laboratorio usando un filtro lento con zeolita, carbón activado, grava y cáscara de *Moringa oleifera* Lam. como lechos filtrantes sin tratamiento previo. Diferentes modelos matemáticos fueron probados para describir la concentración de cafeína en función del tiempo de operación y profundidad del filtro. Se encontró que el modelo que mejor describe los datos experimentales en el caso del carbón activado como lecho es el Modelo de Clark, mientras que, para la zeolita, grava, y cáscara de Moringa *oleifera* lam. fue un modelo deducido que se obtuvo combinando el modelo de filtración de Iwasaki e Ives en conjunto con un balance de masa a través del filtro. La capacidad de adsorción para cada medio filtrante fue cuantificada encontrando la masa de cafeína que es retenida por unidad de masa de lecho filtrante. Esta fue: (19.58 ± 4.17), (32.36 ± 5.16), (9.08 ± 1.01), y (129.98 ± 48.01) [µg/g] en promedio para el carbón activado, la zeolita, grava y cáscara de *Moringa oleifera* respectivamente. A una profundidad fija de lecho, el medio que más removió cafeína fue la zeolita, mientras que el medio que más removió cafeína por unidad de masa fue la cáscara de *Moringa oleifera* Lam. En general, el sistema de filtración no fue lo suficientemente eficiente como proponen otros estudios para realizar un escalamiento; un mejoramiento en la efectividad del empaquetamiento del filtro es sugerido para futuras investigaciones.

Palabras Clave: Contaminantes emergentes, filtración lenta de arena, cafeína, *Moringa oleifera* Lam., adsorción.

Abstract

The study of Emerging Contaminants is of substantial importance for humans and animals; these may alter their reproductive systems as well as increasing health risks. Most of these species infiltrate in the environment and, consequently, to animals through wastewater discharges which is why an effective removal system is required. Slow sand filtration is suggested to be not only the cheapest, but also the most efficient wastewater treatment according to the World Health Organization. In this investigation, caffeine was chosen as a polar organic model of emerging contaminants, being the most abundant compound in one of the most representative discharges of the Metropolitan District of Quito (DMQ). A laboratory scale dynamic filtration analysis of caffeine removal was done using a filter packed with untreated zeolite, activated carbon, gravel and *Moringa oleifera* Lam. Husk. Different breakthrough mathematical model curves were tested to describe caffeine concentration as a function of operation time and filter depth. It was found that the model that best fitted activated carbon´s experimental data was Clark's model, while for zeolite, gravel and *Moringa oleifera* Husk, it was a deduced model obtained by combining Iwasaki and Ives equations, along with a mass balance around the filter. The adsorption capacity of each filtering medium for this particular system was quantified finding the mass of caffeine retained per unit mass of filtering bed. These were (19.58 ± 4.17), (32.36 ± 5.16), (9.08 ± 1.01), and (129.98 ± 48.01) [μg/g] for activated carbon, zeolite, gravel, and *Moringa oleifera* husk, respectively. At a fixed bed depth, the filtering medium that removed most caffeine was zeolite, while the medium that removed most caffeine per unit mass was the *Moringa oleifera* Lam. Husk. The overall filtration system was not as efficient as other studies would prefer for a scale up; a better packing effectiveness is suggested for future investigations.

Key Words: Emerging Contaminants, Slow Sand Filtration, caffeine, *Moringa oleifera* Lam., adsorption

Table of Contents

Index of Tables

Index of Figures

1. Introduction

The study of Emerging Contaminants (ECs) has been gaining substantial importance from the area of Chemical and Environmental Engineering to aquatic Ecological Studies. ECs are defined by the US EPA as "new chemicals without a regulatory status and which impact on environment and human health are poorly understood" (Deblonde, Cossu-leguille, & Hartemann, 2015). The significance of these contaminants lies in the fact that they come from everyday used items such as pharmaceuticals, personal care products, fuel additives, and energized drinks, among others (Bardeló, 2014). Research has found over 200 different pharmaceuticals in rivers water globally (Petrie, Barden, & Kasprzyk-hordern, 2014) in which a significant amount of them are Endocrine Disruptors (Remtavares, 2017). These are chemicals that may interfere to produce "adverse developmental, reproductive, neurological, and immune effects in both humans and wildlife" (NIH, 2014). For instance, estrogen present in birth control pills can lead aquatic organisms to develop hermaphroditism phenomena, infertility, and loss of male identity (Campillo, 2015). Because of the water cycle, some of these species are consumed back and can lead to an increase in the probability of developing breast cancer and pregnancy issues in women. Additionally, some of these contaminants have feminizing effects on men that can inflict their reproductive functions (Rubén, 2013). Overall, ECs are now one of the major concerns and a permanent world menace regarding aquatic ecosystems; and in long terms, a harm to human beings.

Most of the studies to research and eliminate ECs have been done primordially in Europe, North America, Australia and China; however, little research has been done in South American countries (Pazmiño, 2016). Ironically, these are the countries that need the most help to prevent damage to marine life. Taking Ecuador as an example, it has approximately 8% of all animal species in the world from which it has around 4.5% of all presumed fish that can be affected by ECs (EmbassyEcuador, 2015). Ecuador's Capital, Quito, has established a program to reduce contamination from its rivers. This has been done by the EPMAPS (Empresa Pública Metropolitana de Agua Potable y Saneamiento de Quito), the entity in charge of provision of drinkable water, sanitary and pluvial sewage services through the entire water cycle. The program aims to manage wastewater treatment and discharge, complying with current environmental regulations in the city of Quito and in the D.M.Q, the Metropolitan District of Quito (EPMAPS, 2016). Nevertheless, the project does not embrace ECs treatment, which is why an ECs removal method is highly suggested for Ecuador's aquatic ecosystem preservation. There have been studies done along the San Pedro – Guayllabamba – Esmeraldas river, the

watercourses that follows the wastewaters discharges in Quito, and results have revealed that there are, in fact, persistent ECs (carbamazepine and acesulfame) and other organic ECs (caffeine, steroidal estrogens) that degrade along the 300 km flow (Voloshenko-Rossin, et al., 2015). Wastewater samples were taken directly from the DMQ discharge, and there is a relatively high concentration of organic ECs; the most abundant of them is Caffeine with a concentration of 5597 [µg/L] (Voloshenko-Rossin, et al., 2015). Even though results indicate that caffeine eventually degrades, there has not been evidence to suggest that its degradation products are harmless to aquatic organisms; any presence of caffeine along rivers with living organisms may represent a risk to their health (T Moore, L Greenway, L Farris, 2008). Due to its water solubility, caffeine is considered as a model for all kinds of polar organic compounds to be registered as secondary contaminants (González, 2016). Besides, Caffeine may also serve as a model for other types of ECs, which can help understand and investigate its behavior against different treatments. Overall, the use of caffeine as the main EC investigated may be the most imperative and significant one in Ecuador's case.

One of the main candidates suggested to remove ECs is the *Moringa oleifera* Lam. plant. This species is a drought resistant tree, native to the Himalayas in northwestern India, that has already been cultivated in subtropical areas in Ecuador (Leone et al., 2015). As a matter of fact, there are *Moringa oleifera* plantations across the coastal area of Ecuador, mainly in Pedernales and Guayaquil. The physical chemical properties of this crop has made it a powerful coagulant and antimicrobial agent used for wastewater treatment; previous studies have revealed its high adsorption capability with heavy metals (Sharma, Kumari, Srivastava, & Srivastava, 2006). There is evidence suggesting that the Moringa's seed extract has an affinity to organic compounds reflected in the adsorption of Carmine-Indigo Dye (Beltra & Sa, 2009) and removal of tetracycline antibiotic (Santos et al., 2015). Batch experiments that targeted caffeine as a contaminant using the *Moringa oleifera* Seed has also been achieved; apparently, the protein extract in the seed interacts with caffeine and eventually removes it from water (Troya, 2017). Whereas it is essential to study the Moringa's Seed for wastewater treatment, plantations in Ecuador aim to produce the seed mainly to process and sell it as a variety of food products such as tea, capsules and vegetable oil (Ecuamoringa, 2010). However, the *Moringa oleifera* Husk is currently being discarded as waste and even though it is not used in any food industry, it has been proved that it can be applied for adsorption removal of antibiotics such as norfloxacin (Wuana et al., 2016). The Moringa's husks and pod husks have even been used to develop high

quality microporous activated carbons (Mcconnachie, Warhurst, Pollard, & Chipofya, 1996), which is why it can be a potential specie for adsorbing caffeine.

Along with the *Moringa oleifera* plant, there are other candidates that may be used for the removal of caffeine. This includes activated carbon (Sotelo, Rodríguez, Álvarez, & García, 2012), zeolite (Izod, 1982) and pulverized construction rocks which is most often referred to as gravel. Most of these materials appear to remove organic compounds by adsorption phenomena thanks to Van der Waals forces (either induced, permanent or transient electric dipoles) between contaminants and adsorbents. Due to its relatively weak interaction energy (10-100 meV), materials that experience physisorption may be used in slow sand filters, as they can be cleaned and reused several times (Bruni, 2011). Hence, these can be incorporated in slow sand filters as an efficient way to remove the ECs of interest. Unlike other treatments for ECs such as AOP (Advanced Oxidation Processes) like fenton, photo-fenton and photocatalysis, slow sand filters require very little mechanical power, chemical or replaceable parts to work (Tech Brief, 2000). The World Health Organization has even expressed that "under suitable circumstances, slow sand filtration may be not only the cheapest and simplest but also the most efficient method of water treatment" (World Health Organization, 2011). Incorporating slow sand filters may result as the most practical way to treat contaminants in wastewater plants as it only needs to be coupled to the final process, before discharging it to effluent streams.

In order to carry out an effective investigation, filtration dynamics needs to be investigated; it is of significant importance to investigate the contaminant removal mechanism that takes place inside the filter. Different filter beds may have different models that adapt to specific cases, which is why every medium needs to be studied independently before a combination is done. The first variable of interest that needs to be examined is caffeine concentration (dependent variable) as a function of operation time and filter bed depth (independent variables). There are numerous other control variables that should be taken into consideration such as temperature, packaging effectiveness, water flow; however, most of them are implicit in the breakthrough curve model's parameters that are going to be utilized (Peric, Trgo, & Vukojevic, 2008).

Before fabricating a pilot scale filter, it is fundamental that the first investigations are carried out in a smaller case dynamic filter. When the essential mechanisms are well known, a larger scale design will be secure and more efficient. Research studies have determined that an effective standard model proposal for this smaller scale dynamic filter is a cylinder-shaped

borosilicate filter with 11 mm diameter and 60 cm height (Vargas, 2015). A standard size filter bed has also been suggested with a diameter size of approximately 3-5 mm; this is the approximate size range of the bed filter materials. In order to test a medium blanc, inert glass beads with the appropriate size range are selected. All the proposed studies and considerations may help to the design, construction and the correct management of a larger scale dynamic filter.

2. Objectives

The general objective of this project was to perform a dynamic analysis of slow sand filters using caffeine as the model contaminant, with *Moringa oleifera* Lam. husk, Zeolite, Activated Carbon, and Gravel as filtering beds without any further treatment. The ultimate goal of the investigation is to provide the basis of dynamic removal of pollutants so that it serves for future escalation purposes. The specific objectives of this project were to i) obtain experimental data for the level curves of caffeine concentration as a function of time and filter depth, ii) determine and develop a breakthrough model curve that best fits each type of filtering medium, and iii) quantify the adsorption capability of each filtering bed with respect to caffeine as a contaminant.

3. Theoretical Framework

3.1 Filtration Mechanisms

Within Slow Sand Filters, there are five mechanisms (refer to Figure 1 for an illustrative example) that are responsible for the filtration removal of contaminants. These are:

 1) Straining: occurs when the opening between the filter´s bed media is smaller than the contaminant diameter and the particles get retained in the openings.

2) Inertial Separation: Uses the principles of inertia to separate the contaminant from the water flow. It usually happens when there is a rapid change in fluid flow.

3) Interception: It happens when the contaminant passes at a certain distance (1 radius of itself) and makes contact with the filter bed.

4) Diffusion: Arises when random motion of contaminants causes the contaminant to interact with the filter bed. This species then creates an area of lower concentration to which other contaminants diffuse to be captured.

5) Electrostatic Attraction: This category corresponds to the fixation of contaminants in the filtration medium due to adsorption phenomena as a result of Van der Waals forces.
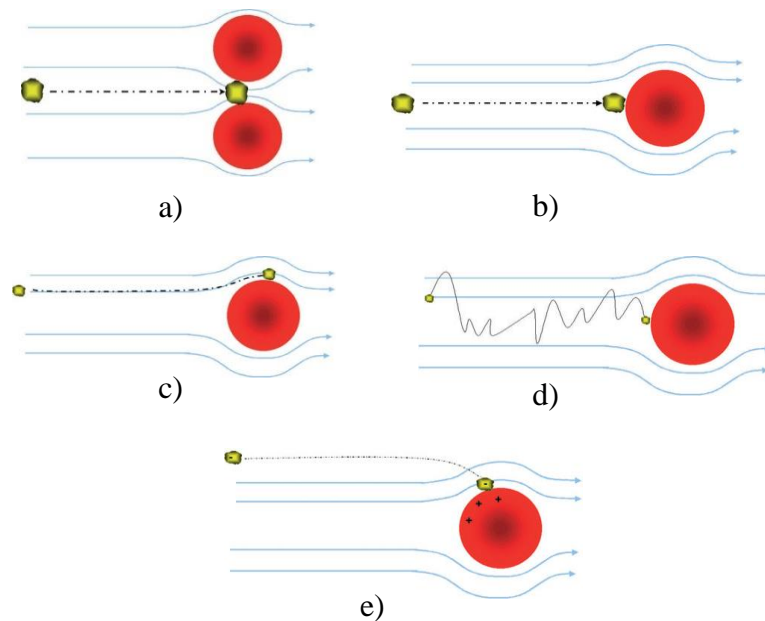
Figure 1. The five different filtration mechanisms that may take place in a slow sand filter: a) Straining b) Interception c) Diffusion d) Inertial Separation and e) Electrostatic Attraction (Camfil, 2000).

Notice that the first 4 removal mechanisms (Straining, Interception, Diffusion and Inertial Separation) take place with relatively large particles, but not so with low concentration molecules dissolved in water; most of them rely on mechanical forces. Conversely, electrostatic attraction involves not only dissolved solids, but atoms, ions and molecules. Most ECs that interact with filter beds will get removed due to adsorption by this means; the other filtration mechanisms are negligible for ECs.

3.2 Types of Filtering Beds

The different types of filtering beds used in this investigation are presented next, as well as the relevant information about them regarding filtration.

3.2.1 *Moringa oleifera Husk*

The main *Moringa oleifera* Husk provider for this project was "Ecuamoringa", an Ecuadorian company that processes Moringa mainly into capsules, teas, and oils. However, they do not use its husk; it is literally a waste material for them. The plantations of Ecuamoringa's providers are located in the Coast of Ecuador, specifically in the province of Santa Elena. The husk was obtained as shown in Figure 2.

Figure 2. *Moringa oleifera* Husk obtained by our main provider, "Ecuamoringa".

The Husks had not received any further physical or chemical treatment; they are the husks that had just been taken off from their seeds. An important aspect to consider when taking into consideration the husk as a filtering bed is that it is not spherical, and its size range varies significantly. For practical purposes, the larger husks were preferred for filling up the filtration column, rather than the small ones. Even though it is complex to do a size analysis distribution for this, for practical purposes it can be said that, for the average husk, its length, width and height were 0.57, 0.45, and 0.10 cm, respectively. These values were the average dimensions of the husk. This is represented in Figure 3. Research carried out in the University of Edinburgh and University of Malawi demonstrates that with a steam pyrolysis, these husks may form a high quality microporous system used for adsorption (Mcconnachie et al., 1996). This may lead to the suggestion that using the Husk without any further treatment may result in a physisorption with caffeine.

0.57 cm 0.57 cm

0.45 cm
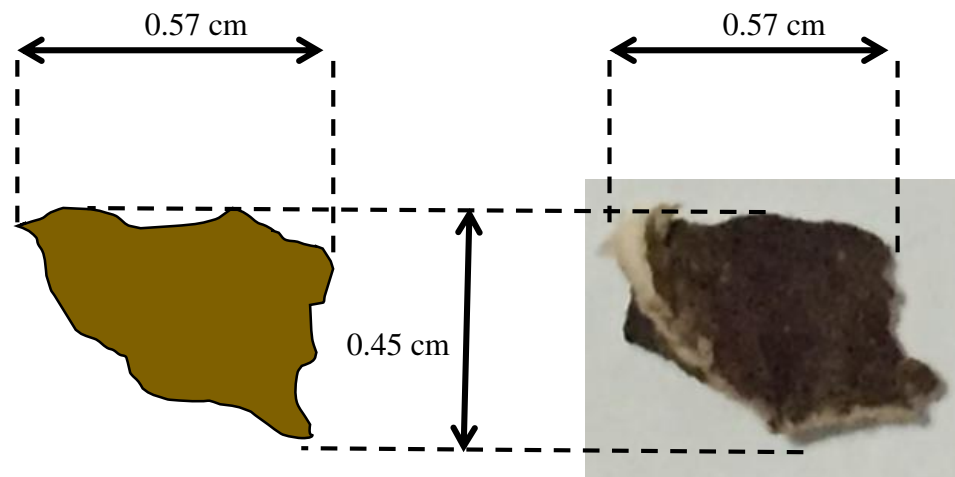
Figure 3. Cross-Section representation of the average types of *Moringa oleifera* Husks that were chosen for this investigation.

3.2.2 *Zeolite*

The zeolite used was provided by AvalChem, an Ecuadorian Company dedicated to the development of projects regarding water treatment plants industrial effluent treatment.

a) b)
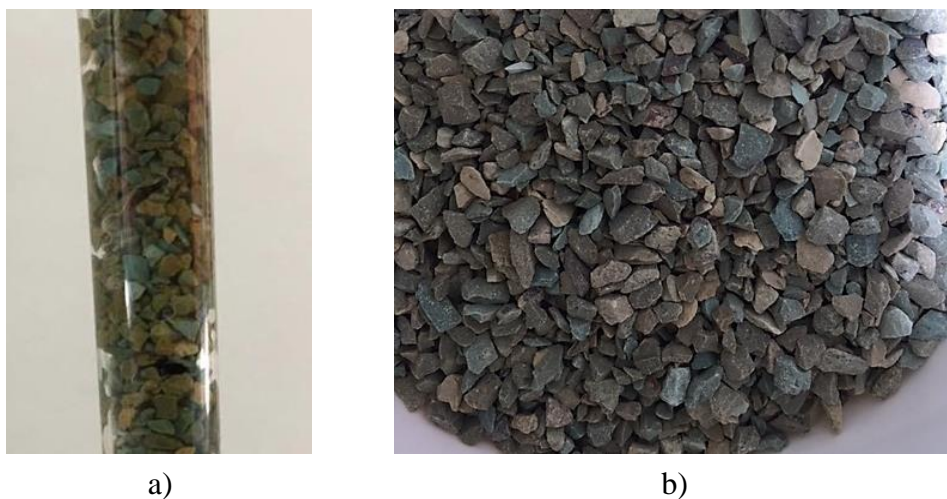
Figure 4. Zeolite provided by AvalChem shown in a a) packed column and b) in a container just after delivery.

For the average unit of zeolite, its length, width and height was 0.31, 0.22, and 0.20 cm respectively (Figure 5).

0.31 cm

0.22 cm
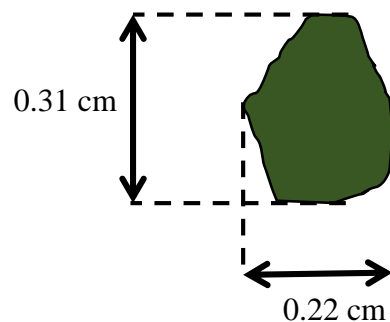
Figure 5. Cross-Section representation of the average unit of zeolite used.

Zeolite is an aluminium silicate characterized for being a three-dimensional structure with pores that consists mainly of silicon, aluminium and oxygen ions. It is the aluminium ions which cause negative areas to be present which is why it is a good adsorbent for polar and water-soluble substances, including caffeine (EPA, 1999). In contrast with other filtering beds, Zeolite's adsorption capacity is not reduced greatly for low pollutant concentrations; thus, it can be suggested that it is more suitable for working in the parts per million (ppm) concentration range.

3.2.3 Activated Carbon

Avalchem was also the provider of Activated Carbon. This was obtained as shown in Figure 6.

a)   b)
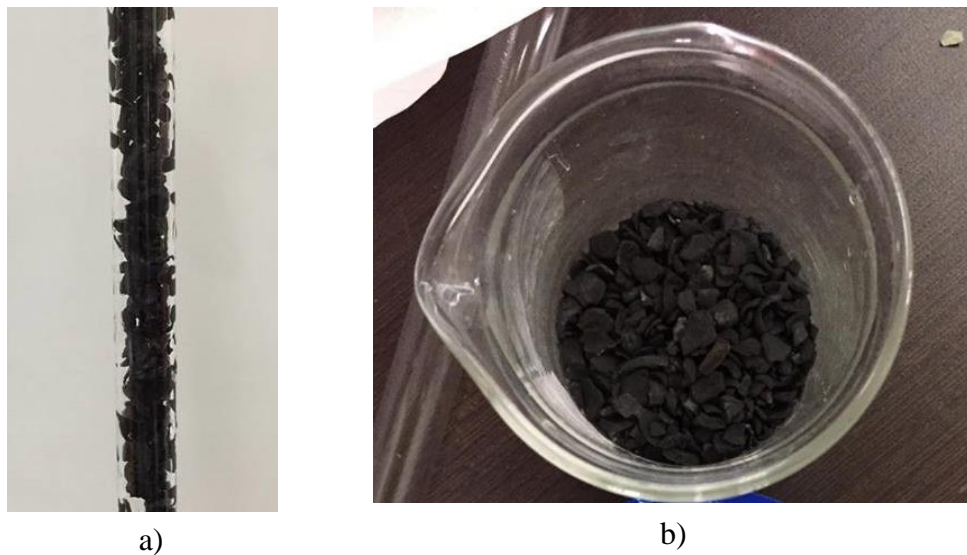
Figure 6. Activated Carbon provided by AvalChem shown in a a) packed column and b) in a beaker just after the delivery.

The average unit of Activated Carbon had a length, width and height of 0.49, 0.33, and 0.27 cm respectively (Figure 7).

0.49 cm

0.33 cm
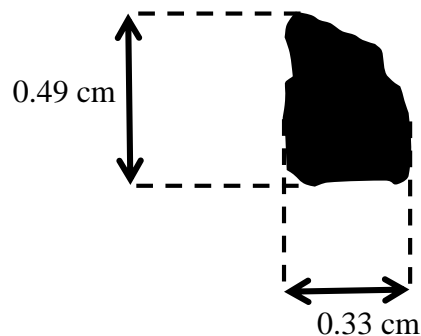
Figure 7. Cross-Section representation of the average unit of zeolite used.

Activated Carbon has the capacity to adsorb water-dissolved pollutants through surface interactions between these species and carbon graphitic platelets. The interactions include mainly Van der Waal and induced dipole forces. The platelets induce neutral organic molecules into intra-molecular dipoles where they get attracted into the carbon's pores or adsorption spaces (Nowicki, 2016). Powdered activated carbon has faster adsorption kinetics and a higher adsorption capacity compared to granular activated carbon; nevertheless, this may cause a dramatic hydraulic head loss in the column when implemented to it. This is the reason why granular activated carbon is preferred. Moreover, granular activated carbon compared to powder, only requires about one-fourth the amount of carbon between influent and effluent.

3.2.4 Gravel

The actual gravel used for this investigation was obtained from the fine sand used in construction materials found in any local hardware store (Figure 8). The gravel used was separated from the other components of the fine sand by washing it with water while using a kitchen sieve to retain the components of interest. The types of components obtained are shown in Figure 9.

Figure 8. Fine Sand found at any local hardware store.

a)   b)

Figure 9. The different components obtained from fine sand: a) the gravel used
for the filtering bed, and b) the rest of the fine sand components.

Experimental data showed that for every 1000 grams of fine sand, 570 grams of filtering gravel was obtained. Moreover, the average particle of gravel had a length, width and height of 0.71, 0.52 and 0.48 cm respectively (Figure 10).
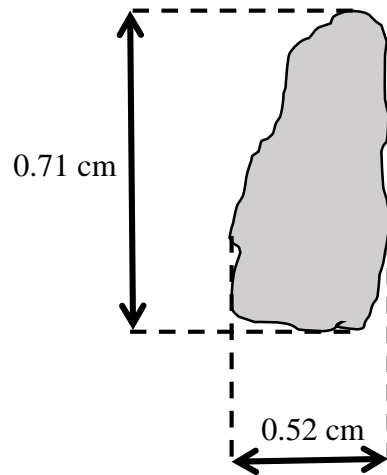
Figure 10. Cross-Section representation of the average unit of gravel used.

Previous studies have developed an iron oxide coated and natural gravel for the treatment of heavy metals in urban drainage systems (Norris, Pulford, Haynes, Dorea, & Phoenix, 2013). Results portray that the adsorption mechanism is similar as the one depicted with activated carbon with Van der Waal forces. Thus, this interaction may also result in the removal of caffeine from water.

3.2.5 Glass Beads

The glass beads are in effect anti bumping granules that may serve as a blank in conjunction with the borosilicate column. This may represent each filtering bed if it did not had present the physical chemical properties of adsorption.

<center>a)   b)</center>
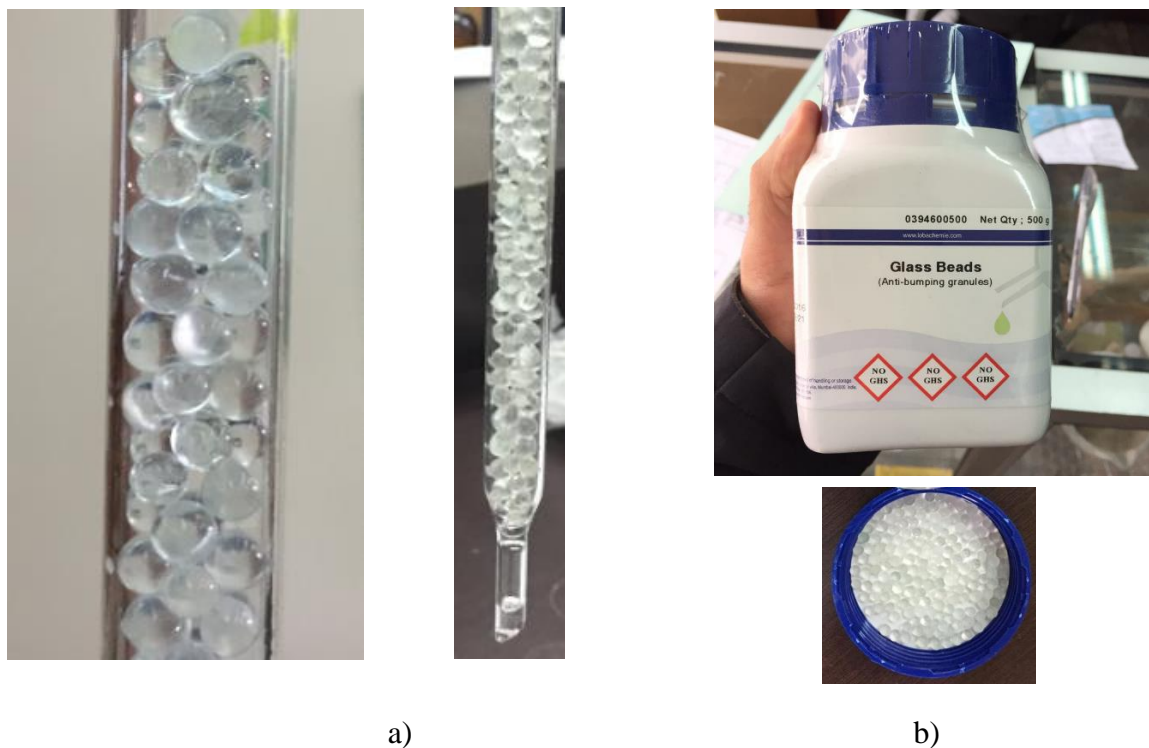
Figure 11. Glass Beads used as filtering bed present in a) the borosilicate column, and b) in its respective container.

The Glass Beads may be treated as perfect spheres with a range of diameter between 0.15 – 0.30 cm.

3.3 Breakthrough Curves

Although classical filtration models have been developed, these depend mainly upon mechanical forces rather than electrostatic ones. For instance, the Iwasaki and Ives equations work with the assumption that the main forces operating in the removal of particles are gravitational ones such as Interception and Inertial Separation (Valencia, 1972). The Mintz and Krishtul equations take the premise that solid particles are retained in the filter bed, which later becomes unstable and then detaches continuously with water flow. Evidence suggests that this does not happen with the adsorption of caffeine (Sotelo et al., 2012). Deb's equation is based on the Iwasaki and Ives model considering local increments of concentration with respect to time. Nevertheless, this model takes fuller's earth as a contaminant instead of low concentration molecules. Additionally, some of the parameters used in these equations, such as the impediment module, σ, are not time-independent which makes its resolution unnecessarily complex for the purpose of this investigation (Valencia, 1972).

The models that do study electrostatic attractions as the main filtration mechanisms in slow sand filters are portrayed within the construction of breakthrough curves. These curves reflect a measure of the effectiveness and efficiency of a column filter taking into consideration distinct operation parameters and variables. They are normally obtained by plotting column effluent concentration as a function of treatment time or effluent volume. An Ideal breakthrough curve would be as depicted in Figure 12:
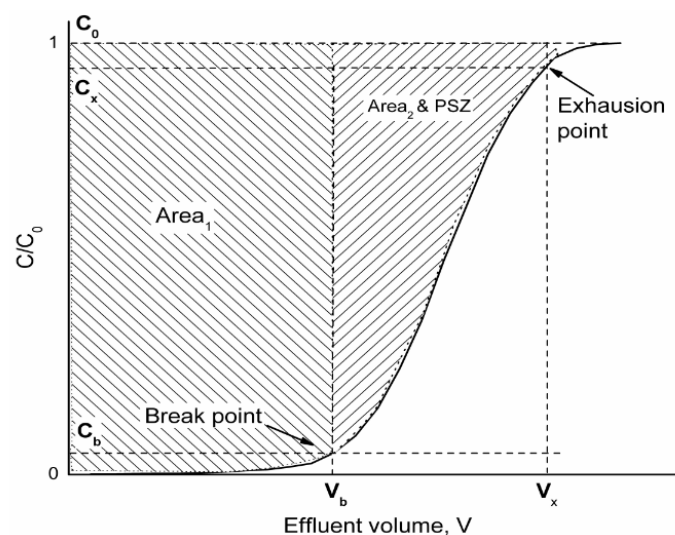
Figure 12: Ideal breakthrough curve. Dimensionless effluent concentration, C/C_0, is plotted against Effluent Volume (Tailor, 2011).

There are certain characteristics that can be obtained from these curves. The breaking point concentration is the maximum acceptable concentration of the adsorbates which is usually 0.5.

The breakthrough capacity can be defined as "the mass of the adsorbate removed by the adsorbent at break point concentration" (Tailor, 2011). Similarly, the degree of column utilization is the mass adsorbed at breakthrough point divided by the mass adsorbed at complete saturation. Finally, the exhaussion capacity is the mass of the adsorbate removed by unit weight of the adsorbent at saturation point. These quantities may be calculated by the following expressions based on Figure 12:

$$Breakthrough\ Capacity = Area_1 * C_0 \tag{1}$$

$$Exhaussion\ Capacity = (Area_1 + Area_2) * C_0 \tag{2}$$

$$Degree\ of\ Column\ Utilization\ (\%) = \frac{Area_1}{(Area_1 + Area_2)} * 100 \tag{3}$$

The breakthrough curves used to calculate the expressions depicted in equations (1), (2) and (3) may be obtained by the distinct models proposed by different authors. There are five main models that will be tested in this project. These are mentioned next.

3.3.1 Bohart-Adams Model

This model is presumably the most used one for breakthrough curves modelling, which is why it is essential to know its derivation and assumptions.

If a molar balance of a chemical species "A" over a differential cylinder is applied, it will lead to the continuity equation (Bird, Stewart, & Lightfoot, 2002):

$$\frac{\partial C_A}{\partial t} + \frac{1}{r}\frac{\partial(rN_{Ar})}{\partial t} + \frac{1}{r}\frac{\partial(N_{A\theta})}{\partial \theta} + \frac{\partial(N_{Az})}{\partial z} = R_A \tag{4}$$

Where C_A is the concentration of species A, N_A is the molar flux of A, and R_A is typically presented as the net rate at which moles of A are created in the control volume by chemical reactions. Nonetheless, for the purpose of the context, this last term may represent the net rate at which moles of A are being removed thanks to the adsorption capabilities of a filter. In the end, R_A is a measure of the amount of moles of A being generated or removed. This term can be written as $R_A = kC_A(\bar{q} - q_s)$ where $\bar{q}$ is the uptake adsorbate, q_s is the equilibrium uptake, c_A is concentration of A, and k is the adsorption coefficient.

But the molar flux can be rewritten as the product of concentration and velocity i.e. $N_A = C_A v$. Taking the axial coordinate z as the depth of the filter, and assuming the gradient molar flux only takes place in this direction:

$$\frac{\partial C_A}{\partial t} + v \frac{\partial C_A}{\partial z} = \left(\frac{1-\varepsilon}{\varepsilon}\right) k C_A (\bar{q} - q_s) \tag{5}$$

Notice that an expression for the void fraction parameter, ε, has been introduced as the removal of contaminants will also depend on this.

The boundary conditions for solving (5) are obtained realizing that at the beginning of the operation the bed is free of adsorbate, and when there is no bed depth, then the effluent concentration will be the same as the influent concentration:

$$\bar{q} = 0 \qquad \text{when} \qquad t = 0 \tag{6}$$

$$C = C_0 \qquad \text{when} \qquad z = 0 \tag{7}$$

Taking the dimensionless variables for time τ and length ξ after solving the differential equation, yields:

$$\frac{C}{C_0} = \frac{e^\tau}{e^\tau + e^\xi - 1} \tag{8}$$

The dimensionless variables are:

$$\tau = k C_0 \left(t - \frac{z}{v}\right) \tag{9}$$

And

$$\xi = \frac{k q_s z}{v} \left(\frac{1-\varepsilon}{\varepsilon}\right) \tag{10}$$

Where parameters k and q_s involve aggregate effects of mass transfer, pore diffusion, and adsorption kinetics. These parameters can be find using non-linear regression by computational methods, or by linearizing equation (8) that can be rewritten as:

$$\frac{C_0}{C} - 1 = e^{\xi - \tau} - e^{-\tau} \tag{11}$$

But the term $e^{-\tau}$ is usually negligible, and as time increases the term z/v can also be ignored. Then, applying the natural logarithm to both sides will give the conventional Adams-Bohart model:

$$\ln\left(\frac{C_0}{c} - 1\right) = \frac{kq_s z}{v}\left(\frac{1 - \varepsilon}{\varepsilon}\right) - kc_0 t \tag{12}$$

For practical uses, equation (8) will be used for modeling breakthrough curves.

Overall, this model assumes that the adsorption rate is proportional to the residual capacity of the adsorbent as well as the concentration of the contaminant of interest (Han et al., 2009).

3.3.2 Thomas model

This model was used for the design of the maximum adsorption capacity a filter bed can have, and is one of the most widely used methods in column filter theory (Thomas, 1943). The main assumptions of the model are: negligible axial and radial dispersion in the filter, the adsorption acts as a pseudo second-order reaction rate, there is a constant column void fraction, and the intra particle diffusion and external resistance during mass transfer are considered negligible (Ansari, Seyghali, Muhammad-khan, & Zanjanchi, n.d.)

The expression is as follows:

$$\frac{C}{C_0} = \frac{1}{1 + e^{\left(\frac{kqz}{Q}\right)} e^{(-kC_0 t)}} \tag{13}$$

Where C is the effluent contaminant concentration, C_0 is the influent contaminant concentration, k is a kinetic coefficient, q is the adsorption capacity of the column, t is the operation time, z is the filter bed depth, and Q is the water flow of the influent stream.

3.3.3 Yoon-Nelson Model

This model assumes that "that the rate of decrease in the probability of adsorption for each adsorbate molecule is proportional to the probability of adsorbate adsorption and the probability of adsorbate breakthrough on the adsorbent" (Han et al., 2009). The main advantage of this model is that it does not require complicated data from the adsorbate characteristics or

the physical properties of the bed filter (Aksu & Gönen, 2004). The equation is expressed as follows:

$$\frac{C}{C_0 - C} = e^{(kt - k\tau)} \tag{14}$$

Where C is the effluent contaminant concentration, C_0 is the influent contaminant concentration, t is operation time, k is a rate constant (min^{-1}), and τ is the time required for 50% adsorbate breakthrough. For the purpose of this investigation, it is of significant importance to have an explicit relation not only with time, but with filter depth. In this model, the depth is implicit in the value of τ. In fact, this term can be decomposed in the product of depth, L [cm], and a proportionality factor, F$_1$ [s/cm]. This last factor may be found experimentally as the other parameters when optimizing the model. Considering this, the final expression will be:

$$\frac{C}{C_0 - C} = e^{(kt - kF_1 L)} \tag{15}$$

3.3.4 The Clark model

This kinetic model adopts the assumption that sorption behavior of pollutants follows the Freundlich adsorption isotherm, while the sorption rate is determined by outer mass transfer (Peric et al., 2008). The final expression yields as:

$$\frac{C}{C_0} = \left(\frac{1}{1 + Ae^{-rt}}\right)^{\frac{1}{n-1}} \tag{16}$$

Where C is the effluent contaminant concentration, C_0 is the influent contaminant concentration, t is operation time, A and r are parameters of the kinetic adsorption, and n is a constant. Similar to the Yoon-Nelson model, the parameter r may be decomposed in the product of filter depth, L [cm], and a proportionality factor F$_2$ [cm^{-1}] which yields:

$$\frac{C}{C_0} = \left(\frac{1}{1 + Ae^{-LF_2 t}}\right)^{\frac{1}{n-1}} \tag{17}$$

3.3.5 Deduced Model from a Bulk Mass Balance

An expression for the variation of caffeine concentration with respect to time can also be deduced using the principles of mass balance taking the control volume of the entire filter. As seen in

Figure *13*, from a mass balance in the filter:

$$\dot{m}_{caf.in} - \dot{m}_{caf.out} = \dot{m}_{caf.acc}$$

Where $\dot{m}_{caf}$ denotes the molar flow of caffeine in mol/m^3, then

$$\dot{V}C_0 - \dot{V}C = \frac{d}{dt}[VC]$$

Where $\dot{V}$ is the fluid flow [m^3/s] of caffeine solution, C_0 is the inlet caffeine concentration [mol/m^3], and V is the volume [m^3] of the system.

Applying the product rule for derivatives:

$$\dot{V}C_0 - \dot{V}C = C\frac{dV}{dt} + V\frac{dC}{dt} \tag{18}$$
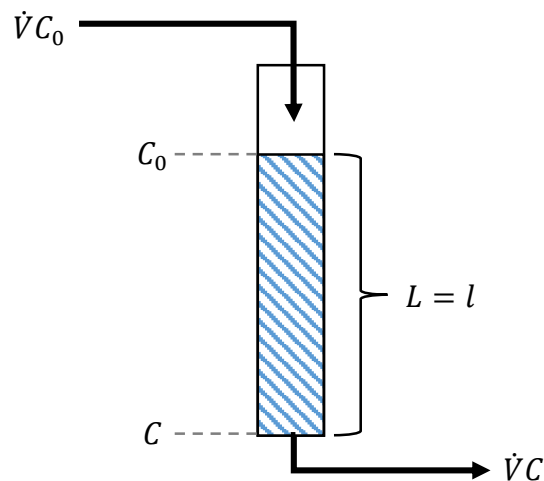
Figure 13. Filter diagram with a depth length "l" applied for a mass balance.

The term $\frac{dV}{dt}$ should be taken into consideration if the contaminant removed from water was a colloid or suspension that would eventually reduce the effective volume of the filter. In this case, the interaction of caffeine with the bed does not affect significantly the filter's volume; $\frac{dV}{dt} = 0$.

$$\dot{V}C_0 - \dot{V}C = V\frac{dC}{dt} \tag{19}$$

$$C_0 - C = \tau \frac{dC}{dt}$$

Where $\tau = \frac{V}{\dot{V}}$

$$\int \frac{dC}{C_0 - C} = \frac{1}{\tau} dt$$

$$-ln(C_0 - C) = \frac{t}{\tau} + A$$

Where A is the integration constant

$$C_0 - C = A'e^{-\frac{t}{\tau}}$$

$$C = C_0 - A'e^{-\frac{t}{\tau}} \tag{20}$$

Let C_{rem} be the concentration of the caffeine solution right after it passes through the filter (When $t = 0$). Then:

$$C_{rem} = C_0 - A'e^{-\frac{0}{\tau}}$$

$$C_{rem} = C_0 - A'$$

$$A' = C_0 - C_{rem} \tag{21}$$

Substituting (20) back into (21):

$$C = C_0 - (C_0 - C_{rem})e^{-\frac{t}{\tau}} \tag{22}$$

Notice that C_{rem} depends on the length of the filter as well as the material used in the filtering bed. If there is a filter with a fixed depth and unique material, the term C_{rem} remains constant.

The differential expression can also be approached using a Laplace transformation. The result depicts that its analogy to a 1ˢᵗ order retard element.

Applying Laplace transformation to equation (19).

$$\dot{V}L\{C_0\} - \dot{V}L\{C\} = VL\left\{\frac{dC}{dt}\right\}$$

$$\dot{V}C_0 - \dot{V}C' = V(sC' - C_{t=0})$$

Where C' denotes the Laplace transformation of the variable C

$$\dot{V}C_0 - \dot{V}C = VsC - VC_{t=0}$$

Assuming an ideal filter in which the filter medium has $C_{t=0} = 0$, then

$$\dot{V}C_0 - \dot{V}C = VsC$$

$$VsC + \dot{V}C = \dot{V}C_0$$

$$C(Vs + \dot{V}) = \dot{V}C_0$$

$$\frac{C}{C_0} = \frac{\dot{V}}{Vs + \dot{V}} \tag{23}$$

$$\frac{C}{C_0} = G = \frac{1}{Ts + 1} \tag{24}$$

Where G is the transmittance and T is the time constant or, in this case, the residence time.

This is the same expression for the transmittance of a Resistance-Capacitance circuit in Figure 14.
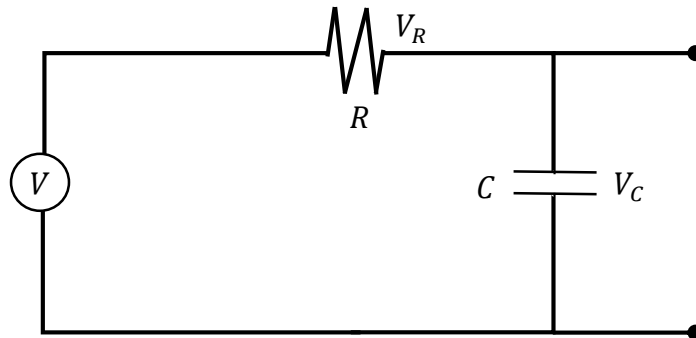
Figure 14. Resistance-Capacitance circuit in series.

Taking V as the input variable and V_C as the output variable the result of the transmittance is the same as equation (24). The time constant T is equal to the product of Resistance and Capacitance. It can be inferred that

$$T = RC = \frac{V}{\dot{V}} \tag{25}$$

The resistance is considered to be the inverse of the volumetric flow rate. A greater flow rate will generate a smaller resistance to transfer the new concentration to the capacity V. The advantage of solving the differential equation this way is that the analogy of capacitance may be appreciated; it is a measure of the effective volume of the filter. This volume represents

indirectly the capacity of the filter to adsorb caffeine. A greater effective volume will show a greater capacitance. As shown in Figure 15, if a packed medium has a greater volume, the water flow will have a prolonged interaction with the medium; therefore, a higher adsorption.

a)   b)
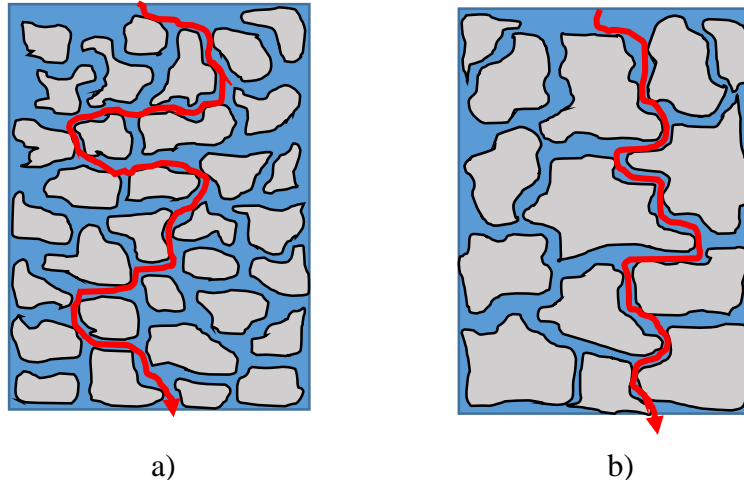
Figure 15: The different "effective volumes" of a filter. A greater effective volume (a) will have more ways in which a liquid may flow than a medium with a lower effective volume (b).

It may be observed that the mass balance at the beginning is taking into consideration the filter as a Continuously Stirred Tank Reactor (CSTR), which is why the result resembles this system when there is a step function as the input variable. This premise makes the assumption that the volume V obtained in the equations is not directly the volume from the filter, but rather a representation of what the volume would be if the filter was a CSTR. This is the reason why it may appear that the volume of the filter is significantly bigger when adjusting experimental models. As the discussed volume is implicit in the time constant (residence time) it is convenient to express this value in a different form. Studies regarding slow sand filters have used the time constant as follows (Valencia, n.d.):

$$T = \frac{CL}{Q^n} \tag{26}$$

Where L is the depth of the filter, C is a constant, Q is the flow rate, and n is an exponent.

Moreover, the initial concentration entering the filter can be considered as the step function $C_0 = C_0 u(t)$, and therefore $\acute{C}_0 = \frac{C_0}{s}$. Substituting this values back to equation (5) will give:

$$\acute{C} = \frac{C_0}{s(Ts + 1)}$$

Applying Inverse Laplace:

$$C = C_0 \left(1 - e^{-\frac{t}{\tau}}\right) \tag{27}$$

But considering real initial conditions, that is $C = C_{rem}$ when $t = 0$, the solution gives the same as equation (22).

Similarly, the relation between filter length and concentration can be found using the Iwasaki model. This theory suggests that particle removal is proportional and first order with respect to the filter depth when the media is homogenous. The mathematical model is constructed as shown:

$$\frac{dC}{dL} = -\lambda C \tag{28}$$

Where C is the concentration of caffeine, L is the length of the filter depth, and λ is the filter coefficient. Notice that $\frac{dC}{dL}$ represents the particle removal.

Solving for C as a function of L:

$$\int \frac{dC}{C} = - \int \lambda dL$$

$$\ln C = -\lambda L + B$$

$$C = B'e^{-\lambda L} \tag{29}$$

But if the depth of the filter is null, i.e. when there is no filtering bed, then, the concentration after the filter is the same as the one entering. That is, $C = C_0$ when $L = 0$.

Applying this boundary condition:

$$C_0 = B'e^0$$

$$C_0 = B'$$

Suggesting that the concentration of the contaminant with respect to the depth of the filter is as follows:

$$C = C_0 e^{-\lambda L} \tag{30}$$

The coefficient λ is the efficiency for the layer dL of the filter. Iwasaki proposed that λ is a constant with respect to L, suggesting that for a determined time, each layer will have the same

efficiency for the removal of contaminants. Not often, this is not the case for the variable time. As time progresses, the filtering bed will start to saturate; hence, the impediment module λ will also decrease. This variation of λ with respect to time can be taken into consideration when describing the condition in which C_{rem} is defined. When $t = 0$, λ will be become a fixed value λ_0. So by definition:

$$C_{rem} = C_0 e^{-\lambda_0 L} \tag{31}$$

Which can then be replaced back to obtain a final expression that relates explicitly the relationship between concentration with length and time:

$$C = C_0 - C_0\left(1 - e^{-\lambda_0 L}\right)e^{-\frac{t}{T}} \tag{32}$$

Where

$$T = \frac{CL}{Q^n}$$

Equation (32) is the "deduced model" from a bulk mass analysis and will be referred like this for the rest of this investigation.

4. Methodology

The methodology may be divided into the preparation of the filtering system, the experiments regarding the generation of breakthrough curves, and the instrumental chemical analysis.

4.1 Column Packing and Preparation

When the borosilicate columns were obtained, they were cleaned up by adding a 0.1 M NaOH solution until completely filled. Subsequently, they were washed with distilled water so that a final solution of pure ethanol could be introduced to fill up the column. This was left for 2 minutes before it was released. Finally, the empty columns were left to dry overnight so that any species left inside the column could evaporate.

When packing the columns with the filtering beds, each bed (with the exception of *Moringa oleifera* Husk) was carefully washed with water until all possible contaminants (such as dirt or small rocks) were carried away. Then, there were left to dry out at room temperature in a time period of 3 hours. Afterwards, each filtering bed was placed in the borosilicate column up to the desired depth; a gentle shake was also given so as to ensure a better packing. Finally, 100 mL of water were passed through the column with the filtering bed to guarantee that the fluid pathway was also cleaned.

In the case of *Moringa oleifera* Husk, a different approach was taken. As the husk became brittle after being dried out at room temperature, the mechanical properties could have also changed. Moreover, the packing was complicated as very often the husk got stuck inside the column and became so tight it completely blocked the fluid flow. For these reasons, the following method was used:

Firstly, the *Moringa oleifera* Husk was cleaned and washed with the help of a sieve for a time period of 1 minute (Figure 16 a-b). A small quantity of this husk was then added to the column entrance and gently pushed inside with the help of a rod (Figure 16 c-d). This was placed until the bottom of the column, and it was always checked that the husk did not block the pathway. The procedure was repeated for the rest of the husk until the column was packed with the desired depth (Figure 16 e-f).

Figure 16. Packing procedure for the *Moringa oleifera* Husk inside the borosilicate column. The husk was cleaned (a), washed (b), then added to the top of the column (c) and gently pushed by a rod (d) until it reached its bottom (e) so that the rest of the husk could be packed tightly (f).

4.2 Construction of Breakthrough Curves

The idea behind breakthrough curves is to analyze the behavior of the contaminant concentration across the filter as a function of time and medium depth. In order to obtain accurate and precise results, other fixed variables and parameters needed to be controlled. One of these parameters was flow; this procedure required a mechanism that could regulate fluid flow and maintain it approximately constant during the entire operation time.

4.2.1 Filtering system using a Micro-dropper

The first section of the project was achieved using a micro-dropper followed by the filter as showed in Figure 17.
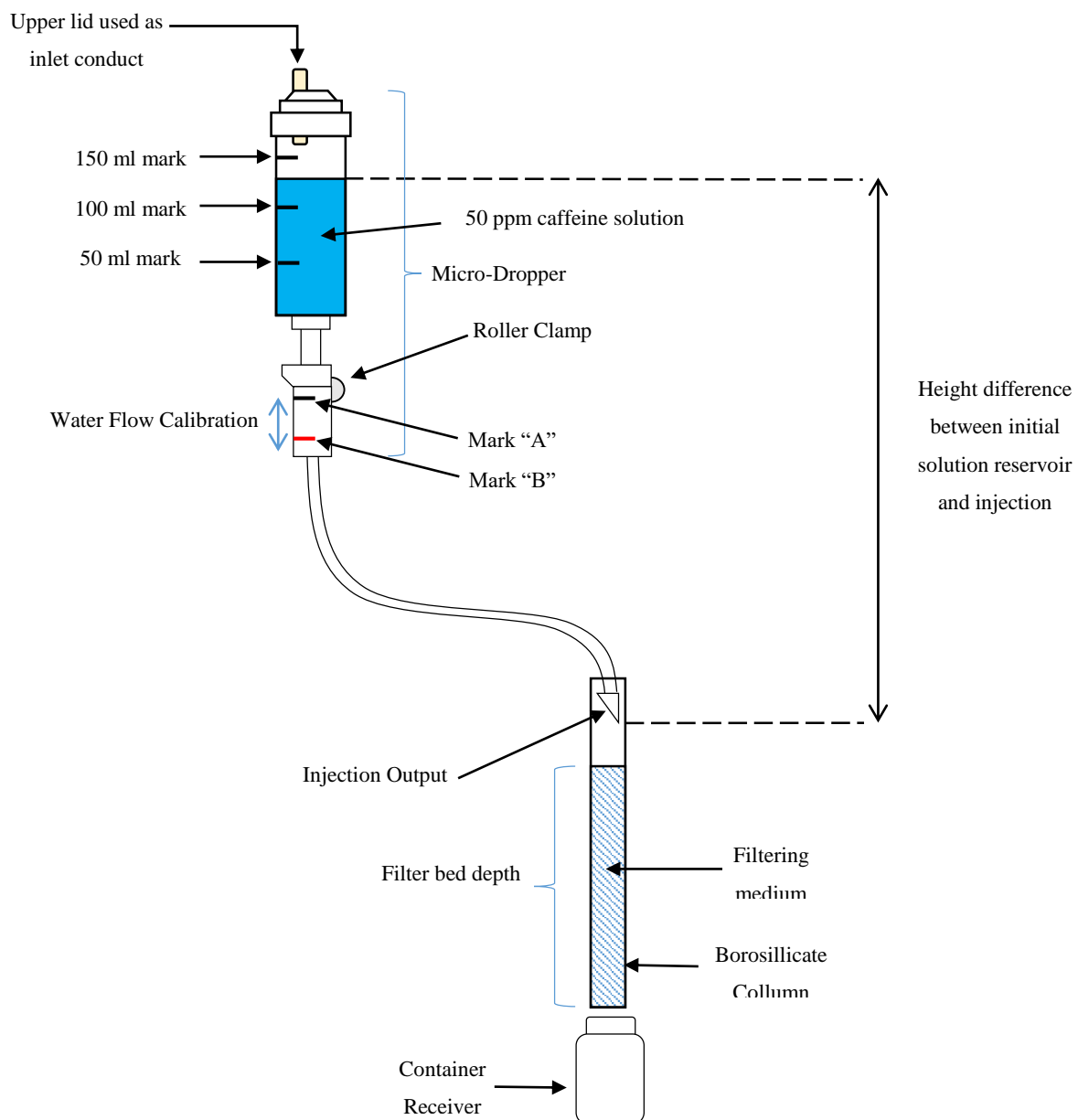
Figure 17. Scheme of the Micro-Dropper system used for the analysis of Breakthrough Curves.

The system worked using gravity as the driving force for fluid flow and could be regulated with the roller clamp. A hole was done on the upper lid of the micro-dropper in order to create an input conduct where the caffeine solution could be stored. The micro-dropper was filled with caffeine solution (50 ppm) until the 100 mL mark by default. The height difference between the initial solution reservoir and injection output was 90 cm. In these conditions, the position of the roller clamp was experimentally regulated and marked so that it included a relatively low fluid flow (Mark "A") and a relatively high fluid flow (Mark "B").

4.2.2 Filtering system using a peristaltic pump

For the second section of this project, a peristaltic pump was used as the system that could regulate fluid flow. Depending on the velocity mark, the water flow increased or decreased. In order to standardize its flow, the time taken for a specific volume of water to fill was recorded (Figure 18). This was done for every mark in the pump.
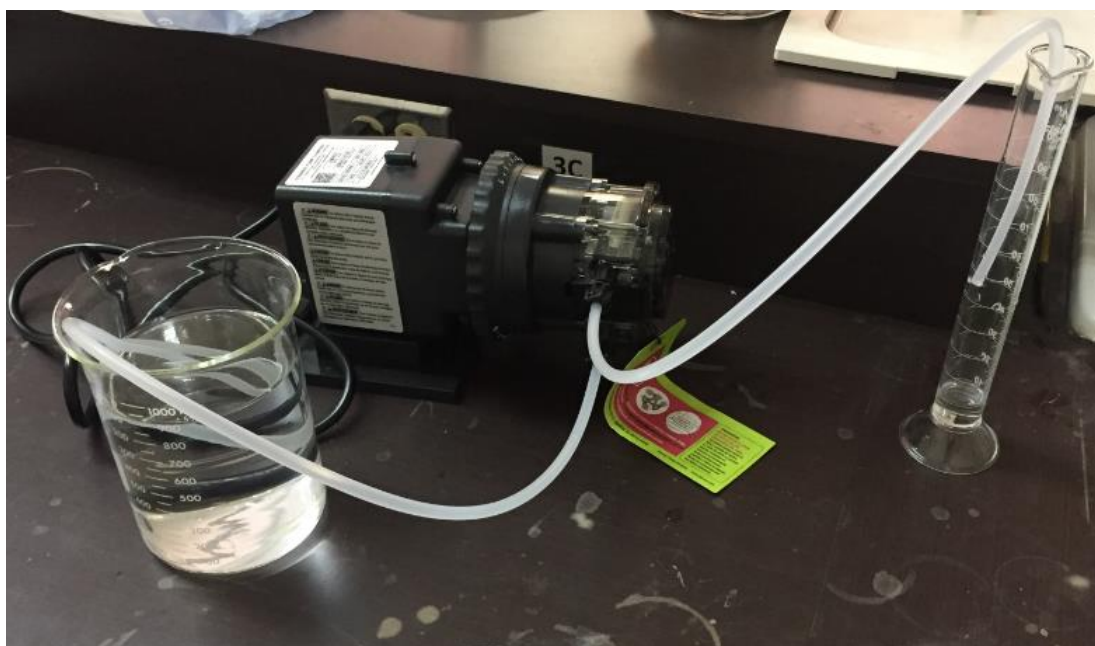
Figure 18. Operating peristaltic pump for the standardization of its fluid flow.

The selected fluid flow in the peristaltic pump was chosen based on which resembled the most as the fluid flow in the micro-dropper system.

With both systems ready, the column needed to be filled and prepared depending on which variable was going to be fixed and measured (e.g. caffeine concentration as a function of time or depth). Each filter medium was thoroughly washed in a beaker with distilled water to make sure they were effectively cleaned up. Then, the column was packed up at a specific height

with the medium (Figure 19) and further washed with distilled water. This was done in order to further clean the theoretical pathway the caffeine solution was going to pass.
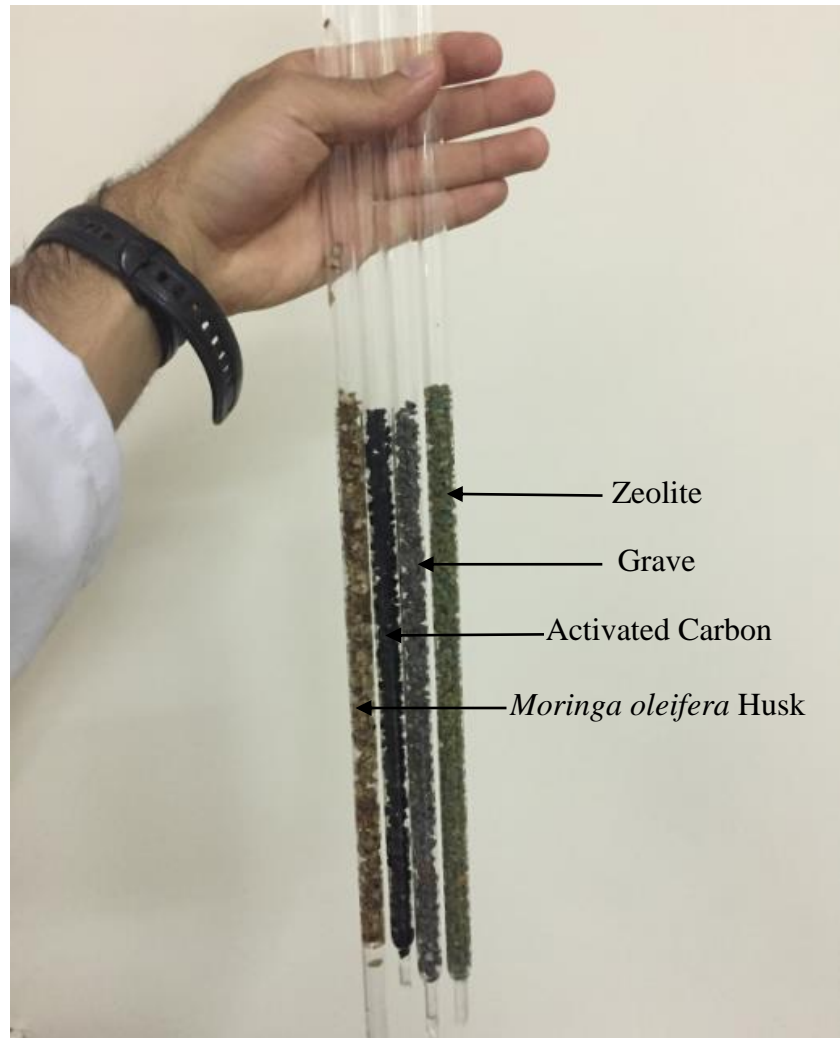
Figure 19. The different filtering beds (*Moringa oleifera* husk, Activated Carbon, Gravel and Zeolite) packed at a specific depth (30 cm).

The porosity of the system was then recorded measuring the volume between spaces in the filtering bed. This was achieved covering the end of the column, and letting distilled water fill up to the end point of the filtering bed. Then, the end of the column was released so that water could be collected and weighted. This is shown in Figure 20. The importance of this measure is reflected on the effectiveness of the filter packaging; not every time the columns are packed, they are done in the same exact way. Measuring the spaces in between the filtering beds may be used as a way to quantify this variation. However, for a specific filtering medium with a fixed bed depth, this volume was ensured to be approximately equal reflecting a similar filter packaging and consequently, an appropriate reproducibility of the system.
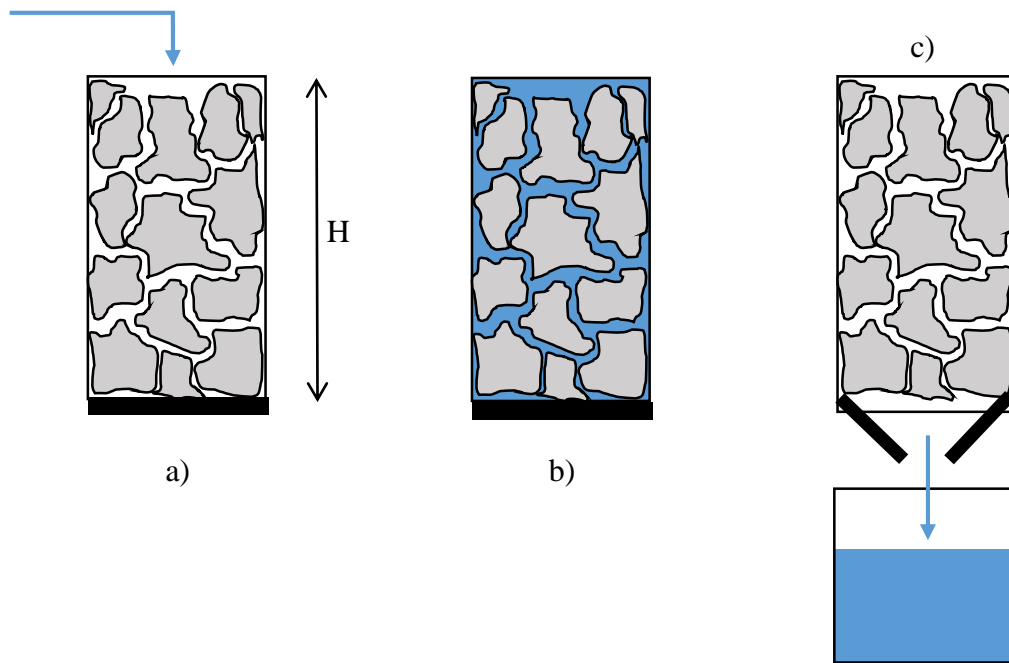
Figure 20. System used for measuring porosity. the end of the column is covered
(a) so water can fill up until a desired height in the filter (b) this amount of water
can then be (c) released and measured.

4.2.3   *Concentration as a function of time*

Once the micro-dropper and filter were ready, the roller clamp was turned to the low flow mark. In the case of the peristaltic water pump, it was turned on into a specific position corresponding to a particular water flow; i.e. the same one as that of the roller clamp. The operation time begun when the first drop of the outflow appeared at the end of the filter (time = 0). The effluent was collected at 15 s, 30 s, 1 min, 2 min, 3 min, 4 min, 5 min and 6 min in separate containers. It is important to point out that the time used for collecting data varied for every material, as some got saturated faster than others. For every time, the solution obtained had a margin of $\pm$ 5 seconds; for instance, for the 1-minute data, the solution was collected between 55 and 65 seconds. After the 6th minute, there was a last measure taken in which the solution was collected for an entire minute. This allowed an approximate measure of the fluid flow that occurred for the entire run in the micro-dropper's case. This was done for all filtering bed types. The overall operating system is shown in Figure 21.

Figure 21. Overall operating system for the analysis of breakthrough curves.

4.2.4 Concentration as a function of depth

Similarly, concentration was monitored as a function of depth at a fixed time. The column was filled with every medium filter so that its height varied between 10 and 50 cm. As each filtering medium had distinct removal effectiveness, the selected depth was not exactly the same for every single case. For instance, a species with a high percentage removal capacity would require a lower filter depth than a species with a low percentage removal. If there is a low depth selected in both cases, the species with a lower percentage removal will get saturated instantly; henceforth, the results would not be as significant as for this species in particular as if a larger filter depth were chosen. Basically, the depth was selected independently for each type of filtering bed. The selected depths for each type of bed is shown in Table 1. For every case, a caffeine solution of 50 ppm was allowed to flow at the low velocity mark.

Table 1. Selected depths for each type of filtering medium.

No. of Depth	Filtering Bed Depth [cm]			
	Activated Carbon	Zeolite	Gravel	*Moringa oleifera* Husk
1st Depth	27.0	26.0	54.0	46.0
2nd Depth	22.5	23.0	37.0	35.0
3rd Depth	18.0	18.0	27.0	27.0
4th Depth	13.0	13.0	18.0	15.0

For every scenario, caffeine concentration was analyzed using High Performance Liquid Chromatography (HPLC) or UV-VIS absorbance depending on the case, explained as follows.

4.3 HPLC Analysis

High Performance Liquid Chromatography was operated in reverse phase with a Non-Polar C-18 column. The mobile phase used was a solution of $CH_3OH : CH_3COOH : H_2O$ (15:1:34) v/v/v. The analyzed samples were stored in plastic flasks which were then degasified to allow any air particles trapped in the solution to escape. The characteristic peak of caffeine regarding HPLC analysis was found experimentally at a given retention time as in the artificial water this was the only existent species. The Area below this characteristic peak as well as the peak's height were measured in order to quantify caffeine concentration. To compute the peak's height and the area below the peak, the PeakSimple Chromatography Software was used. For a detailed procedure of the operation of the HPLC refer to Appendix A.

4.4 UV-VIS Spectrograph Analysis

The CECIL 2021 spectrograph was used along with a 10 mm quartz cuvette. At the beginning, the spectrograph was operated in spectrometer mode in order to obtain the complete spectra of an artificial solution of caffeine and identify at which wavelength did the maximum absorbance took place. The spectrograph was then set in spectrophotometer mode at this particular wavelength to measure absorbance and eventually quantify caffeine concentration. For a more in detail methodology of how the samples were analyzed using the UV-VIS Spectrograph, refer to Appendix B.

4.5 Generation of Calibration Curves

Calibration curves were constructed for both the UV-VIS Spectrophotometer and High Performance Liquid Chromatography (HPLC). This was done preparing an artificial stock solution of 1000 ppm caffeine from the Sigma-Aldrich Caffeine Powder. Consequently, caffeine solutions with specific concentrations (0, 5, 15, 30, 50 and 60 ppm) were prepared with the help of a micro pipette and a Florence flask.

In the case of UV-VIS spectroscopy, quantification was done measuring the absorbance for each sample at a wavelength of 273.5 nm. When using HPLC, both, the height and the area below the characteristic peak of caffeine were measured for each concentration.

To further test the reproducibility of the instrument along with the storage conditions of caffeine solutions, two calibration curves were performed: one when this whole investigation started (June 2017), and a second one after the investigation ended (October 2017).

5. Results and Discussion

5.1 Calibration Curves

5.1.1 UV-VIS Calibration Curve.

The caffeine spectrum obtained from the UV-VIS Spectrograph is presented in Figure *22*.
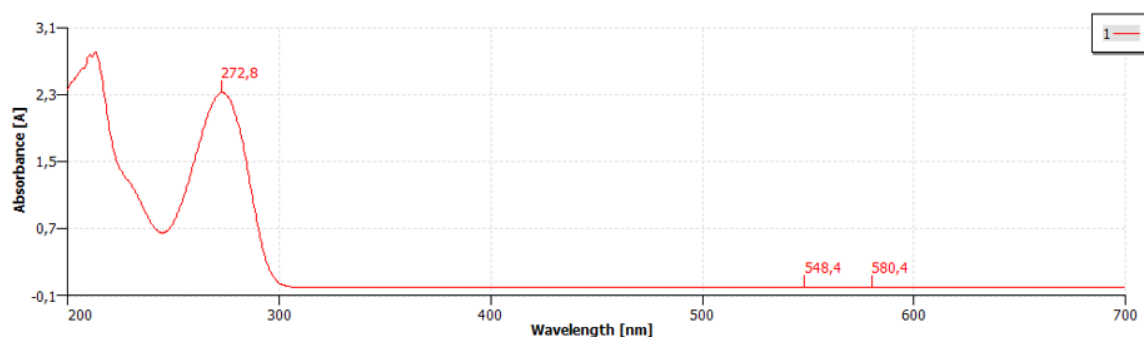
Figure 22. UV-VIS Caffeine spectrum of caffeine (50 ppm).

There was one characteristic peak in the spectrograph at a wavelength of 273.5 nm. Note that the first peak of the spectrum (205 nm) corresponds to distilled water, which is why it is not taken into account. The specific data for this calibration curve is found in Appendix C, from which Figure 23 was constructed.
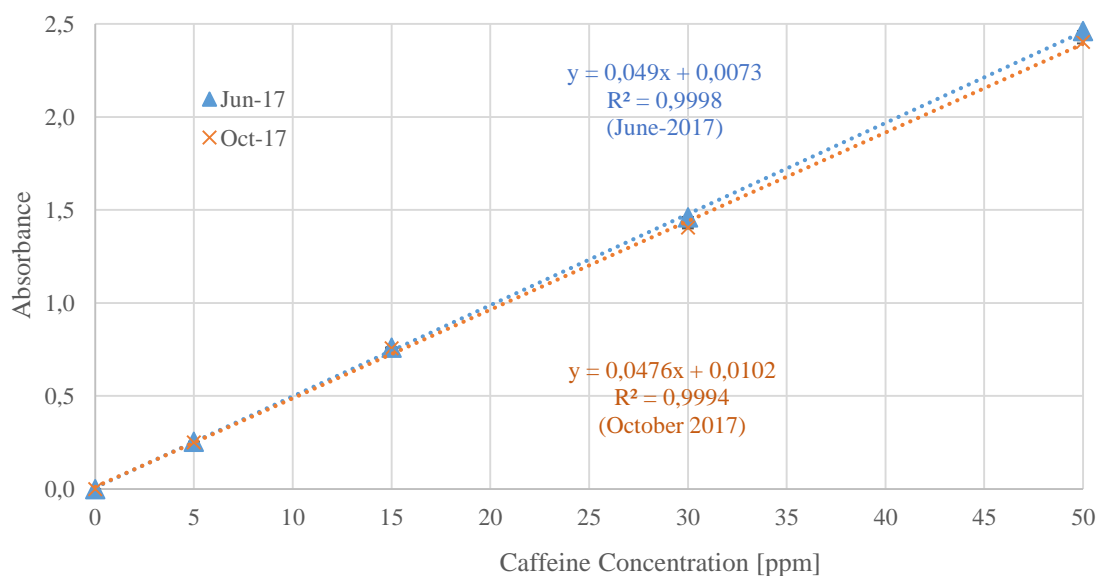
Figure 23. Calibration Curves Graphs using UV-VIS Spectroscopy at 273.5 nm (5 months apart).

Note that the 60 ppm data was omitted as the absorbance portrayed started to show deviations from Beer's Law. It appears that the linearity functions correctly between the range of 0 and 50 ppm caffeine.

5.1.2   HPLC Calibration Curve.

The chromatogram obtained when analyzing a pure caffeine solution in an HPLC reverse phase is shown in Figure 24:
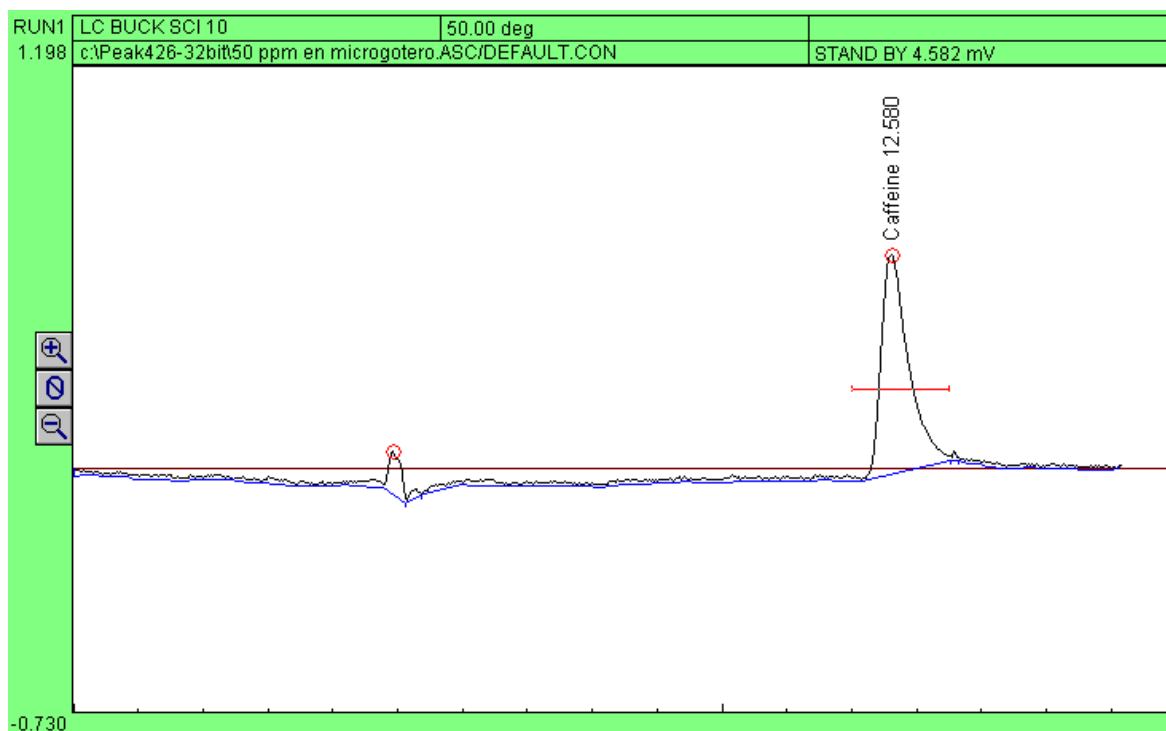
Figure 24. HPLC Chromatogram for an artificial solution of caffeine 15 ppm.

The first interference in the chromatogram makes reference to the dilution effect of water, while the second peak corresponds to caffeine. Using the corresponding Stationary Phase (C-18 column) in conjunction with the selected mobile phase, it was found that the retention time of caffeine was 12.58 ± 0.5 minutes. It is important to show the chromatogram and find experimentally the retention time of caffeine as in future investigations with real wastewaters this might be used as a reference to identify qualitatively which species is actually caffeine.

For data quantification, the area below the peak and the peak's height could be used. A calibration curve was done for both cases. Refer to Appendix C for the actual calibration curves data. For further information about the chromatograms obtained for these calibration curves refer to Appendix G. The calibration curves of caffeine using the area below the peak and the peak's height are presented in FiguresFigure *25* and Figure *26* respectively.
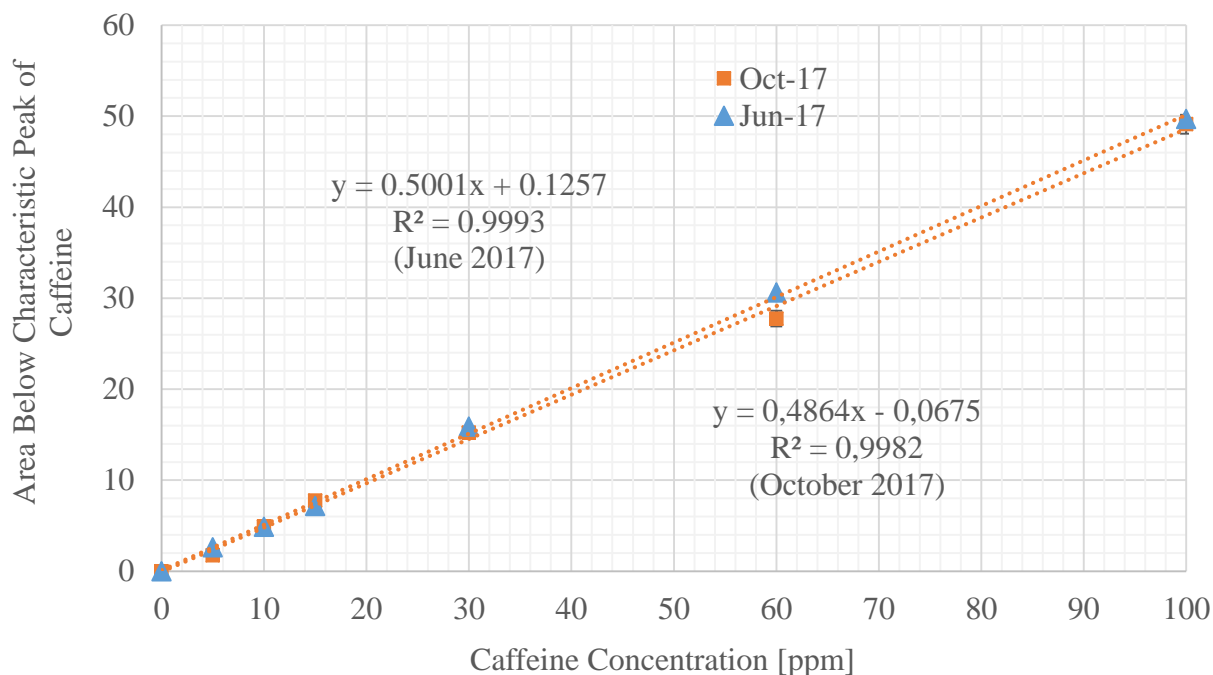
Figure 25. Calibration Curve of Caffeine using the Area Below its Characteristic Peak using an HPLC Chromatogram.
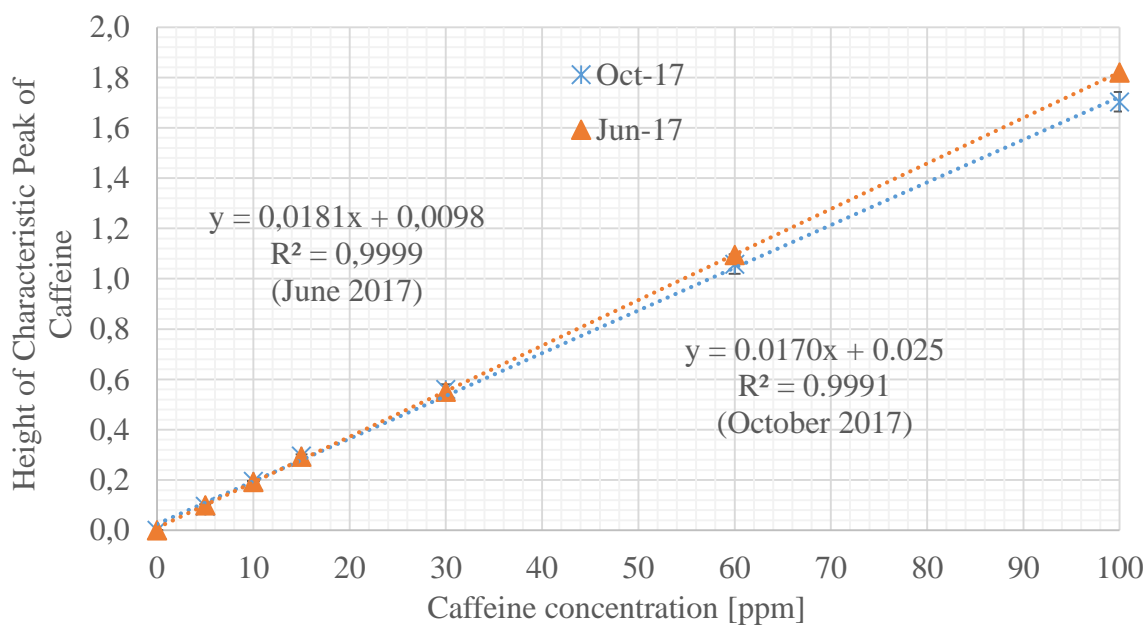
Figure 26. Calibration Curve of Caffeine using its Characteristic Peak Height in an HPLC Chromatogram.

Based on the graphs, the equation used for relating absorbance and concentration for the UV-VIS spectrograph is:

$$C = \frac{A - 0.0073}{0.049} \tag{33}$$

Where C is caffeine concentration in ppm, and A is the absorbance at 273.5 nm.

As for the HPLC, the relationship is given by:

$$C = \frac{A_p - 0.1257}{0.5} \tag{34}$$

Or by:

$$C = \frac{H - 0.0098}{0.0181} \tag{35}$$

Where C is caffeine concentration in ppm, A_p is the area below the characteristic peak of caffeine, and H is the characteristic peak's Height.

5.2 Peristaltic Bomb Calibration

The velocity marks on the peristaltic pump had the following results:

Table 2. Water Flow corresponding to every position in the peristaltic bomb.

| Bomb position | Time [s] to reach 50 ml | | | Average | Water Flow [ml/s] | | % Standard Deviation |
	Test 1	Test 2	Test 3		[ml/s]	[ml/min]	
1	436	434	432	434	0.115	6.912	0.461
1.5	217	218	217	217	0.230	13.825	0.266
2	171	175	172	173	0.292	17.544	1.206
2.5	125	122	126	124	0.400	24.000	1.674
3	107	103	104	105	0.467	28.037	1.989

Bomb Position 1.5 was used in the rest of this work as this resembled the micro dropper system that was used at the beginning of the investigation. Although the peristaltic pump used pulsations to transfer water to the column, while the micro-dropper used a continuous drop to drop flow, both methods provided the same results when tested in the filtering system (Results not shown).

5.3 Concentration as a function of time

Once the filtration system was operational, caffeine concentration was monitored as a function of time for every type of filtering bed at different filter depths. This is shown in the following sections. The most representative data for the construction of these curves is shown in Appendix D. For detailed information about the absorbance of each measurement with its corresponding uncertainty and standard deviation, see Appendix I.

5.3.1   Activated Carbon as the filtering bed

Table 14 in Appendix D presents caffeine concentration data at different operation times on a given filter depth using activated carbon as the filtering bed. Figure 27 illustrates these relationships graphically.
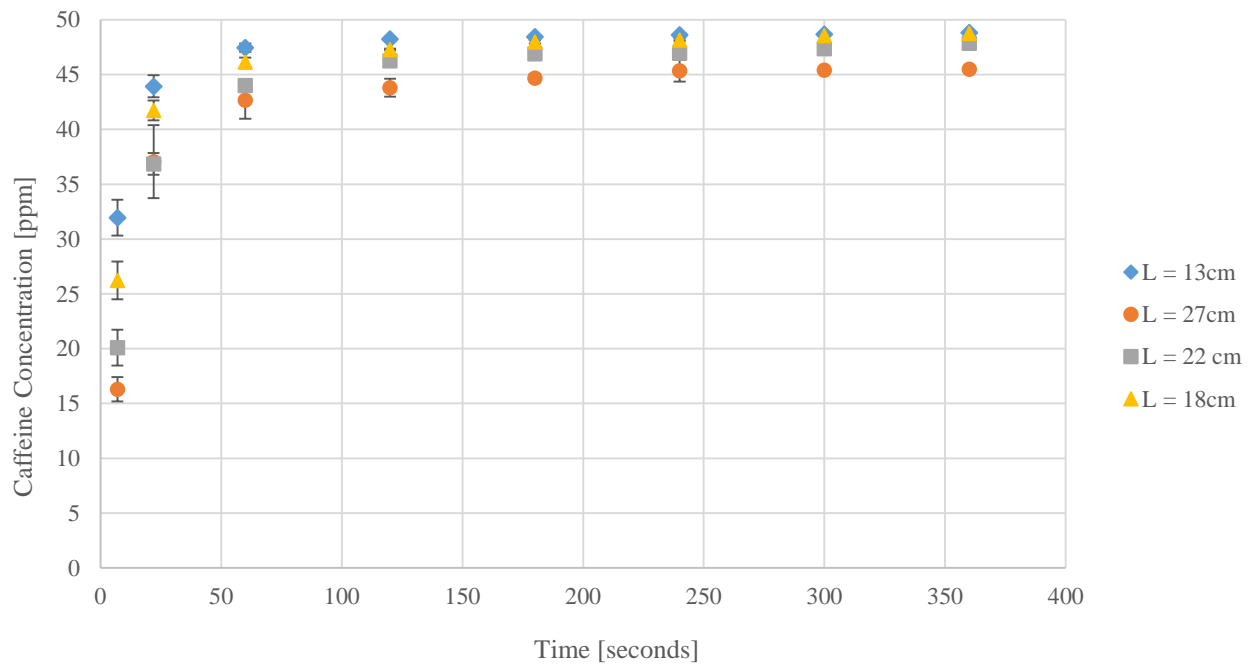
Figure 27. Caffeine concentration as a function of time for different depth lengths (L) using Activated Carbon as filtering bed.

It can be observed that as operation time progresses, the effluent concentration tends asymptotically to the initial influent concentration. Moreover, as the filter depth increases, the outflow caffeine concentration takes a larger time to reach the same concentration as with a smaller filter depth. Also note that the instantaneous variation of caffeine concentration with respect to time is significantly greater at the beginning of the operation compared to the end of the operation. This suggests that a non-saturated bed will have a greater adsorption capacity

than a semi-saturated bed; the attachment of caffeine molecules in the bed seems to decrease the electrostatic attraction that exists between them. It is important to know that this is not always the case. Some studies regarding the removal of heavy metals indicate that a semi-saturated bed actually increase the adsorption capacity of the filter (Muhammad, Parr, Smith, & Wheatley, 1998). This happens as the deposited layer has a greater attraction for metals as the filter itself. In the case of caffeine, even though it is a polar molecule, induced dipole attraction is not sufficient in order to show this behavior. Consequently, if a low caffeine concentration is to be sought, the filter will only be effective for a small amount of time (until 1 minute for most). The behavior of these curves appear to be essentially the same for every type of filtering bed as Figures Figure *28*,Figure *29*, and Figure *31* indicate.

5.3.2   *Zeolite as the filtering bed*

Table 15 in Appendix D presents caffeine concentration data at different operation times on a given filter depth using zeolite as the filtering bed. Figure 28 illustrates these relationships graphically.
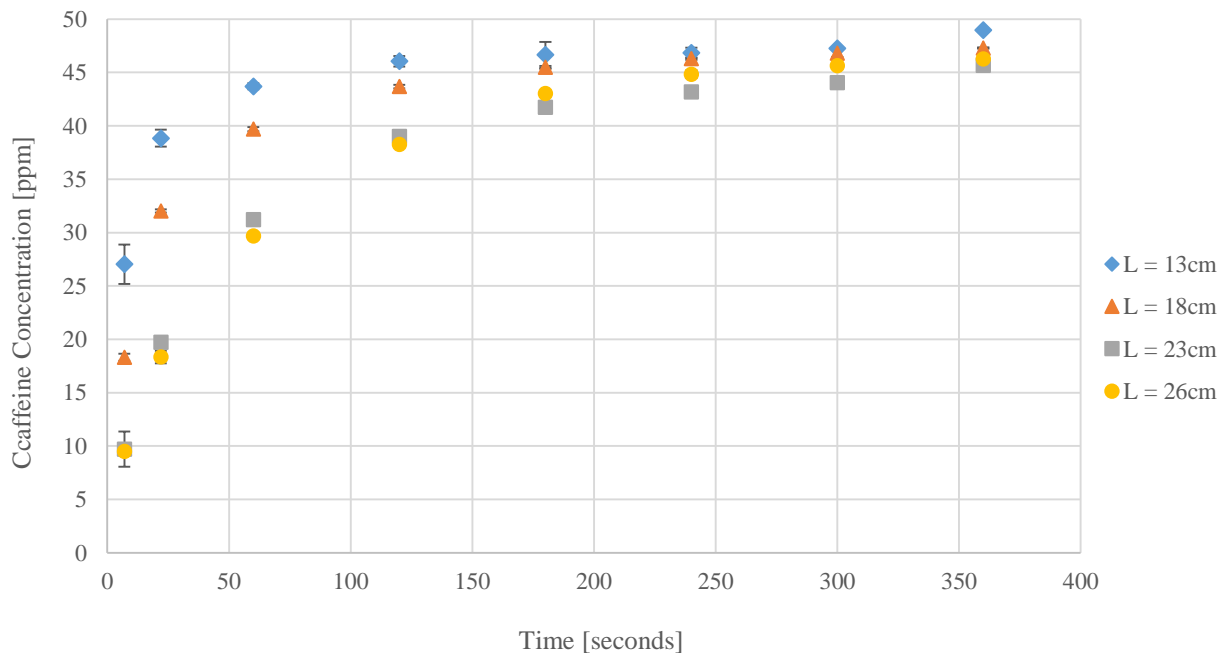
Figure 28. Caffeine concentration as a function of time for different depth lengths (L) using Zeolite as filtering bed.

Comparing zeolite with the rest of the filtering beds, it can be seen that these curves present a much greater resistance to saturation. This is reflected in the curves as the rate of change of concentration with respect to time is lower compared to the other filtering beds. Note that the level curves for zeolite in which L = 13, 18 and 23 cm in Figure 28 are must more

distinguishable than any other type of bed for the same depth difference. It appears to be that Zeolite is the most sensitive medium regarding filtering depth when plotting caffeine concentration vs operation time; a small change in filtering depth creates a large variation in the concentration-time level curve.

5.3.3   Gravel as the filtering bed

Table 16 in Appendix D presents caffeine concentration data at different operation times on a given filter depth using gravel as the filtering bed. Figure 29 illustrates these relationships graphically.
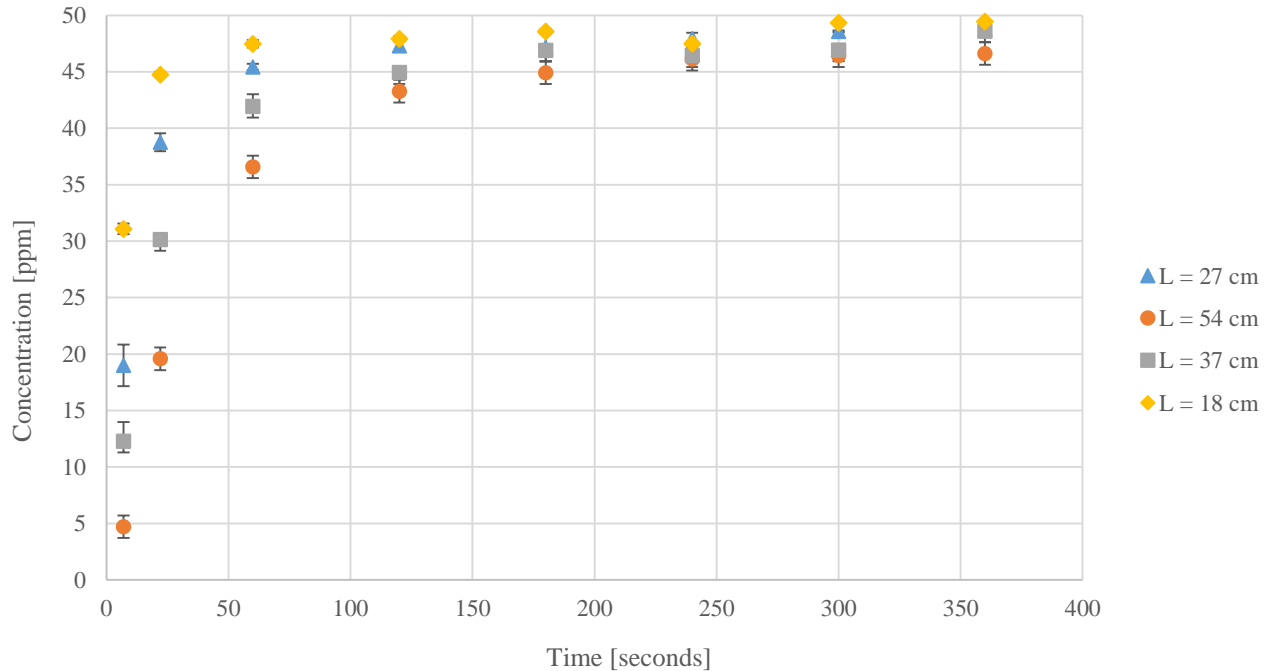
Figure 29. Caffeine concentration as a function of time for different depth lengths (L) using Gravel as filtering bed.

When using Gravel, the different level curves needed to be constructed with the greatest difference in filter depth. It varied from L =18 cm to L = 54 cm as shown in Figure 29. This was because a small change in gravel's filtering depth did not affected significantly its level curves (the complete opposite effect of Zeolite). Even though the filter tends to get saturated rapidly for every level curve, increasing its depth reduces to a great extent caffeine concentration at the beginning of the operation. This behavior supports the fact that attraction between the media and caffeine is taking place, but loses effectiveness as caffeine gets deposited in a layers.

5.3.4 *Moringa oleifera* **Lam***. Husk as the filtering bed*

The system with *Moringa oleifera* Husk as the filtering bed presented a peculiar behavior. Even though the husk was cleaned thoroughly with water, when water passed through this filter, it gave off a pale yellow solution. This was clearly shown when the samples were taken as a function of time in the containers. This can be visualized next in Figure 30.
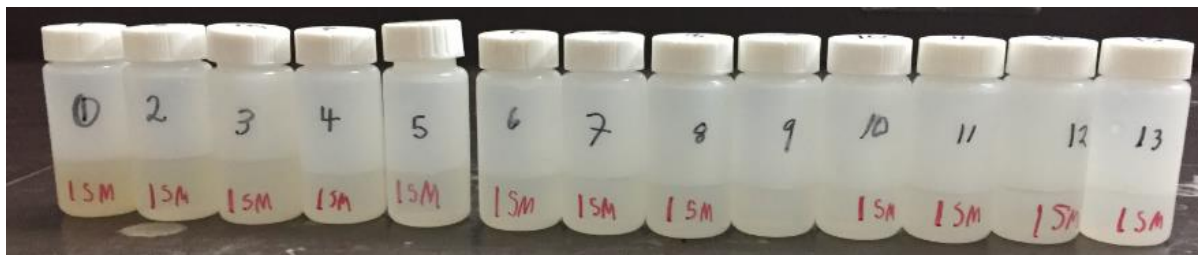
Figure 30. Pale yellow solution given off when the *Moringa oleifera* Husk was used as the filtering bed.

It turned out that these solutions absorbed in a similar wavelength than the characteristic peak of caffeine when analyzed in the UV-VIS spectrophotometer (at 273.5 nm). Actually, the caffeine and this pale yellow solution spectrum overlapped when analyzed in the UV-VIS spectrometer. For instance, in order to quantify caffeine concentration only, Liquid Chromatography needed to be applied (HPLC Analysis). This separated both species at different retention times which was the reason why HPLC analysis was chosen as the main instrumental analysis when using the *Moringa oleifera* Husk as the filtering bed.

Table 17 presents in Appendix D caffeine concentration data at different operation times on a given filter depth using *Moringa oleifera* as the filtering bed. Figure 31 illustrates these relationships graphically.
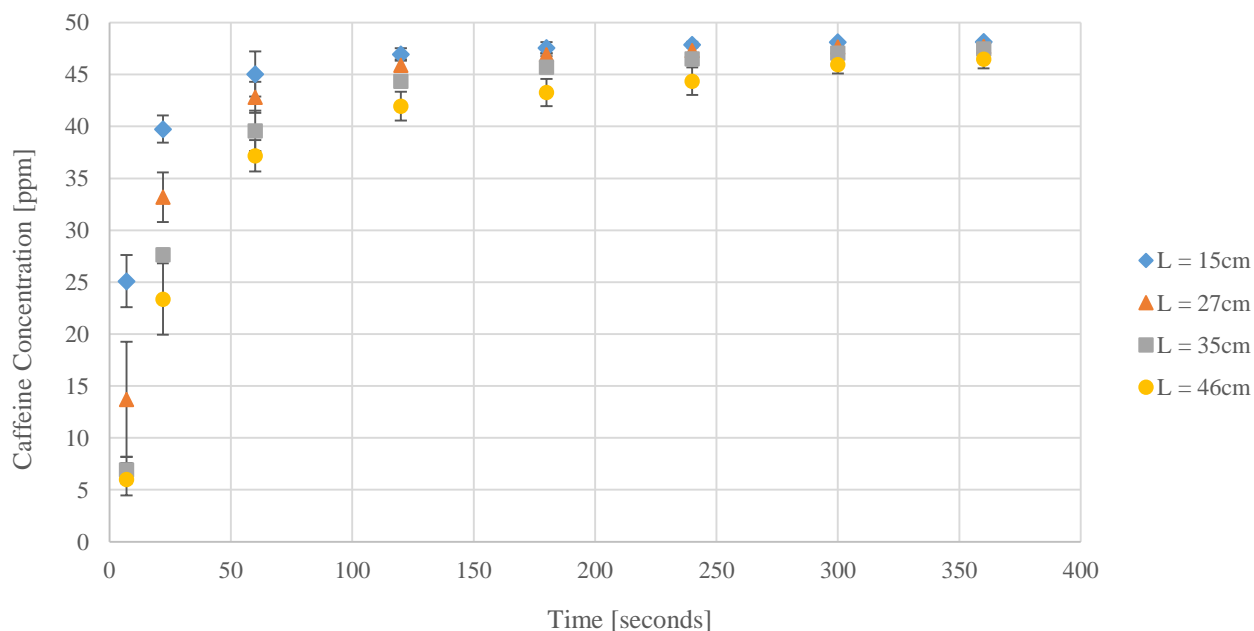
Figure 31. Caffeine concentration as a function of time for different depth lengths using *Moringa oleifera* Lam. husk as filtering bed.

The level curves corresponding to *the Moringa oleifera* husk resembles the behavior of the rest of the filtering beds; electrostatic attraction is taking place which is why caffeine is getting removed. From this aspect, it may be inferred that the husk can actually be used and compared with the rest of the filtering beds. Note that the error bars are much more noticeable in Figure 31 than any other graph. The husk's morphology and column packing varied in every case which is why even though the filtering depth could be the same, the system inside could differ. It was this constant variation that indirectly made the results fluctuate more and consequently, have a larger uncertainty.

5.4 Concentration as a function of depth

Appendix E presents the most representative data for caffeine concentration at different filter depths on a given operation time for each bed individually. Appendix J has these complete set of data. Figures 34-37 illustrates this corresponding relationships graphically.

5.4.1   Activated Carbon as the filtering bed.
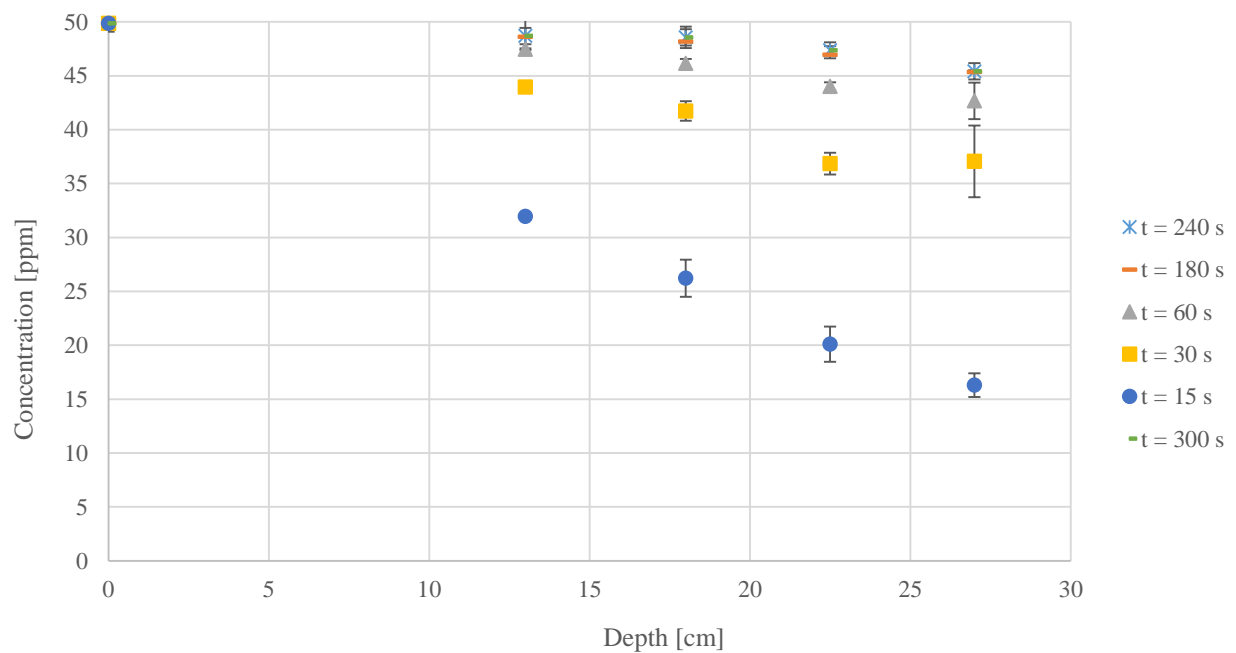
Figure 32. Caffeine concentration as a function of depth for different operating times (t) using Activated Carbon as the filtering bed.

5.4.2 *Zeolite as the filtering bed.*
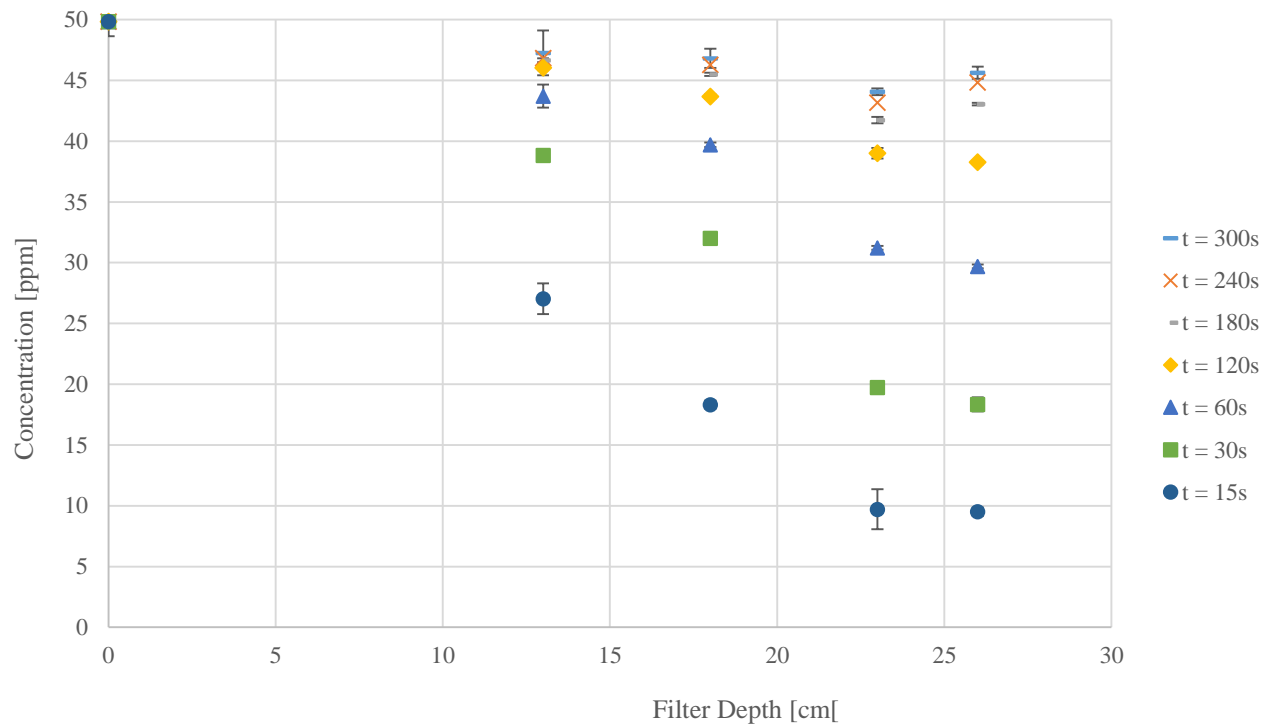
Figure 33. Caffeine concentration as a function of depth for different operating times (t) using Zeolite as the filtering bed.

5.4.3 *Gravel as the filtering bed*
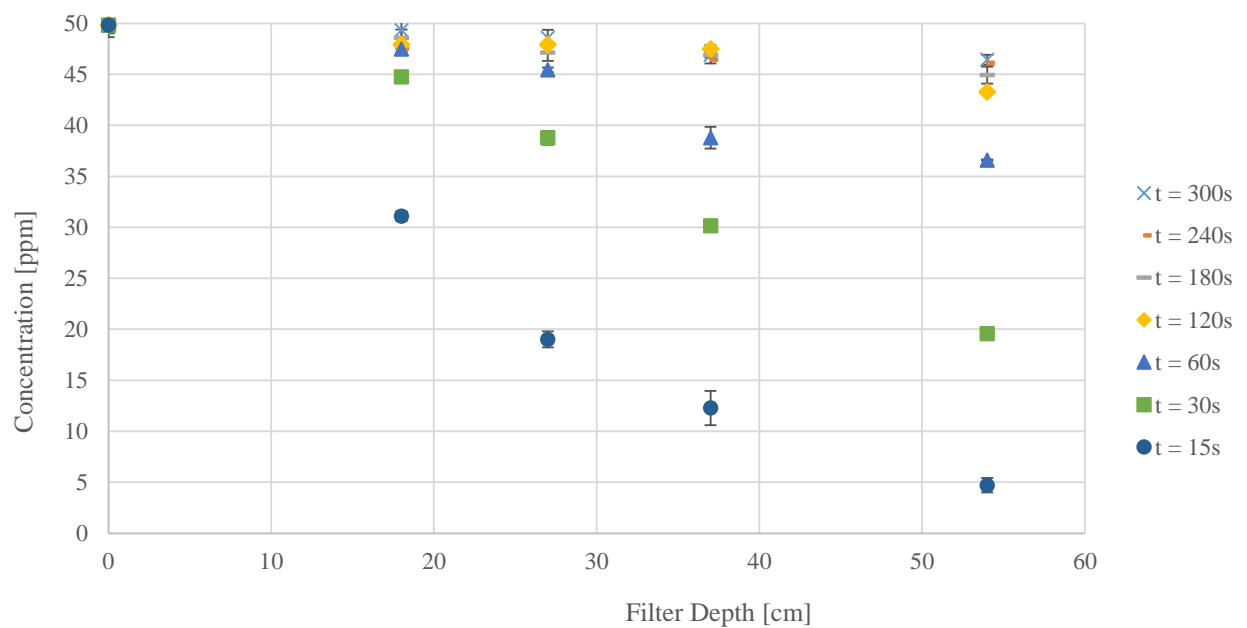
Figure 34. Caffeine concentration as a function of depth for different operating times (t) using Gravel as the filtering bed.

5.4.4 *Moringa oleifera* **Lam.** *Husk as the filtering bed*
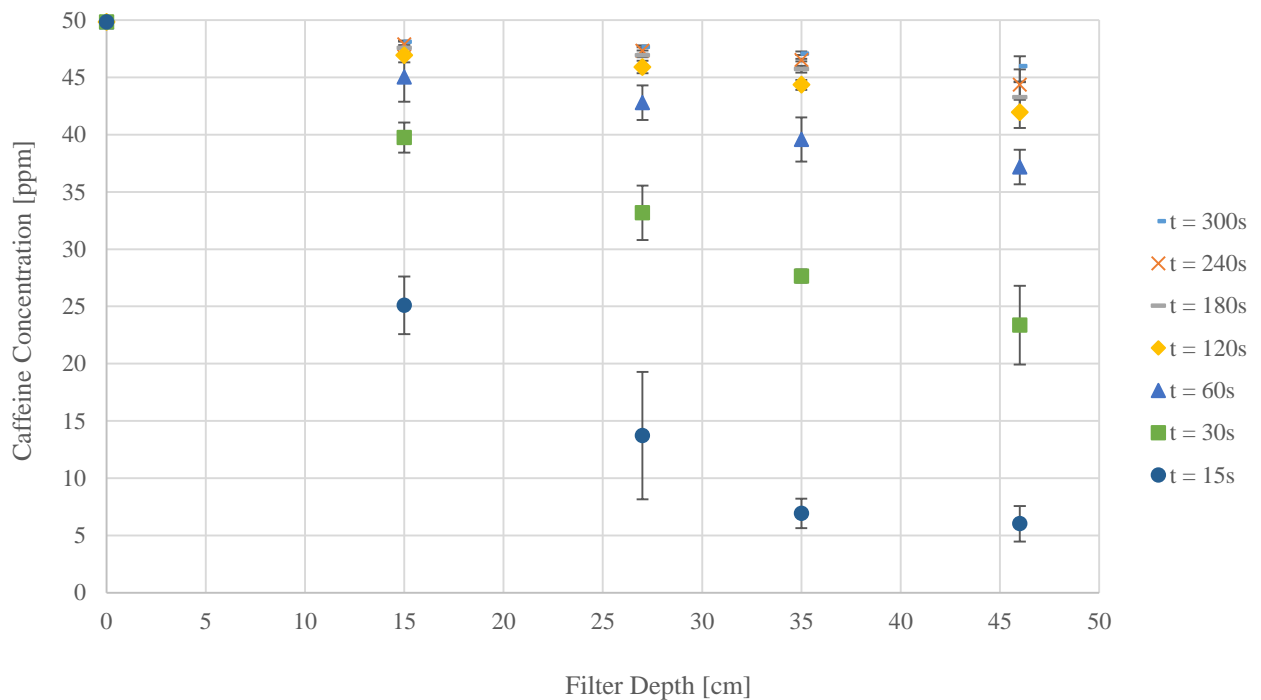
Figure 35. Caffeine concentration as a function of depth for different operating times (t) using *Moringa oleifera* husk as the filtering bed.

The behavior of caffeine concentration with respect to filter depth appears to be the same for every filtering bed. At the beginning, when the filtering bed begins to fill the column, the caffeine concentration appears to decrease lineally with respect to the bed depth. This linear range appears to be for the first 22, 18, 27, and 27 cm for activated carbon, zeolite, gravel, and *Moringa oleifera* husk respectively. After this range, caffeine removal starts to lose effectiveness and the rate of change of caffeine concentration decreases. Apparently, with a lower contaminant concentration the removal effectiveness of a bed layer decreases. Actually, this is exactly what Iwasaki and Ives proposed with their filtering and clarification water theory (Valencia, 1972). In fact, equation (28) expresses that the variation of concentration with respect to a filtering bed layer (in this case, caffeine removal with respect to filter depth) is proportional to its concentration. i.e. a greater caffeine concentration will lead to a greater caffeine removal with a fixed layer "L", and a lower caffeine concentration will lead to a lower caffeine removal with the same fixed layer "L". It is important to highlight the fact that this model works with the assumption that the main operating forces that remove contaminants are gravitational flows, but this is not necessarily the case when removing caffeine; experimental discrepancies may be attributed to this.

The level curves regarding Figures Figure *32*, Figure *33*, Figure *34* and Figure *35* are mostly significant when the operation time is low. As operation time progresses, the level curves are closer to each other and the resolution (understanding it as the ability to distinguish curves from each other) between them is lost. The only filtering bed that has a higher resolution at an advanced operating time is Zeolite.

5.5 Filter Standardization

Most of the results regarding filtering beds refer to their filter depth rather than its mass; however, these two quantities are directly related. It is significant to know this relationship as this will be used in analyzing how much caffeine can a specific bed mass adsorb and retain. In order to see the variation of the filter's bed mass with respect to its depth, the mass of each medium was recorded at specific filter lengths. The actual data for each bed is portrayed in

The gradient of the lines in Figure 36 depicts the proportional relationship between the mass of the filtering medium, and its corresponding depth in the column. These are found to be 0.433 [g/cm], 0.873 [g/cm], 0.075 [g/cm], and 0.861 [g/cm] for activated carbon, zeolite, *Moringa oleifera* husk, and gravel respectively. For a graphical representation of each bed individually, see Appendix F.
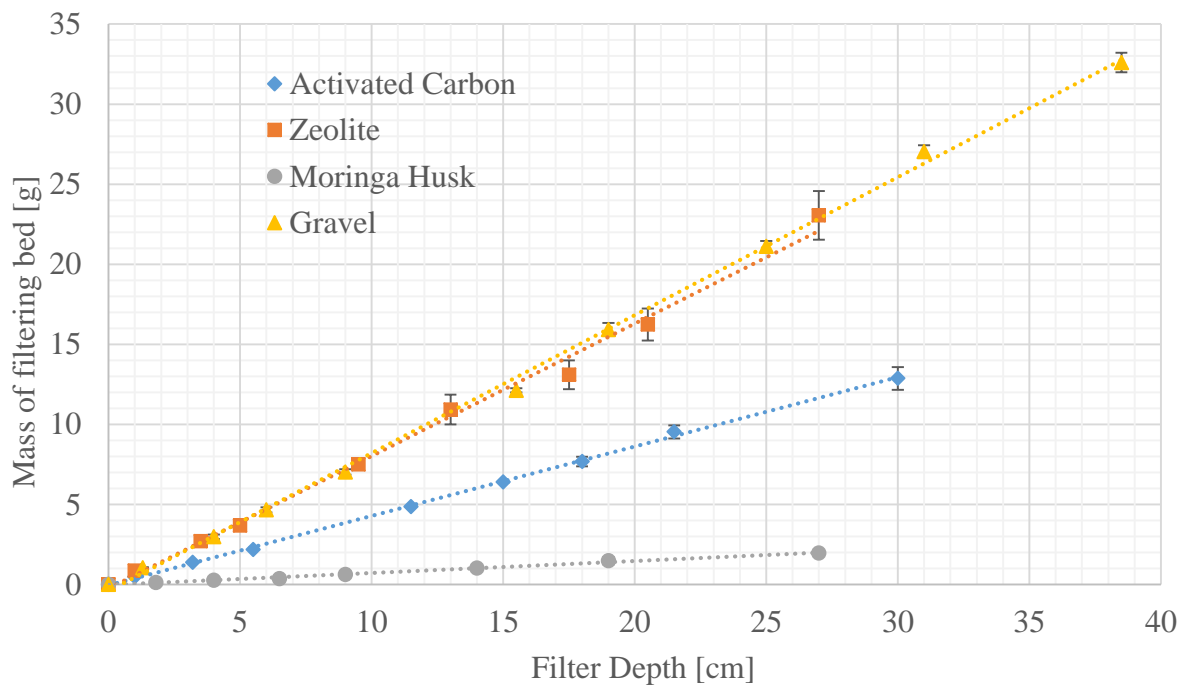
Figure 36. Mass of the distinct type of filtering mediums as a function of their corresponding filter depth in the column.

The first qualitative observation that could be corroborated using instrumental analysis (HPLC and UV-VIS Spectroscopy) is that, in fact, the phenomena that removes caffeine in the filtering system is adsorption. This can be verified by referring to the UV-VIS spectrum before and after operation (Figure 37).

a)

b)
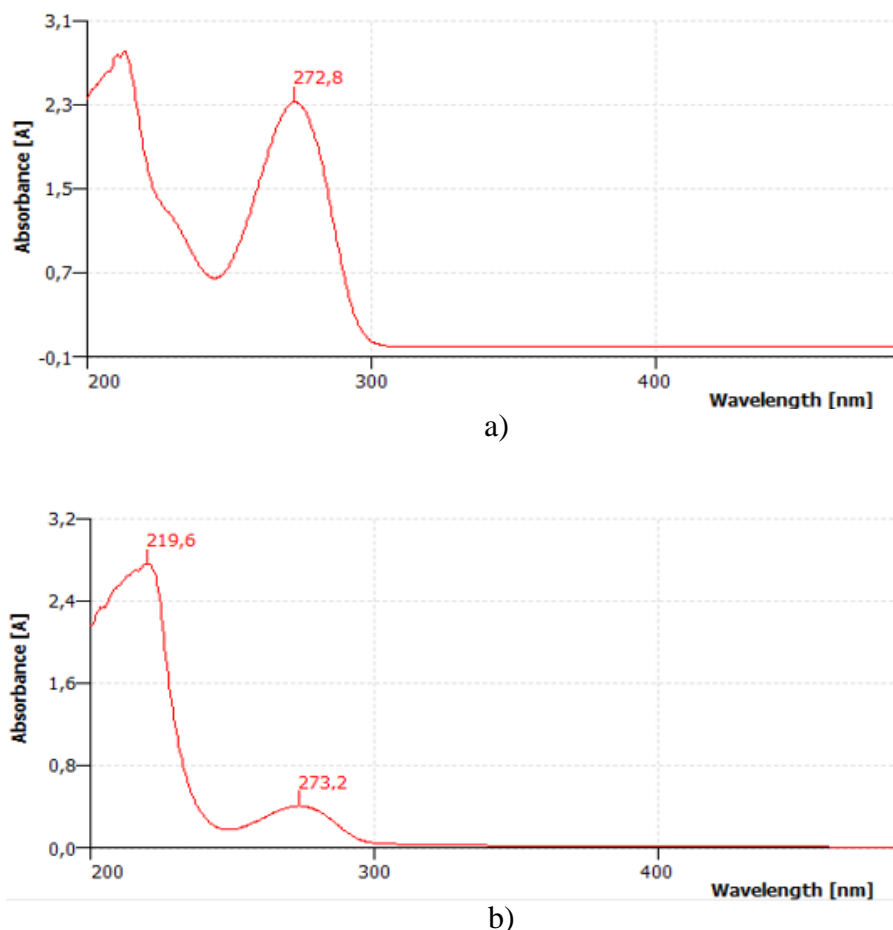
Figure 37. UV-VIS spectrum of a caffeine artificial solution before (a) and after (b) dynamic filtration using Gravel as the filtering bed (t = 10s, L = 26 cm).

Note that the shape of the UV-VIS Spectrums for all filtering beds behaved the same way as the one on Figure 37. If the caffeine molecule would have had degraded or broken down, like in Advanced Oxidation Processes, the spectrum before and after would have had noticeable different peaks at different wavelengths. This is not the case; the characteristic peak of caffeine after the treatment only decreased, maintaining its original shape. This highlights the fact that caffeine is only getting retained by a physical-chemical phenomenon, adsorption. To ensure that the interaction between caffeine and the filtering beds was mainly physical (i.e. without chemical bonding), a backwash with distilled water was applied to every filtering system after it saturated. The effluents were analyzed and each was found to be with caffeine (their UV-

VIS spectrum matched exactly with the caffeine spectrum). If there was any chemical bonding whatsoever, the backwash solution would not have had the presence of caffeine at all.

Additionally, HPLC analysis was used to detect if any species other than caffeine was present in the filter effluent. UV-VIS spectroscopy was complemented with HPLC analysis as this last one would notice different species that absorb at a same wavelength. The chromatograms obtained after the artificial solution passed each filtering bed were similar as those shown next in Figure 38.

a)

b)
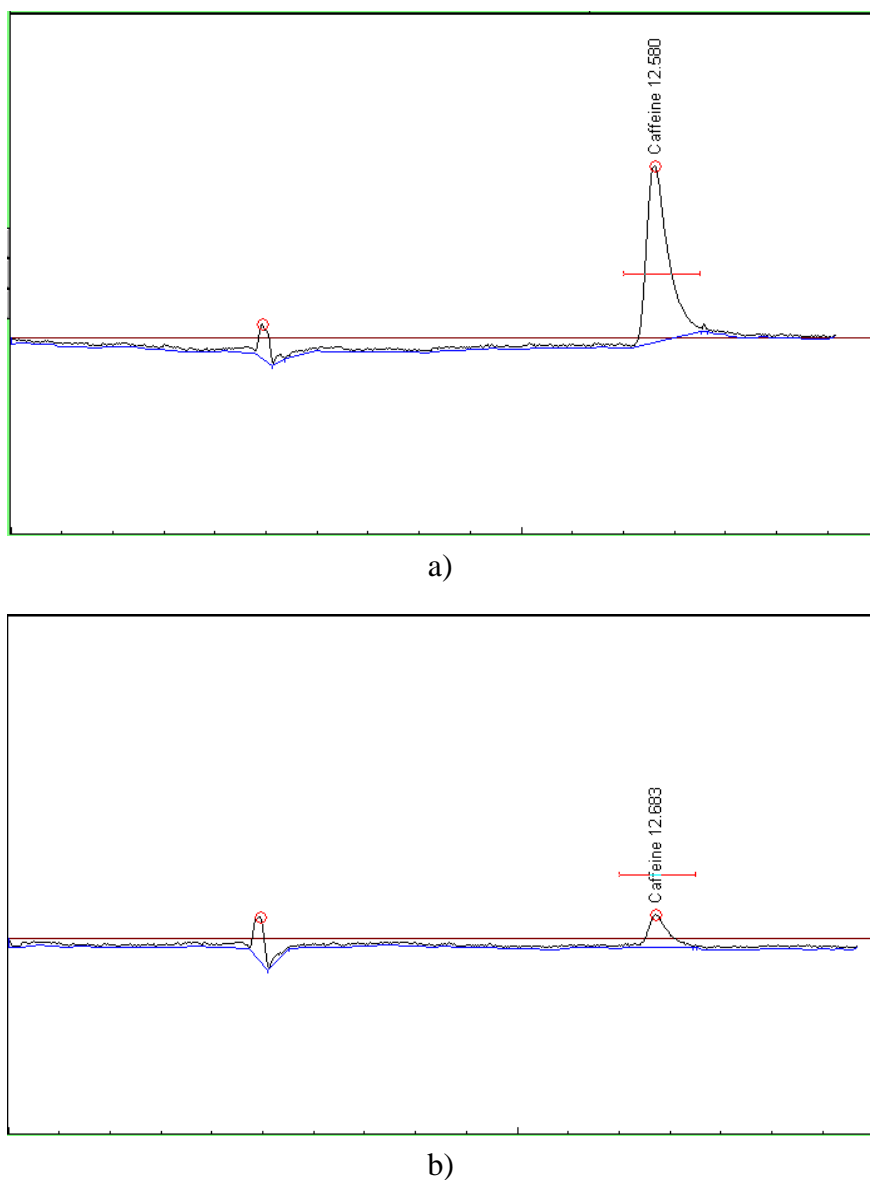
Figure 38. HPLC Chromatogram (a) before and (b) after filtration using *Moringa oleifera* Husk as the filtering bed (L = 26 cm).

As there were no other peaks other than the one corresponding to the retention time of caffeine, it was inferred that there were no other species produced.

The five different models discussed previously were tested on each breakthrough curve for every filtering bed. The parameters and variables for every model were optimized for each case in order to obtain a best fit model. This was performed using the "Solver" complement in Microsoft Excel. The following results show the experimental data and each model with its corresponding optimized parameters. A table with the values of these parameters was included. Also, the models were numbered in ascending order from best to worst to describe which model best fitted the experimental data. These were based on the value of the Minimum Mean Squared Error (MMSE) for each model.

5.6 Best Fit Models for Activated Carbon
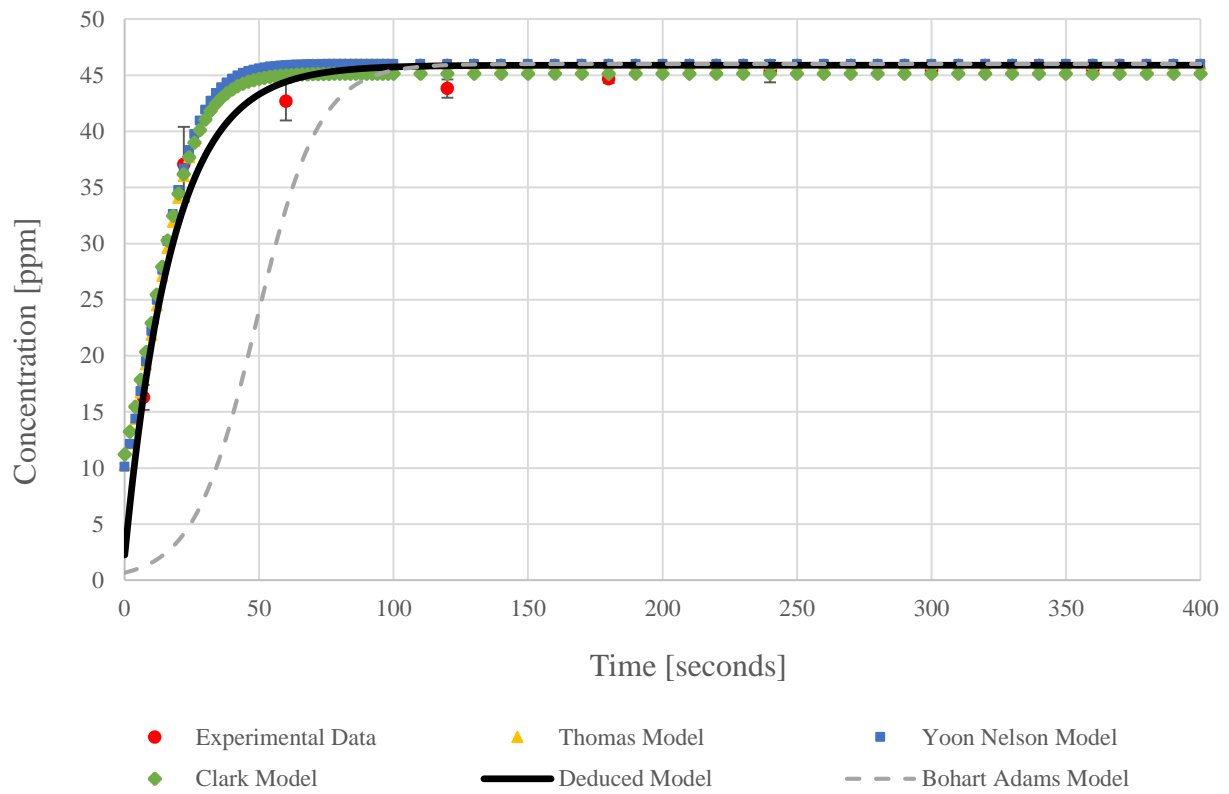
Figure 39. Best fit models of breakthrough curves for the adsorption of Caffeine ($C_0 = 46$ ppm) using Activated Carbon as the filtering bed (Depth = 27 cm) at a flow of 13.83 mL/min.

Table 3. Optimized parameters for each breakthrough curve model using Activated Carbon as the filtering medium.

Deduced Model	c [cm^2]	n [-]	λ_0 [cm^{-1}]	MMSE
(2)	0.569	0.0966	0.112	1.677
Bohart Adams Model	k [s^{-1}]	q$_s$ [-]	ε [-]	63.750
(5)	0.00187	5.0946×10^{-5}	0.9998	
Thomas Model	k [s^{-1}]	q [cm^2]		2.515
(3)	0.00250	4.261		
Yoon Nelson Model	k [s^{-1}]	F$_1$ [s/cm]		2.635
(4)	0.120	0.392		
Clark Model	r [s^{-1}]	n [-]	F$_2$ [cm^{-1}]	1.562
(1)	0.114	2.005	0.113	

5.7 Best Fit Model for Zeolite
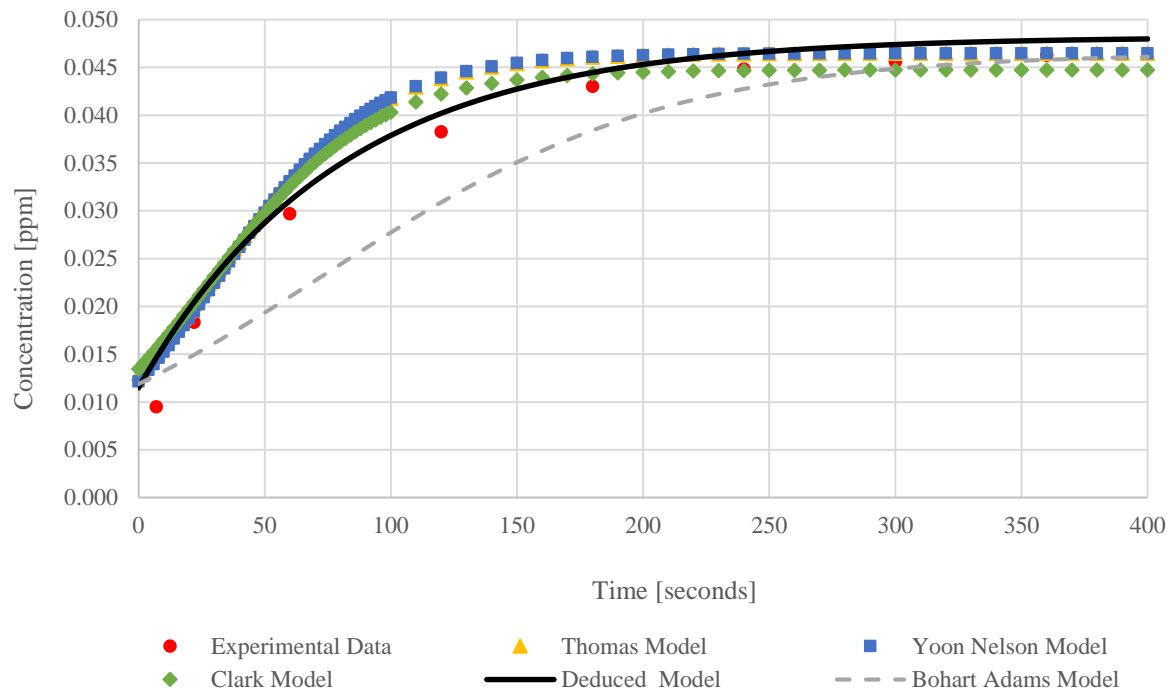
Figure 40. Best fit models of breakthrough curves for the adsorption of Caffeine ($C_0 = 46$ ppm) using Zeolite as the filtering bed (Depth = 26 cm) at a flow of 13.83 mL/min.

Table 4. Optimized parameters for each breakthrough curve model using Zeolite as the filtering medium.

Deduced Model	**c [cm²]**	**n [-]**	**λ_0 [cm⁻¹]**	**MMSE**
(1)	1.398	0.5265	0.055	8.931
Bohart Adams Model	**k [s⁻¹]**	**q_s [-]**	**ε [-]**	18.926
(5)	0.000314	1.935	0.7140	
Thomas Model	**k [s⁻¹]**	**q [cm²]**		17.080
(4)	0.000674	12.483		
Yoon Nelson Model	**k [s⁻¹]**	**F_1 [s/cm]**		15.541
(3)	0.032	1.233		
Clark Model	**r [s⁻¹]**	**n [-]**	**F_2 [cm⁻¹]**	10.536
(2)	0.0306	2.010	0.0909	

5.8 Best Fit Model for Gravel
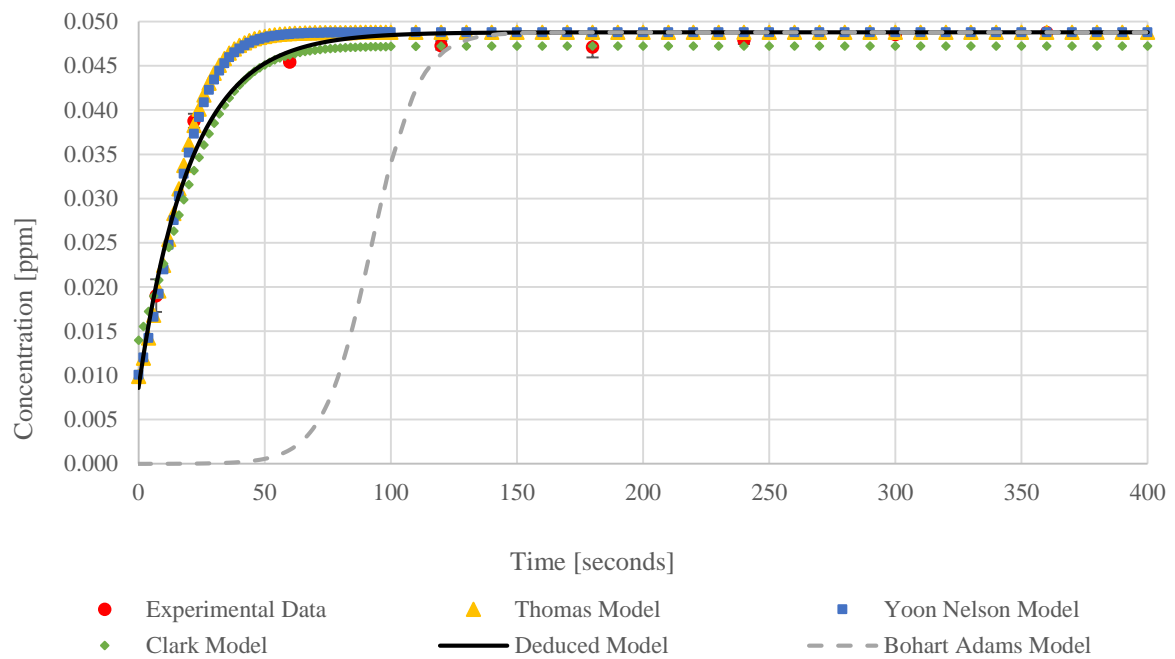
Figure 41. Best fit models of breakthrough curves for the adsorption of Caffeine ($C_0 = 46$ ppm) using gravel as the filtering bed (Depth = 27 cm) at a flow of 13.83 mL/min.

Table 5. Optimized parameters for each breakthrough curve model using gravel as the filtering medium.

Deduced Model	c [cm^2]	n [-]	λ_0 [cm^{-1}]	MMSE
(1)	0.755	0.0056	0.064	2.691
Bohart Adams Model	k [s^{-1}]	q$_s$ [-]	ε [-]	643.248
(5)	0.002162	9.505×10^{-7}	0.9874	
Thomas Model	k [s^{-1}]	q [cm^2]		9.064
(3)	0.002477	4.706		
Yoon Nelson Model	k [s^{-1}]	F$_1$ [s/cm]		8.615
(2)	0.115	0.434		
Clark Model	r [s^{-1}]	n [-]	F$_2$ [cm^{-1}]	9.337
(4)	0.0786	2.008	0.0895	

5.9 Best Fit Model for *Moringa oleifera* Husk
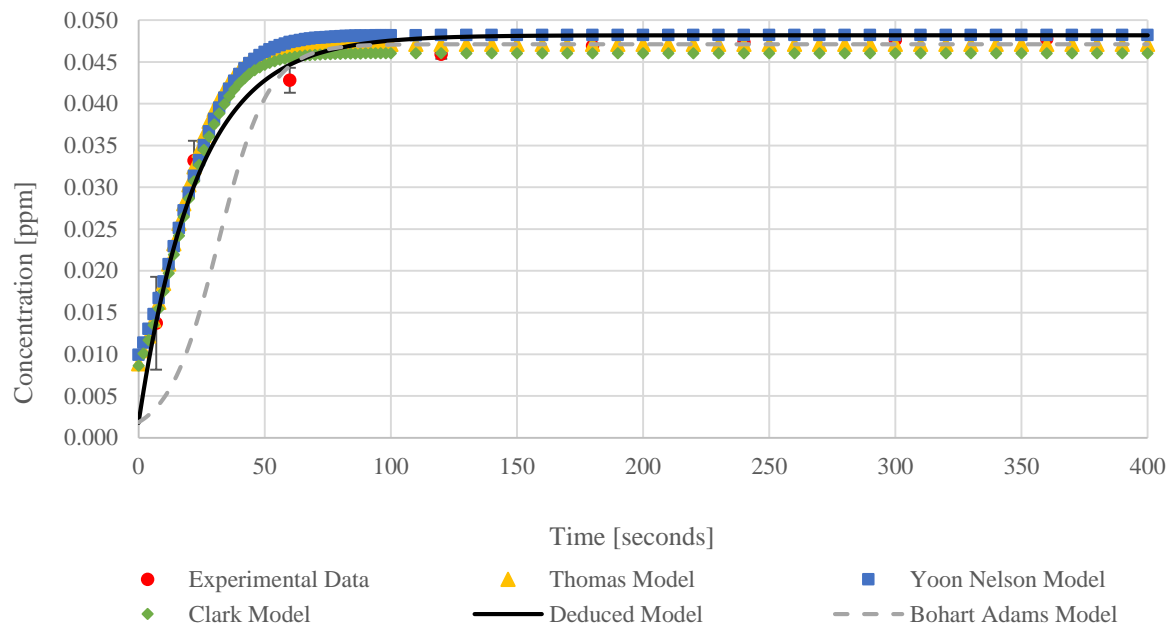
Figure 42. Best fit models of breakthrough curves for the adsorption of Caffeine ($C_0 = 46$ ppm) using *Moringa oleifera* Husk as the filtering bed (Depth = 27 cm) at a flow of 13.83 mL/min.

Table 6. Optimized parameters for each breakthrough curve model using *Moringa oleifera* husk as the filtering medium.

Deduced Model (1)	c [cm²]	n [-]	λ_0 [cm⁻¹]	MMSE
	0.517	0.3473	0.122	3.538
Bohart Adams Model (5)	k [s⁻¹]	q_s [-]	ε [-]	286.517
	0.002087	8.019×10⁻⁵	1.000	
Thomas Model (3)	k [s⁻¹]	q [cm²]		7.627
	0.002130	5.860		
Yoon Nelson Model (4)	k [s⁻¹]	F_1 [s/cm]		8.968
	0.090	0.559		
Clark Model (2)	r [s⁻¹]	n [-]	F_2 [cm⁻¹]	6.559
	0.0988	2.012	0.1652	

5.10   Comparison Between Filtering Mediums

A direct measure of the efficiency of filtering mediums may be achieved by plotting the percentage of caffeine removal as a function of time for a fixed bed depth. This was done for every filtering medium. Figure 43 shows the actual caffeine removed vs. operation time, while in Figure 44, the best models that fit experimental data. Note that the efficiency removal is a function of time because as time progresses, the filter will continue to saturate; the ability to retain caffeine will then decrease.
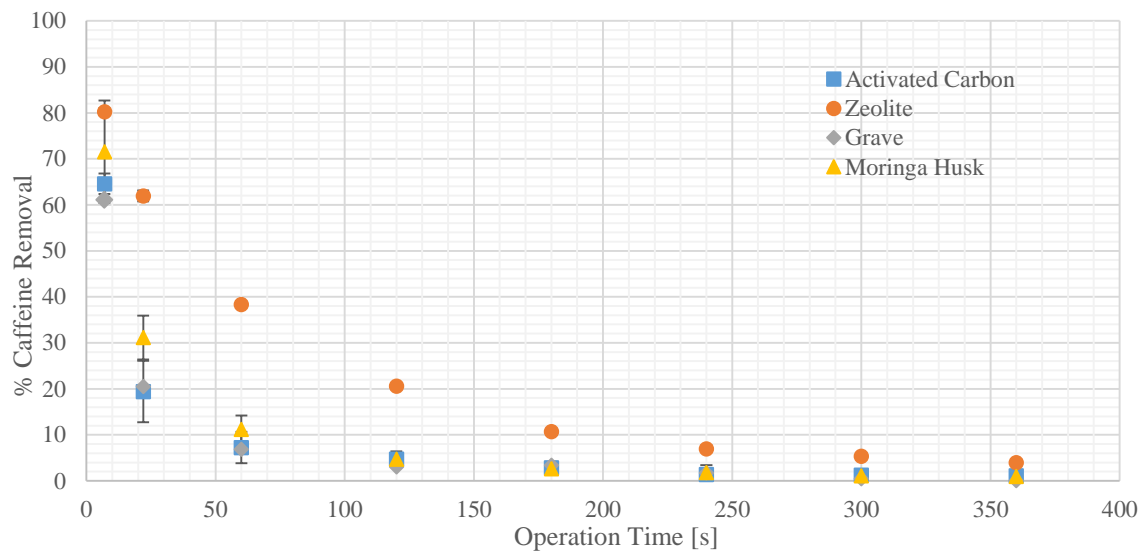
Figure 43. Percentage of caffeine removal as a function of time for different filter mediums (Depth = 27 cm).
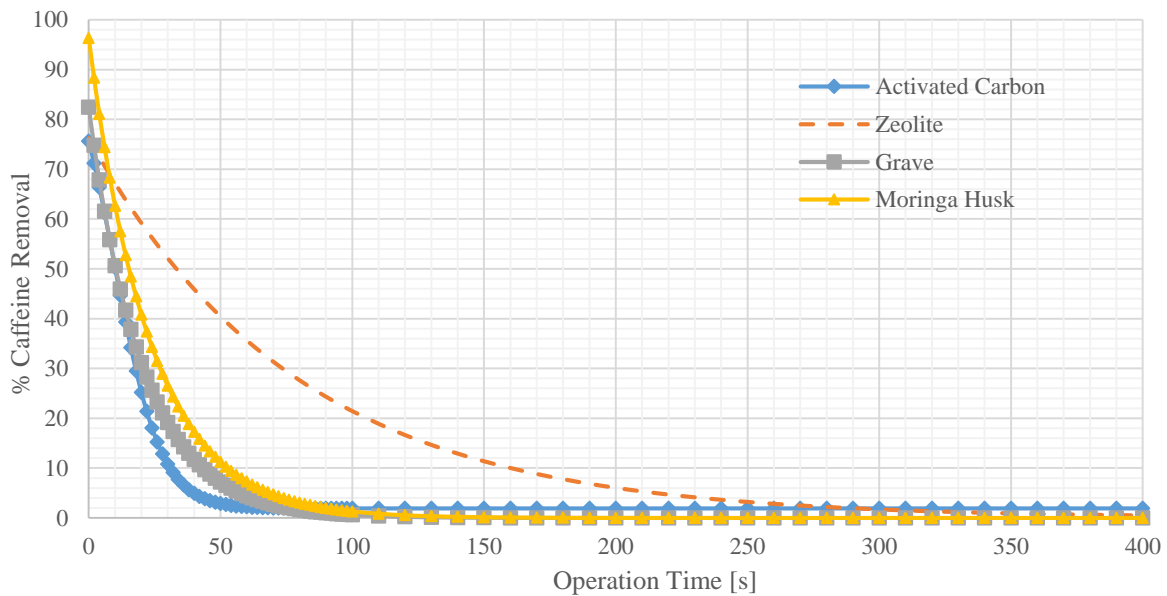
Figure 44. Percentage of caffeine removal (applying the models that best describe experimental data) as a function of time for different filter mediums (Depth = 27 cm).

Note that the comparison between medium beds were carried out at a selected depth of 27 cm. where all filters were tested and experimented. From Figure 43 it can be observed that the filtering bed that maintains the highest percentage caffeine removal through operation time is zeolite. However, based on the models that best describe experimental data on Figure 44 it can be inferred that zeolite does not produce the highest percentage of caffeine removal at the beginning of the operation. When the first drop of the effluent appears (when t = 0), the percentage of caffeine removal of zeolite is barely 75% while other beds such as *Moringa oleifera* husk and gravel present a percentage removal of 96% and 81% respectively. From this perspective, zeolite will be preferred as the filtering medium if the priority is to maintain a high percentage removal through time. However, other beds such as the *Moringa oleifera* husk or gravel will be preferred if what is sought is to obtain an instantaneous caffeine removal at the beginning of the operation.

5.11   Breakthrough Curves Analysis

In order to calculate the operational parameters from the classical models of breakthrough curves, the results were processed so that dimensionless concentration (C/C_0) could be plotted against effluent volume taking Figure 12 as reference. The conversion between operation time to effluent volume was done taking into account the water flow control variable (13.83 mL/min). Comparing these type of breakthrough curves for each medium filter at a depth of 27 cm. the following results were obtained using the best models.
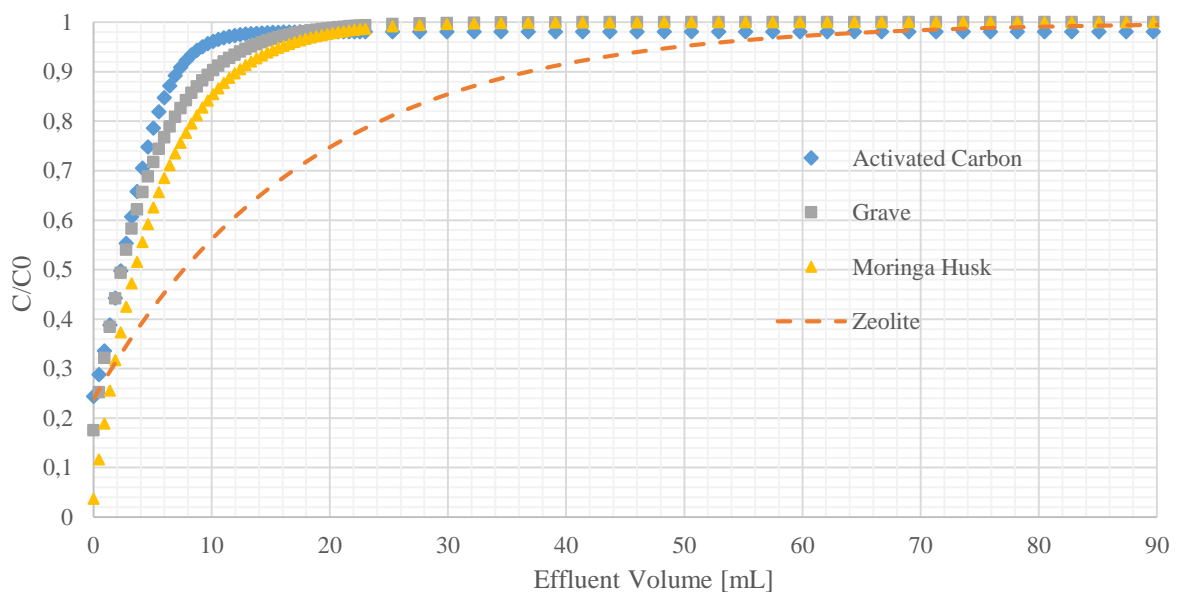
Figure 45. Classical Breakthrough Curves for different medium filters at a depth of 27 cm.

At the beginning of the operation, the adsorption capacity of each filtering bed was the highest as it did not contain any pollutant; its surface could take up most caffeine. As time progressed, the bed started to become saturated and so, the effluent concentration started to increase and tend to C_0.

Comparing Figure 45 with the ideal breakthrough curve shown in Figure 12, it may be observed that the breaking point for every graph is almost instantaneous, and so, it is negligible. This makes the breakthrough capacity along with the percentage degree of column utilization virtually null for the interaction of caffeine with every filtering bed. This could be a reflection of the relatively small interaction forces between caffeine and the filtering medium if compared to other pollutants. For example, investigations with similar filtering beds have shown a much greater adsorption capacity when the contaminants were dye or heavy metals (Beltra & Sa, 2009). The fact that caffeine is a polar organic molecule may explain this.

Nevertheless, other studies regarding caffeine removal using granulated activated carbon in a filtering bed have in fact showed a much greater efficiency through a noticeable breaking point at an advanced operation time (Sotelo et al., 2012). The main difference between this last investigation with the presented project was that the chosen fluid flow was lower and the column packing was compressed to a much higher efficiency. Even though one of the indirect aims of this project was to use the filtering beds as they were without any further treatment, evidence claims that this is actually necessary in order to gain a better removal capacity and a more evident breaking point. Packing efficiency may be increased by reducing the particle size and compressing it more inside the column. Only when this is achieved, the results can be comparable. This may be applied not only for activated carbon, but also for zeolite, gravel and *Moringa oleifera* Husk.

Some studies regarding removal of pollutants in wastewater suggest that a common breaking point should be reached after 100 mL of effluent volume in order to consider a scale up. This is the case of the biosorption of phenol in a continuous packed bed (Aksu & Gönen, 2004). As it may be observed from Figure 45, after 100 mL of effluent volume the filter practically got saturated; the packing system with the column needs to be redesigned to achieve this. It is important to consider how does the concentration-time graphs compare to other species as this will serve as a reference when considering a scale up. Most of the breakthrough curves found experimentally tend to have their breaking point in the first couple of hours (when operating at a similar water flow). For example, adsorption of methylene blue in a fixed-bed column using

phoenix tree leaf powder has a breaking point after an operation time of 1 hour with a fluid flow of 1 mL/min (Han et al., 2009). This value should be taken into account as reference for future works as it considers a possible scale up. The presented difference is quite noteworthy when comparing the results obtained shown in Figures Figure *39* - Figure *42*. Methylene blue may represent a basic organic dye that is present in wastewaters which is why it may be compared to other pollutants such as caffeine. The study serves as a reference denoting that the breaking point needs to occur much longer in order to consider the filtering system as a potential candidate for pollutants in wastewater treatment plants. Overall, the kinetic parameters for every model highlighted in tables Table *3*- *Table 6* are lower than the ones obtained in studies regarding caffeine removal with other filtering beds (Sotelo et al., 2012).

Most of the breakthrough curves appear to be best represented by the "Deduced Model" with the exception of activated carbon. When using activated carbon as the filtering bed, Clark's Model was the mathematical expression that best adapted experimental data. Clark's model works with the assumption that sorption behavior of contaminants follows the Freundlich adsorption isotherm which suggests that a multilayer is formed. If a multilayer is formed, technically the contaminants are going to be continuously adsorbed into the bed even past saturation. This could actually be the reason why in Figure 27 the different level curves seem to have different asymptotes; a larger filter depth will signify a larger surface area where caffeine could continuously form a multilayer. Thus, as the bed continues to filter out more caffeine, the effluent will not tend to the influent concentration, but tend to a relatively lower one which highlights that the sorption rate is determined by the outer mass transfer step. This also occurs with zeolite and *Moringa oleifera* husk as Clark's model is the second model that best fits experimental data. Actually, an investigation concerning the removal of lead ions from aqueous solutions suggests that zeolite in a filtering bed follow Clark's kinetic model of adsorption (Peric et al., 2008). On the other hand, gravel is the only bed that does not consider Clark's model as one of the best expression to describe its data. Henceforth, evidence points out that gravel does not follow the Freundlich adsorption isotherm. Further experiments should be carried out to test whether each bed follows the Freundlich or Langmuir adsorption isotherm.

The exhaussion point, however, does exist for every graph presented in this project. The caffeine retained in every filtering bed can then be calculated; as a matter of fact, the area englobed between the curve for a particular model and $C/C_0 = 1$ will give a direct relationship on how much caffeine did that filter bed retain. Using this criteria, it can be seen that the bed

that adsorbed caffeine the most was zeolite, followed by *Moringa oleifera* Husk, Gravel, and Activated Carbon respectively.

Taking zeolite as an example of the filtering bed, the area englobed between its curve and $C/C_0 = 1$ is found to be 14.0988 [mL]. multiplying this value by the initial caffeine concentration (0.0482 mg/mL) will give 0.6796 [mg] which is in fact, its exhaussion capacity. This suggests that in that particular filtering bed of zeolite with a depth of 27 cm, a quantity of 0.6796 mg of caffeine is retained. Considering Avogadro's Number and that the molar mass of caffeine is 194.19 [g/mol] it can be found that there are $1.0288*10^{-6}$ and $6.1959*10^{17}$ moles and molecules of caffeine respectively.

It is essential to obtain a relationship that indicates how much caffeine will be retained per mass of filtering bed as this will be the practical information that may be used when considering a possible escalation. From the filter standardization results it is known that 27 cm of zeolite will have around 21 grams of zeolite. The actual measured value was 21.06 g. Finding the quotient of the exhaussion capacity (in grams) and this last value will give the relation between mass of caffeine retained to the mass of zeolite. This was 3.236×10^{-5} for zeolite. Moreover, the unit mass of the filtering beds (Figure 46) can be weighed and so, the total mass of caffeine may be determined.

Figure 46. Filtering Bed Units.

The unit mass of zeolite weighed 0.0202 g, and so, the total mass of caffeine retained in this unit could be calculated: $0.0202 \, [g] \times 3.236 \times 10^{-5} = 6.5368 \times 10^{-7} [g]$.

So that particular single unit of zeolite with a mass of 0.0202 grams has a capability of adsorbing approximately 0.65368 μg of caffeine. This was applied for every filter length (L = 26, 23, 18, 13 cm for the case of zeolite) in order to obtain a standard deviation and consequently, an uncertainty. Processing the results, it was found that in average, the unit mass of zeolite adsorbed $5.640 \times 10^{-7} \pm 1.007 \times 10^{-7}$ g of caffeine. This information was processed for each filtering bed and is summarized in

Table 7.

Table 7. Adsorption characteristics of the different types of filtering beds with respect to caffeine.

Adsorption characteristic	Activated Carbon	Zeolite	Gravel	*Moringa oleifera* Husk
Mass of caffeine retained [g] in filtering bed (L =27 cm)	0.0002154	0.0006796	0.0001998	0.0002600
Moles of retained Caffeine in filtering bed (L = 27 cm)	1.1093×10^{-6}	3.4995×10^{-6}	1.0288×10^{-6}	1.3387×10^{-6}
Molecules of retained Caffeine in filtering bed (L = 27 cm)	6.6801×10^{17}	2.1074×10^{18}	6.1959×10^{17}	8.0619×10^{17}
Mass of retained caffeine/Mass of filtering bed [μg/g]	19.58 ± 4.17	32.36 ± 5.16	9.08 ± 1.01	129.98 ± 48.01
Mass of unit bed [g]	0.0469	0.0202	0.2111	0.0073
Mass of caffeine retained per unit bed [μg]	1.100 ± 0.20	0.564 ± 0.10	1.681 ± 0.22	1.196 ± 0.46

From the information obtained, the best filtering beds will depend on what variables are considered a priority. For instance, if the main goal is to achieve a maximum removal with a fixed bed depth, zeolite will be chosen. However, if the purpose is to obtain the most pollutant

retention with the least amount (mass) of medium, then the *Moringa oleifera* Husk will be the best filtering bed. On the other hand, if there is an economic analysis on which is the cheapest and the most abundant filtering bed that could be used, then gravel will appear as the best candidate. A combination of these beds may result in the optimum dynamic filtration system if an escalation is desired.

6. Conclusion

In conclusion, a dynamic filtration analysis was achieved using caffeine as the contaminant model with Zeolite, Activated Carbon, Gravel and *Moringa oleifera* Husk as the filtering beds. Chemical Instrumental Analysis through the use of UV-VIS Spectroscopy and High Performance Liquid Chromatography corroborated the fact that the mechanism which removes caffeine in the presented system is adsorption. Under a fluid flow of 13.83 [mL/min] with a concentration of 50 ppm, caffeine concentration was monitored as a function of operation time and filter bed depth obtaining individual level curves for each variable. For each type of filtering medium, different mathematical models were tested to see which one fitted best each experimental set of data. These included the Bohart-Adams model, Thomas model, the Yoon-Nelson model, the Clark Model, and a deduced model from Iwasaki & Ives equations in conjunction with a mass balance around the filter. It was found that the model that best adapted to activated carbon as the filtering bed was Clark's model, while for zeolite, gravel and *Moringa oleifera* Husk, it was the deduced model. The breakthrough capacity and percentage degree of column utilization for every filtering medium with caffeine was virtually null due to the low value of their breaking points. Based on different studies regarding similar filter beds with similar contaminants, it was found that the system proposed on this investigation is not efficient for a scale up. The different parameters obtained experimentally depicted a relatively low adsorption kinetics which is why it is suggested to improve the filtering system by increasing the packing effectiveness and reduce the fluid flow. Overall, caffeine removal has a lower effectiveness than other contaminants like dye or heavy metals with similar filtering beds. Nevertheless, an exhaussion capacity was found, which permitted the quantification of the adsorption capabilities of each medium for this particular system. When having a fixed bed depth, the medium that removed the most caffeine was zeolite, followed by *Moringa oleifera* husk, activated carbon, and gravel. At a bed depth of 27 cm, these retained a quantity of 0.6796, 0.2600, 0.2154, and 0.1998 mg of caffeine, respectively. Taking into account the relation of filter bed depth with its corresponding mass for every medium, the mass of caffeine retained per mass of filtering bed [μg/g] could be calculated. This was 19.58 ± 4.17, 32.36 ± 5.16, 9.08

$\pm$ 1.01, and 129.98 $\pm$ 48.01 for activated carbon, zeolite, gravel, and *Moringa oleifera* husk respectively. Additionally, analyzing the average filter bed units for each medium, it was found that these retained 1.10×10^{-6} $\pm$ 2.02×10^{-7}, 5.640×10^{-7} $\pm$ 1.01×10^{-7}, 1.681×10^{-6} $\pm$ 2.19×10^{-7}, $1.196\times10^{-6} \pm 4.59\times10^{-7}$ mg of caffeine per unit of activated carbon, zeolite, gravel, and *Moringa oleifera* husk respectively. The optimal filtering bed will rely on the variables that are considered priorities. If the objective is to remove the maximum amount of caffeine in a fixed column length, zeolite will be chosen; however, if the main goal is to retain the most caffeine with the least amount of bed mass, then *Moringa oleifera* husk would be recommended. To consider a possible scale up, an increase of the surface area available should be achieved in the system in order for the breaking point to occur at time of 1 hour with a fluid flow of approximately 1 mL/min.

7. Recommendations

This investigation was specifically focused on the dynamics of pollutant removal; nonetheless, a hydraulic analysis may be recommended for determining the possibilities and limitations of a real system. Sometimes the effectiveness of the filtering medium will not only be determined by the pollutant removal, but also by the amount of fluid it is capable of treating per unit time. Henceforth, hydraulic head loss in conjunction with the analysis done in this investigation will ultimately indicate which bed is the best for treating a specific fluid flow.

It is important to notice that even though the characterization of filtering mediums were done with their depth-mass relation, it is not the mass per se that is responsible for adsorption; it is its superficial area. It will be recommended for future investigations to enhance and develop a relation between filtering bed mass to its superficial area. Varying the superficial area of the beds through particle size could also be explored to determine which combination yields the best percentage of pollutant removal considering hydraulic head losses.

As mentioned in the introduction, the filtering systems were constructed in a small scale so that it could then be scaled-up to a pilot plant and consequently, a large water treatment plant. Still, some of the effects and filtration dynamics reported in this investigation would not necessarily apply exactly for larger filters. The column diameter used here was 1.1 cm, but in a real pilot plant filter this will be much wider. It will be of significant importance to explore the effects of increasing the diameter of the column as this will be an approach to scale-up this study to a larger filter.

8. Acknowledgements

9. References

Aksu, Z., & Gönen, F. (2004). Biosorption of phenol by immobilized activated sludge in a continuous packed bed : prediction of breakthrough curves, *39*, 599–613. https://doi.org/10.1016/S0032-9592(03)00132-8

Ansari, R., Seyghali, B., Muhammad-khan, A., & Zanjanchi, A. (n.d.). *Highly efficient adsorption of anionic dyes from aqueous solutions using sawdust modified by cationic surfactant of cetyltrimethylammonium bromide*.

Beltra, J., & Sa, J. (2009). Removal of Carmine Indigo Dye with Moringa oleifera Seed Extract, 6512–6520.

Bird, R., Stewart, W., & Lightfoot, E. (2002). *Transport Phenomena*. John Wiley & Sons. Inc.

Deblonde, T., Cossu-leguille, C., & Hartemann, P. (2015). International Journal of Hygiene and Emerging pollutants in wastewater : A review of the literature. *International Journal of Hygiene and Environmental Health*, *214*(6), 442–448. https://doi.org/10.1016/j.ijheh.2011.08.002

González, N. (2016). Characterization of contaminants by different treatments for their removal in water : Use of Caffeine as a model compound Nicole Belén González Salguero Nicole Belén González Salguero.

Han, R., Wang, Y., Zhao, X., Wang, Y., Xie, F., Cheng, J., & Tang, Mm. (2009). Adsorption of methylene blue by phoenix tree leaf powder in a fixed-bed column : experiments and prediction of breakthrough curves fixed-bed column : experiments and prediction, (September 2015). https://doi.org/10.1016/j.desal.200

Izod, T. P. (1982). REMOVAL OF CAFFEINE BY SELECTIVE ADSORPTION USING ZEOLITE ADSORBENTS.

Leone, A., Spada, A., Battezzati, A., Schiraldi, A., Aristil, J., & Bertoli, S. (2015). Cultivation , Genetic , Ethnopharmacology , Phytochemistry and Pharmacology of Moringa oleifera Leaves : An Overview, 12791–12835. https://doi.org/10.3390/ijms160612791

Mcconnachie, G. L., Warhurst, A. M., Pollard, S. J., & Chipofya, V. (1996). Activated carbon from Moringa husks and pods, 279–282.

Muhammad, N., Parr, J., Smith, M. D., & Wheatley, A. D. (1998). Adsorption of heavy metals in slow sand filters Method used for Batch Adsorption Tests, 346–349.

Norris, M. J., Pulford, I. D., Haynes, H., Dorea, C. C., & Phoenix, V. R. (2013). Treatment of heavy metals by iron oxide coated and natural gravel media in Sustainable urban Drainage Systems, 674–681. https://doi.org/10.2166/wst.2013.259

Peric, J., Trgo, M., & Vukojevic, N. (2008). Testing of Breakthrough Curves for Removal of Lead Ions from Aqueous Solutions by Natural Zeolite-Clinoptilolite According to the Clark Kinetic Equation, (October 2007), 944–959. https://doi.org/10.1080/01496390701870622

Petrie, B., Barden, R., & Kasprzyk-hordern, B. (2014). ScienceDirect A review on emerging contaminants in wastewaters and the environment : Current knowledge , understudied areas and recommendations for future monitoring. *Water Research*. https://doi.org/10.1016/j.watres.2014.08.053

Santos, A. F. S., Matos, M., Sousa, Â., Costa, C., Teixeira, J. A., Paiva, P. M. G., … Costa, C. (2015). Removal of tetracycline from contaminated water by Moringa oleifera seed preparations, *3330*(September), 0–8. https://doi.org/10.1080/09593330.2015.1080309

Sharma, P., Kumari, P., Srivastava, M. M., & Srivastava, S. (2006). Removal of cadmium from aqueous system by shelled Moringa oleifera Lam . seed powder, *97*, 299–305. https://doi.org/10.1016/j.biortech.2005.02.034

Sotelo, J. L., Rodríguez, A., Álvarez, S., & García, J. (2012). Removal of caffeine and diclofenac on activated carbon in fixed bed column. *Chemical Engineering Research and Design*, *90*(7), 967–974. https://doi.org/10.1016/j.cherd.2011.10.012

Tailor, R. (2011). *Adaptation of Bagasse fly ash into zeolites for the removal of phenols from aqueous solution*. Veer Narmad South Gujarat University. Retrieved from http://hdl.handle.net/10603/3037

T Moore, L Greenway, L Farris, G. B. (2008). Assessing Caffeine as an Emerging Environmental Concern Using Conventional Approaches, 31–35. https://doi.org/10.1007/s00244-007-9059-4

Tech Brief. (2000). Slow Sand Filtration.

Thomas, H. (1943). Heterogeneous Ion Exchange ina Flowing System, (2), 1664–1666.

Valencia, A. (1972). *Teoría, Diseño y Control de los Procesos de Clarificación del Agua*. Lima, Perú: CEPIS (Centro Panamericano de Ingenieria Sanitaria y Ciencias del

Ambiente).

Valencia, G. (n.d.). Filtros Biologicos.

World Health Organization. (2011). *Slow Sand Filters*.

Wuana, R. A., Ato, R. S., Iorhen, S., Wuana, R. A., Ato, R. S., & Iorhen, S. (2016). Preparation , characterization , and evaluation of Moringa oleifera pod husk adsorbents for aqueous phase removal of norfloxacin adsorbents for aqueous phase removal of norfloxacin, *3994*(January). https://doi.org/10.1080/19443994.2015.1046150

10.APPENDICES

APPENDIX A: DETAILED METHODOLOGY FOR USING THE HPLC

With the help of a syringe and needle, the samples were taken (Figure 47 a-b) so that the needle could then be replaced with a 45 µm filter (Figure 47 c-d) to filter out solid particles that could block the chromatograph column. A volume of 100 µL was then taken from the filtered samples with the help of a micro syringe (Figure 48 a); this volume was then ejected. In order to clean the syringe and make sure any previous contaminants were expelled, this was done a total of 3 times. A final volume of 100 µL was taken making sure no bubbles were present in the liquid (Figure 48 b). The samples were then injected into the input port of the HPLC.

a)

b)

c)

d)
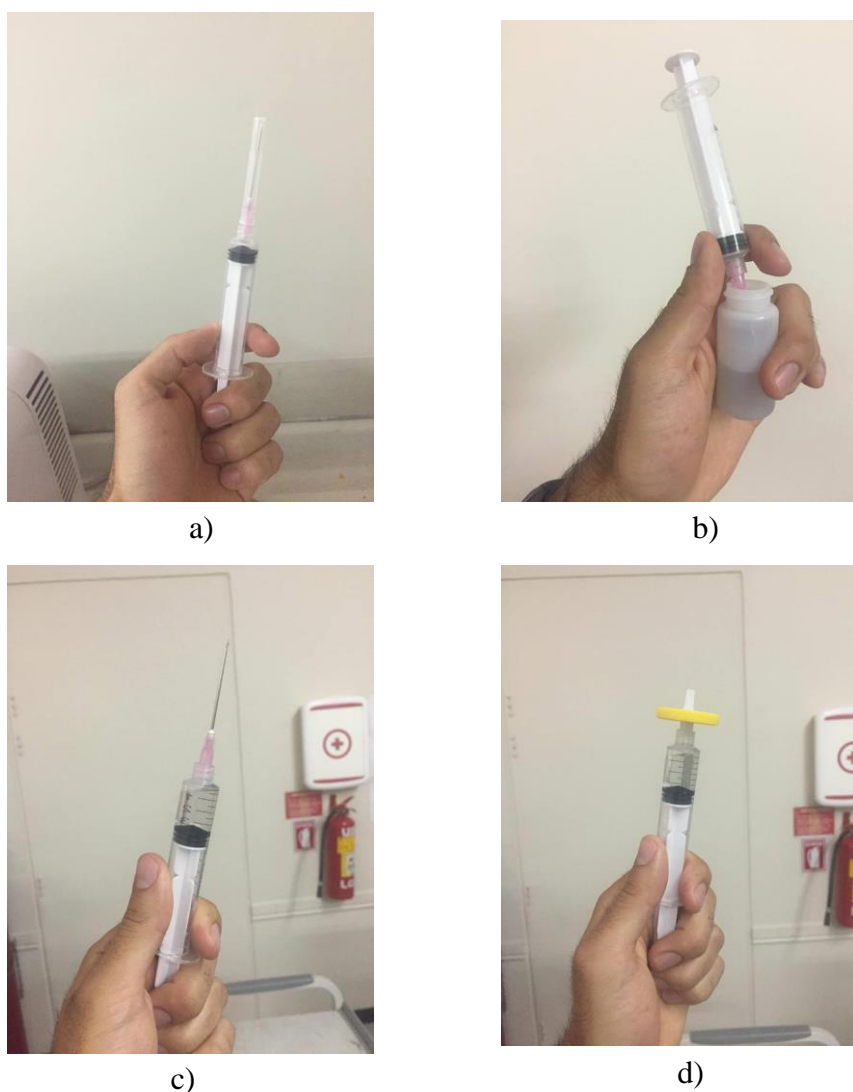
Figure 47. Filtering process before injecting sample in the HPLC column. Samples are absorbed using a syringe (a) & (b) so that the needle (c) could be replaced with a microfilter (d) to make sure no solid particles were injected in the column.

<div style="text-align:center">a)   b)</div>
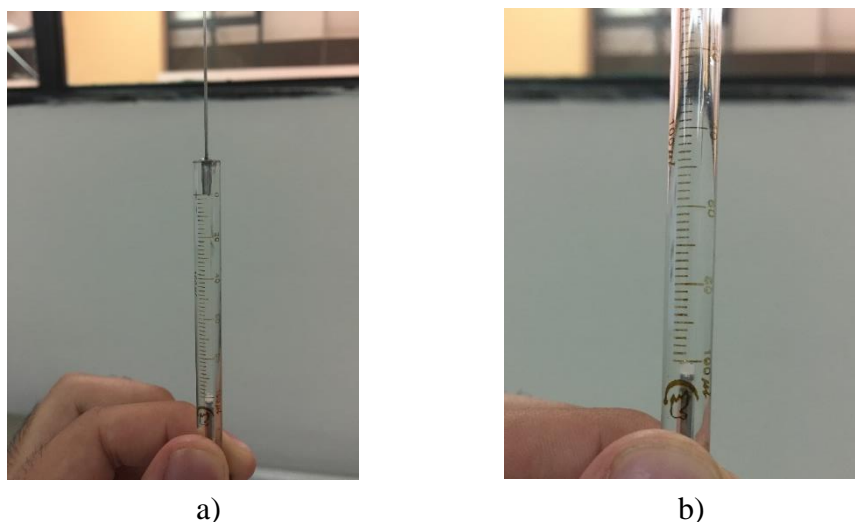
Figure 48. Preparation for the HPLC injection with the microsyringe. A volume of 100 μL was taken (a) making sure no air bubbles are present (b).

APPENDIX B: DETAILED METHODOLOGY FOR USING THE UV-VIS SPECTROMETER

Beforehand, the quartz cuvettes were carefully cleaned with selected wipe-paper making sure the frontal and rear sides did not have any contaminants that could interfere with absorbance readings. The inside of the cuvettes was then cleaned with distilled water to make sure any previous pollutants where expelled. The spectrograph was turned on and left for 5 minutes until the deuterium and tungsten lamp were calibrated and ready to use.

As the experimental samples had only water and caffeine, distilled water was used as the baseline reference. Once this baseline was selected, the first collected sample was transferred in the cuvette until the suggested mark. The cuvette was then positioned on the sample cell of the spectrograph following the corresponding instructions of the instrument. Consequently, the path length, resolution, and maximum absorbance were introduced in the software. To obtain the complete spectrum of the sample solution the wavelength range was selected between 200 nm and 600 nm. The spectrograph was left to run so that the software could record a specific absorbance for each wavelength. This way, a maximum absorbance for caffeine could be noticed at a specific wavelength. This position would then be used for quantifying data. Once the sample was analyzed and recorded, this solution was thrown away and the cuvette was cleaned. This procedure was repeated for every sample.

APPENDIX C: CALIBRATION CURVES DATA

Table 8. Caffeine Calibration Curve data for UV-VIS Spectroscopy (June 2017).

Concentration [ppm]	Absorbance			Average Absorbance	Standard Deviation
	1st Data	2nd Data	3rd Data		
0	0.000	0.000	0.000	0.000	0.000
5	0.254	0.253	0.254	0.254	0.001
15	0.760	0.761	0.760	0.760	0.001
30	1.461	1.459	1.462	1.461	0.002
50	2.460	2.461	2.463	2.461	0.002
60	2.765	2.767	2.765	2.766	0.001

Table 9. Caffeine Calibration Curve data for UV-VIS Spectroscopy (October 2017).

Concentration [ppm]	Absorbance			Average Absorbance	Standard Deviation
	1st Data	2nd Data	3rd Data		
0	0.000	0.000	0.000	0.000	0.000
5	0.251	0.249	0.251	0.250	0.001
15	0.758	0.757	0.754	0.756	0.002
30	1.411	1.402	1.404	1.406	0.005
50	2.405	2.411	2.394	2.403	0.009

Table 10. Data for the Calibration Curve of Caffeine using the Area Below its Characteristic Peak applying HPLC (June 2017).

ppm (caffeine)	Area Below Characteristic Peak				Standard Deviation
	Test 1	Test 2	Test 3	Average	
0	0.000	0.000	0.000	0.000	0.000
5	3.0175	2.6470	2.2266	2.6304	0.3231
10	4.8242	4.8918	4.8918	4.8693	0.0319
15	7.2564	6.9364	7.3294	7.1741	0.1707
30	15.0433	16.3337	16.2972	15.8914	0.5999
60	31.5364	29.4557	30.8892	30.6271	0.8694
100	50.6169	48.2298	50.2215	49.6894	1.0446

Table 11. Data for the Calibration Curve of Caffeine using the Area Below its Characteristic Peak applying HPLC (October 2017).

ppm (caffeine)	Area Below Characteristic Peak				Standard Deviation
	Test 1	Test 2	Test 3	Average	
0	0.000	0.000	0.000	0.000	0.000
5	3.0175	2.6470	2.2266	2.6304	0.3231
10	4.8242	4.8918	4.8918	4.8693	0.0319
15	7.2564	6.9364	7.3294	7.1741	0.1707
30	15.0433	16.3337	16.2972	15.8914	0.5999
60	31.5364	29.4557	30.8892	30.6271	0.8694
100	50.6169	48.2298	50.2215	49.6894	1.0446

Table 12. Data for the Calibration Curve of Caffeine using its Characteristic Peak Height (June 2017).

Caffeine concentration [ppm]	Height of Chacarcteristic Peak				Standard Deviation
	Test 1	Test 2	Test 3	Average	
0	0.000	0.000	0.000	0.000	0.000
5	0.109	0.097	0.094	0.100	0.008
10	0.191	0.194	0.194	0.193	0.002
15	0.299	0.292	0.287	0.293	0.006
30	0.530	0.570	0.554	0.551	0.020
60	1.101	1.131	1.054	1.095	0.039
100	1.776	1.833	1.850	1.820	0.039

Table 13. Data for the Calibration Curve of Caffeine using its Characteristic Peak Height (October 2017).

Caffeine concentration [ppm]	Height of Chacarcteristic Peak				Standard Deviation
	Test 1	Test 2	Test 3	Average	
0	0.000	0.000	0.000	0.000	0.000
5	0.098	0.093	0.096	0.096	0.003
10	0.198	0.192	0.195	0.195	0.003
15	0.299	0.292	0.296	0.296	0.004
30	0.571	0.549	0.561	0.560	0.011
60	1.064	1.052	1.059	1.058	0.006
100	1.711	1.696	1.703	1.703	0.008

APPENDIX D: MOST REPRESENTATIVE DATA USED FOR THE CONSTRUCTION OF CAFFEINE CONCENTRATION AS A FUNCTION OF TIME

Table 14. Caffeine concentration data as a function of time for different depth lengths using Activated Carbon as the filtering bed.

Range of time taken from samples [s]	Represented Time [s]	Caffeine Concentration [ppm]			
		L = 13 cm	L = 18 cm	L = 22 cm	L = 27 cm
0-15	7	31.96	26.23	20.10	16.29
15-30	22	43.94	41.73	36.85	37.07
50-70	60	47.46	46.14	44.01	42.67
110-130	120	48.25	47.29	46.27	43.81
170-180	180	48.45	47.99	46.90	44.67
230-250	240	48.63	48.17	46.96	45.35
290-310	300	48.69	48.57	47.36	45.42
350-370	360	48.82	48.78	47.87	45.50

Table- 15. Caffeine concentration data as a function of time for different depth lengths using Zeolite as the filtering bed.

Range of time taken from samples [s]	Represented Time [s]	Caffeine Concentration [ppm]			
		L = 13 cm	L = 18 cm	L = 23 cm	L = 26 cm
0-15	7	27.041	18.327	9.708	9.511
15-30	22	38.844	32.021	19.742	18.341
50-70	60	43.708	39.695	31.225	29.701
110-130	120	46.062	43.681	39.014	38.273
170-180	180	46.654	45.490	41.735	43.048
230-250	240	46.831	46.293	43.191	44.844
290-310	300	47.266	46.810	44.069	45.633
350-370	360	48.967	47.293	45.674	46.286

Table 16. Caffeine concentration data as a function of time for different depth lengths using Gravel as the filtering bed.

Range of time taken from samples [s]	Represented Time [s]	Caffeine Concentration [ppm]			
		L = 18 cm	L = 27 cm	L = 37 cm	L = 54 cm
0-15	7	31.09	19.01	12.28	4.71
15-30	22	44.76	38.78	30.16	19.59
50-70	60	47.48	45.43	41.95	36.58
110-130	120	47.92	47.31	44.93	43.29
170-180	180	48.58	47.15	46.90	44.93
230-250	240	47.50	47.96	46.44	46.13
290-310	300	49.35	48.57	46.93	46.44
350-370	360	49.46	48.78	48.60	46.63

Table 17. Caffeine concentration data as a function of time for different depth lengths using *Moringa oleifera* Lam. Husk as the filtering bed.

Range of time taken from samples [s]	Represented Time [s]	Caffeine Concentration [ppm]			
		L = 15 cm	L = 27 cm	L = 35 cm	L = 46 cm
0-15	7	25.10	13.71	6.92	6.01
15-30	22	39.75	33.18	27.65	23.37
50-70	60	45.04	42.80	39.58	37.18
110-130	120	46.94	45.91	44.35	41.96
170-180	180	47.57	46.92	45.72	43.27
230-250	240	47.89	47.33	46.52	44.37
290-310	300	48.11	47.65	47.07	45.97
350-370	360	48.14	47.74	47.47	46.48

APPENDIX E: MOST REPRESENTATIVE DATA USED FOR THE CONSTRUCTION OF CAFFEINE CONCENTRATION AS A FUNCTION OF DEPTH

Table 18. Caffeine concentration data as a function of depth for different operating times using Activated Carbon as the filtering bed.

Filter Depth [cm]	Caffeine Concentration [ppm]						
	t = 15 s	t = 30 s	t = 60 s	t = 120 s	t = 180s	t = 240 s	t = 300 s
13	31.96	43.94	47.46	48.12	48.45	48.63	48.69
18	26.23	41.73	46.14	47.86	47.99	48.17	48.57
22	20.10	36.85	44.01	45.98	46.90	46.96	47.36
27	16.29	37.07	42.67	43.54	44.67	45.35	45.42
0	49.85	49.85	49.85	49.85	49.85	49.85	49.85

Table 19. Caffeine concentration data as a function of depth for different operating times using Zeolite as the filtering bed.

Filter Depth [cm]	Caffeine concentration [ppm]						
	t = 15 s	t = 30 s	t = 60 s	t = 120 s	t = 180 s	t = 240 s	t = 300 s
13	27.04	38.84	43.71	46.06	46.65	46.83	47.27
18	18.33	32.02	39.69	43.68	45.49	46.29	46.81
23	9.71	19.74	31.23	39.01	41.74	43.19	44.07
26	9.51	18.34	29.70	38.27	43.05	44.84	45.63
0	49.85	49.85	49.85	49.85	49.85	49.85	49.85

Table 20. Caffeine concentration data as a function of depth for different operating times using Gravel as the filtering bed.

Filter Depth [cm]	Caffeine Concentration [ppm]						
	t = 15 s	t = 30 s	t = 60 s	t = 120 s	t = 180s	t = 240 s	t = 300 s
18	31.09	44.76	47.48	47.92	48.58	47.50	49.35
27	19.01	38.78	45.43	47.92	47.15	47.96	48.57
37	12.28	30.16	38.78	47.48	46.90	46.44	46.93
54	4.71	19.59	36.58	43.29	44.93	46.13	46.44
0	49.85	49.85	49.85	49.85	49.85	49.85	49.85

APPENDIX F: DATA FOR THE STANDARDIZATION OF THE MASS OF THE DIFFERENT FILTERING BEDS WITH RESPECT TO THEIR COLUMN DEPTH

Table 21. Corresponding mass of Activated Carbon with respect to its filter depth in the column.

Length [cm]	Mass [g]				Standard Deviation
	Test 1	Test 2	Test 3	Average	
0.0	0.0000	0.0000	0.0000	0.0000	0.0000
1.0	0.4693	0.4500	0.4724	0.4639	0.0121
3.2	1.3765	1.3664	1.3822	1.3750	0.0080
5.5	2.1739	2.2024	2.1572	2.1778	0.0229
11.5	4.8652	4.8300	4.8432	4.8366	0.0178
15.0	6.3915	6.3400	6.4378	6.3898	0.0489
18.0	7.6780	7.9256	7.3278	7.6438	0.3004
21.5	9.5271	8.7162	9.1660	8.9411	0.4063
30.0	12.8662	12.7200	14.0000	13.1954	0.7006

Table 22. Corresponding mass of Zeolite with respect to its filter depth in the column.

Length [cm]	Mass [g]				Standard Deviation
	Test 1	Test 2	Test 3	Average	
0.0	0.0000	0.0000	0.0000	0.0000	0.0000
1.0	0.8213	0.8611	0.8721	0.8515	0.0267
3.5	2.6964	2.6621	2.7652	2.7079	0.0525
5.0	3.6398	3.5175	3.8923	3.6832	0.1911
9.5	7.2645	7.5706	7.6352	7.4901	0.1980
13.0	9.8462	11.4932	11.4212	10.9202	0.9308
17.5	12.5242	12.6287	14.1231	13.0920	0.8945
20.5	15.1121	16.5771	17.0293	16.2395	1.0022
27.0	21.8909	22.5042	24.7672	23.0541	1.5149

Table 23. Corresponding mass of *Moringa oleifera* Husk with respect to its filter depth in the column.

Length [cm]	Mass [g]				Standard Deviation
	Test 1	Test 2	Test 3	Average	
0	0.0000	0.0000	0.0000	0.0000	0.0000
1.8	0.1029	0.1182	0.1452	0.1221	0.0214
4	0.2773	0.2187	0.2987	0.2649	0.0414
6.5	0.3676	0.3017	0.4215	0.3636	0.0600
9	0.5954	0.5762	0.6872	0.6196	0.0593
14	0.8906	0.9762	1.1869	1.0179	0.1525
19	1.5256	1.2342	1.6721	1.4773	0.2229
27	1.9687	1.8021	2.1242	1.9650	0.1611

Table 24. Corresponding mass of Gravel with respect to its filter depth in the column.

Length [cm]	Mass [g]				Standard Deviation
	Test 1	Test 2	Test 3	Average	
0.0	0.0000	0.0000	0.0000	0.0000	0.0000
1.3	1.0537	1.0627	0.9982	1.0382	0.0349
4.0	2.8437	3.1263	2.9790	2.9830	0.1413
6.0	4.6964	4.7981	4.4726	4.6557	0.1665
9.0	6.8772	7.2142	6.9851	7.0255	0.1721
15.5	12.0091	12.2765	12.0912	12.1256	0.1370
19.0	15.9752	16.3111	15.4821	15.9228	0.4170
25.0	20.8801	21.4921	20.9971	21.1231	0.3249
31.0	26.7231	27.4765	26.8712	27.0236	0.3992
38.5	32.8835	33.0121	31.8921	32.5959	0.6129

APPENDIX G:

HPLC CHROMATOGRAMS FOR THE CALIBRATION CURVE OF CAFFEINE
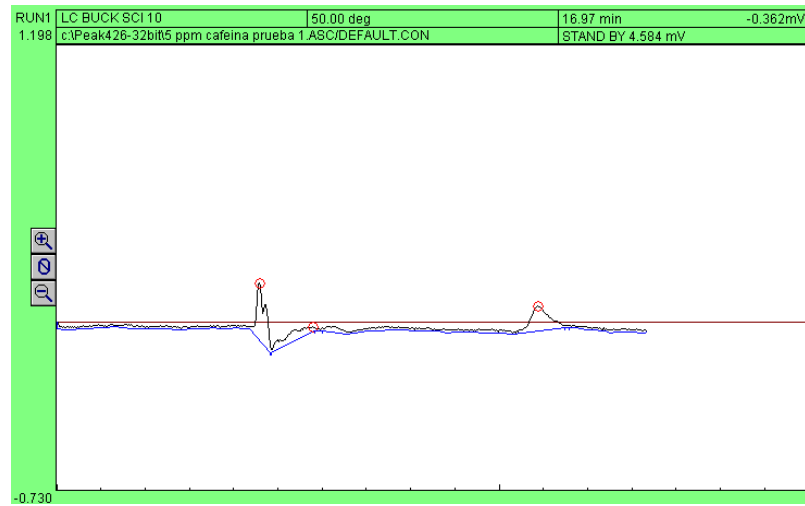
a)
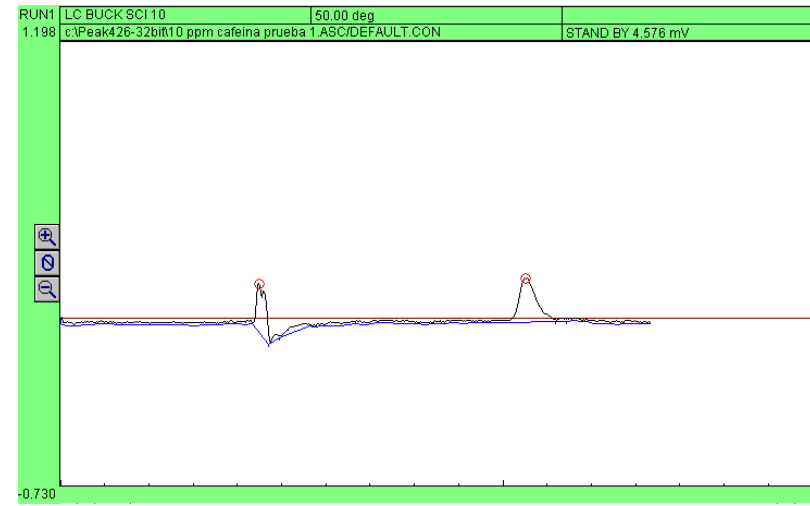
b)

Figure 49. HPLC Chromatograms used for the Calibration Curves of caffeine applying the area below the characteristic peak, and the peak's height. a) 5 ppm b) 10 ppm c) 15 ppm d) 30 ppm e) 50 ppm f) 60 ppm.
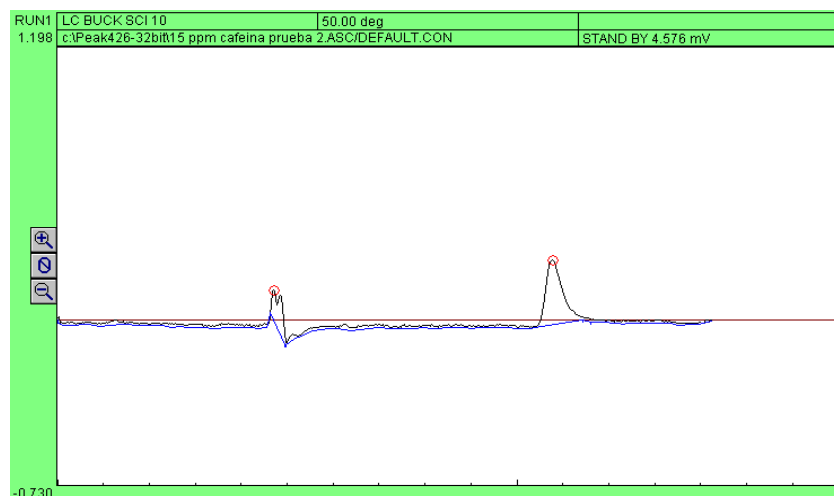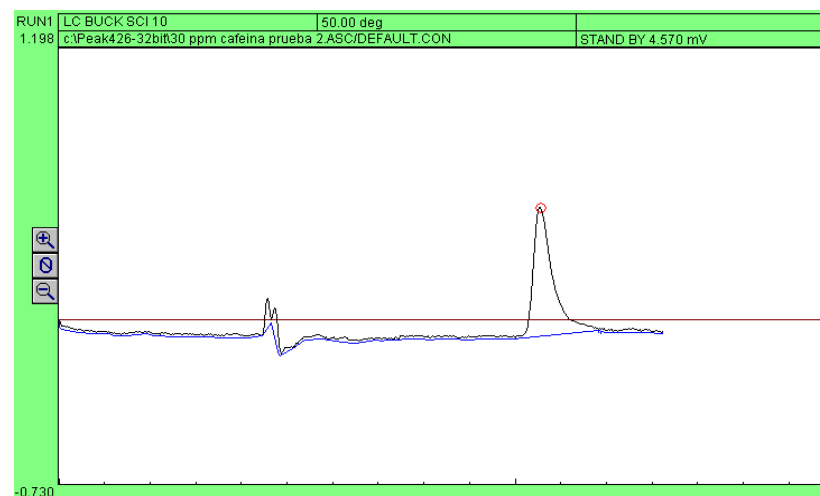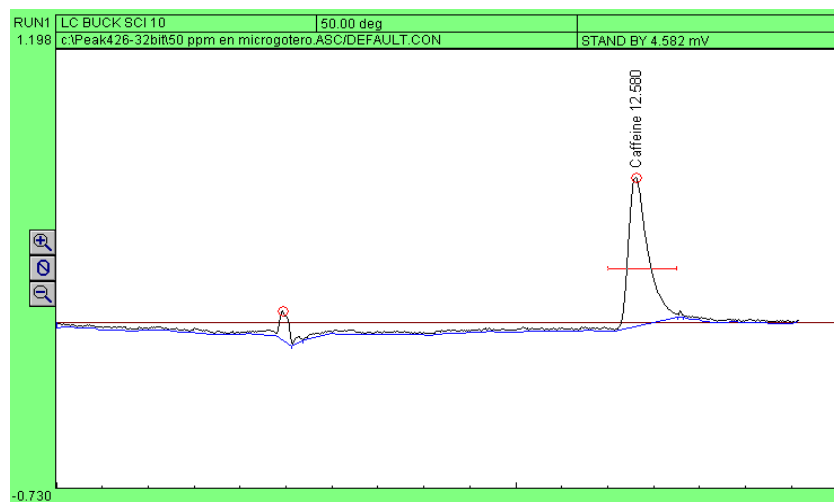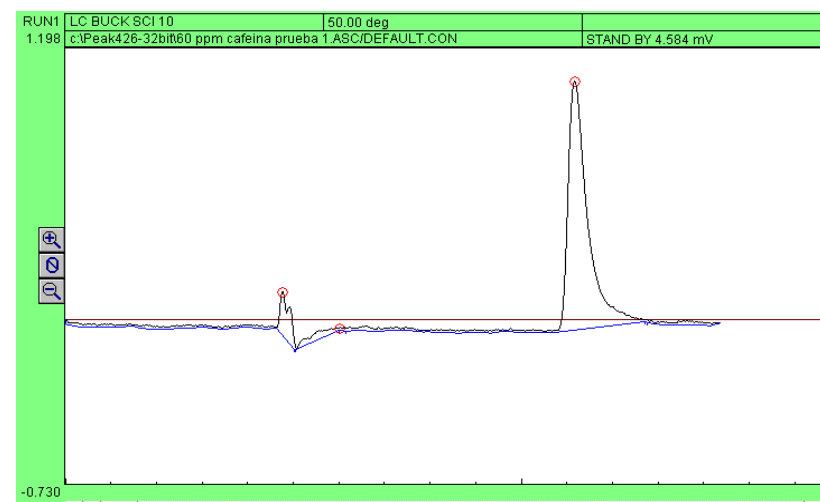
Figure 49. *(Continued)* HPLC Chromatograms used for the Calibration Curves of caffeine applying the area below the characteristic peak, and the peak's height. a) 5 ppm b) 10 ppm c) 15 ppm d) 30 ppm e) 50 ppm f) 60 ppm.

APPENDIX H:

CHARACTERIZATION OF FILTERING BEDS: MASS OF THE FILTERING MEDIUM AS A FUNCTION OF ITS FILTER DEPTH IN THE COLUMN
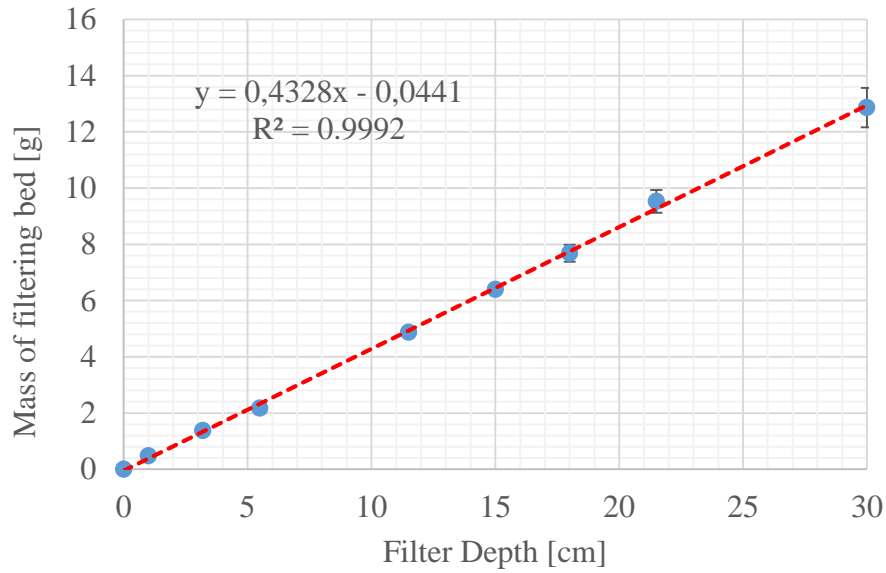
Figure 53. Mass of Activated Carbon as a function of its filtering depth in the column.
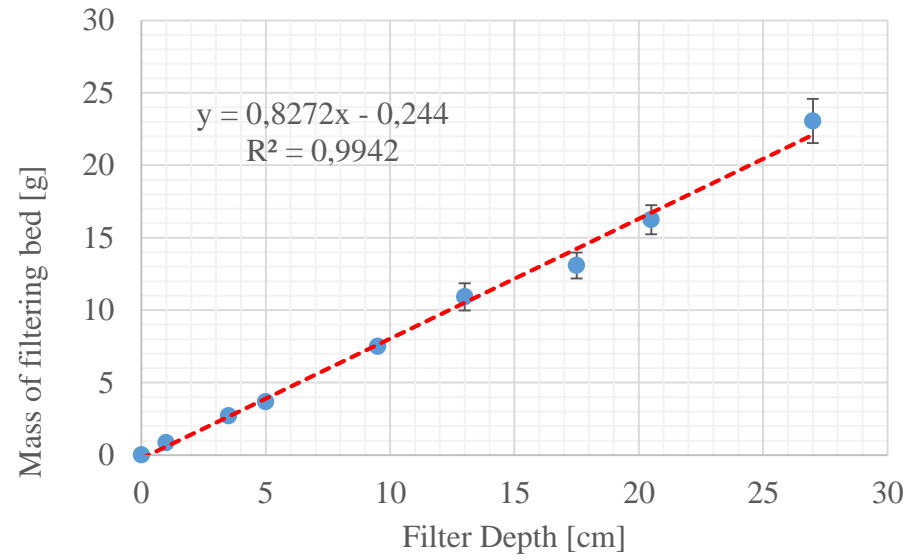
Figure 52. Mass of Zeolite as a function of its filtering depth in the column.
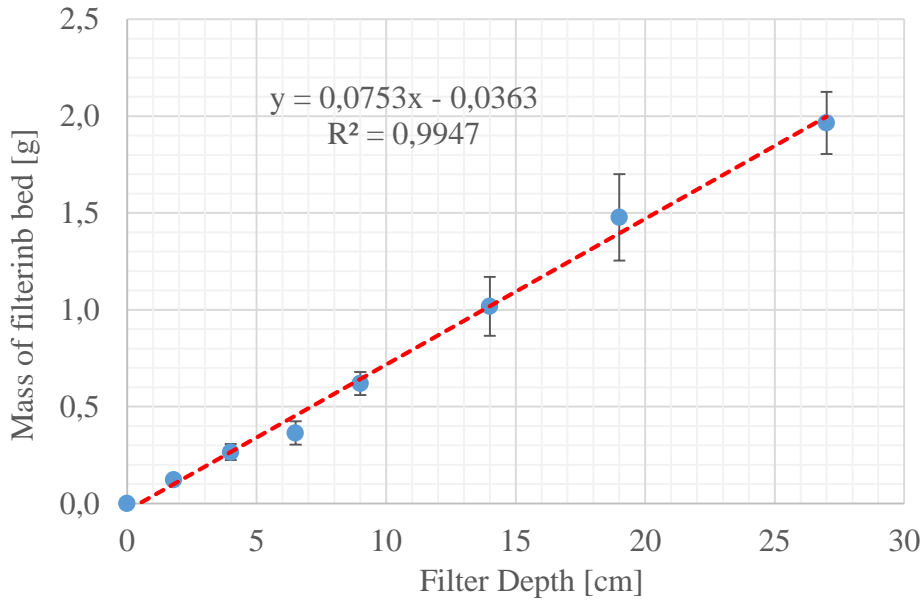
Figure 51. Mass of *Moringa oleifera* Husk as a function of its filtering depth in the column.
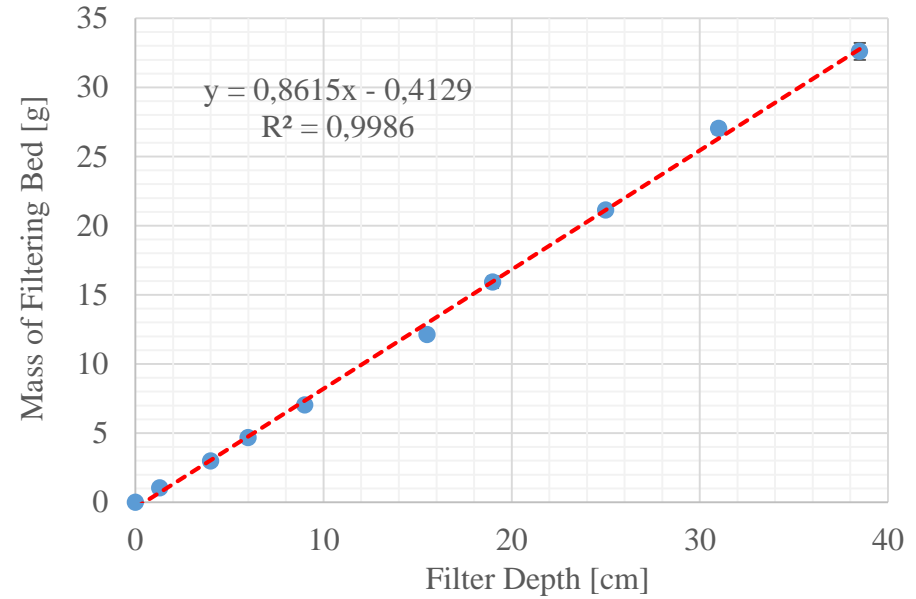
Figure 50. Mass of Gravel as a function of its filtering depth in the column.

APPENDIX I:

CONCENTRATION OF THE DIFFERENT FILTERING BEDS (ACTIVATED CARBON, ZEOLITE, GRAVEL, AND *Moringa oleifera* HUSK) AS A FUNCTION OF TIME

Table 25. Caffeine concentration as a function of time using Activated Carbon as the filtering bed with a depth of 27 cm.

Range of time taken from samples [s]	Represented Time [s]	Absorbance				% Standard Deviation	Concentration [ppm]	Absolute Uncertainty	C/C0	Absolute Uncertainty
		Test 1	Test 2	Test 3	Average					
0-15	7	0.843	0.743	0.831	0.806	6.78	16.29	1.104	0.327	0.0222
15-30	22	1.640	1.954	1.877	1.824	8.97	37.07	3.326	0.744	0.0667
50-70	60	2.003	2.159	2.132	2.098	3.97	42.67	1.696	0.856	0.0340
110-130	120	2.12	2.198	2.144	2.154	1.85	43.81	0.813	0.879	0.0163
170-180	180	2.177	2.213	2.199	2.196	0.83	44.67	0.369	0.896	0.0074
230-250	240	2.175	2.27	2.243	2.229	2.20	45.35	0.996	0.910	0.0200
290-310	300	2.227	2.235	2.236	2.233	0.22	45.42	0.100	0.911	0.0020
350-370	360	2.231	2.239	2.241	2.237	0.24	45.50	0.108	0.913	0.0022

Table 26. Caffeine concentration as a function of time using Activated Carbon as the filtering bed with a depth of 22 cm.

Range of time taken from samples [s]	Represented Time [s]	Absorbance				% Standard Deviation	Concentration [ppm]	Absolute Uncertainty	C/C0	Absolute Uncertainty
		Test 1	Test 2	Test 3	Average					
0-15	7	1.037	1.041	0.899	0.992	8.148	20.10	1.638	0.403	0.0329
15-30	22	1.864	1.809	1.766	1.813	2.709	36.85	0.998	0.739	0.0200
50-70	60	2.179	2.169	2.143	2.164	0.859	44.01	0.378	0.883	0.0076
110-130	120	2.272	2.270	2.281	2.274	0.258	46.27	0.119	0.928	0.0024
170-180	180	2.307	2.305	2.304	2.305	0.066	46.90	0.031	0.941	0.0006
230-250	240	2.301	2.317	2.307	2.308	0.350	46.96	0.164	0.942	0.0033
290-310	300	2.322	2.333	2.329	2.328	0.239	47.36	0.113	0.950	0.0023
350-370	360	2.352	2.351	2.356	2.353	0.112	47.87	0.054	0.960	0.0011

Table 27. Caffeine concentration as a function of time using Activated Carbon as the filtering bed with a depth of 18 cm.

Range of time taken from samples [s]	Represented Time [s]	Absorbance				% Standard Deviation	Concentration [ppm]	Absolute Uncertainty	C/C0	Absolute Uncertainty
		Test 1	Test 2	Test 3	Average					
0-15	7	1.310	1.200	1.367	1.292	6.568	26.23	1.723	0.526	0.03456
15-30	22	2.071	2.001	2.084	2.052	2.175	41.73	0.908	0.837	0.01821
50-70	60	2.252	2.261	2.291	2.268	0.900	46.14	0.415	0.925	0.00833
110-130	120	2.323	2.322	2.329	2.325	0.162	47.29	0.077	0.949	0.00155
170-180	180	2.362	2.351	2.364	2.359	0.296	47.99	0.142	0.963	0.00286
230-250	240	2.362	2.37	2.371	2.368	0.208	48.17	0.100	0.966	0.00201
290-310	300	2.383	2.388	2.39	2.387	0.151	48.57	0.073	0.974	0.00147
350-370	360	2.389	2.401	2.402	2.397	0.301	48.78	0.147	0.978	0.00295

Table 28. Caffeine concentration as a function of time using Activated Carbon as the filtering bed with a depth of 13 cm.

Range of time taken from samples [s]	Represented Time [s]	Absorbance				% Standard Deviation	Concentration [ppm]	Absolute Uncertainty	C/C0	Absolute Uncertainty
		Test 1	Test 2	Test 3	Average					
0-15	7	1.573	1.569	1.578	1.573	0.286	31.96	0.092	0.641	0.00184
15-30	22	2.159	2.158	2.164	2.160	0.148	43.94	0.065	0.881	0.00131
50-70	60	2.329	2.333	2.337	2.333	0.171	47.46	0.081	0.952	0.00163
110-130	120	2.368	2.371	2.375	2.371	0.148	48.25	0.071	0.968	0.00143
170-180	180	2.381	2.379	2.384	2.381	0.105	48.45	0.051	0.972	0.00103
230-250	240	2.388	2.39	2.392	2.390	0.083	48.63	0.041	0.975	0.00082
290-310	300	2.391	2.394	2.395	2.393	0.086	48.69	0.042	0.977	0.00085
350-370	360	2.397	2.401	2.401	2.400	0.096	48.82	0.047	0.979	0.00094

Table 29. Caffeine concentration as a function of time using Zeolite as the filtering bed with a depth of 26 cm.

Range of time taken from samples [s]	Represented Time [s]	Absorbance				% Standard Deviation	Concentration [ppm]	Absolute Uncertainty	C/C0	Absolute Uncertainty
		Test 1	Test 2	Test 3	Average					
0-15	7	0.491	0.474	0.455	0.473	3.805	9.511	0.362	0.191	0.00726
15-30	22	0.934	0.908	0.876	0.906	3.207	18.341	0.588	0.368	0.01180
50-70	60	1.471	1.461	1.456	1.463	0.522	29.701	0.155	0.596	0.00311
110-130	120	1.891	1.883	1.874	1.883	0.452	38.273	0.173	0.768	0.00347
170-180	180	2.121	2.118	2.111	2.117	0.242	43.048	0.104	0.864	0.00209
230-250	240	2.223	2.202	2.189	2.205	0.778	44.844	0.349	0.900	0.00700
290-310	300	2.251	2.243	2.236	2.243	0.335	45.633	0.153	0.915	0.00306
350-370	360	2.283	2.277	2.266	2.275	0.379	46.286	0.175	0.928	0.00352

Table 30. Caffeine concentration as a function of time using Zeolite as the filtering bed with a depth of 23 cm.

Range of time taken from samples [s]	Represented Time [s]	Absorbance				% Standard Deviation	Concentration [ppm]	Absolute Uncertainty	C/C0	Absolute Uncertainty
		Test 1	Test 2	Test 3	Average					
0-15	7	0.398	0.561	0.49	0.483	16.920	9.708	1.643	0.195	0.03295
15-30	22	0.951	1.002	0.971	0.975	2.636	19.742	0.520	0.396	0.01044
50-70	60	1.529	1.545	1.538	1.537	0.522	31.225	0.163	0.626	0.00327
110-130	120	1.901	1.943	1.913	1.919	1.127	39.014	0.440	0.783	0.00882
170-180	180	2.041	2.066	2.05	2.052	0.617	41.735	0.257	0.837	0.00517
230-250	240	2.108	2.138	2.125	2.124	0.708	43.191	0.306	0.866	0.00614
290-310	300	2.153	2.182	2.165	2.167	0.673	44.069	0.296	0.884	0.00595
350-370	360	2.231	2.253	2.252	2.245	0.553	45.674	0.253	0.916	0.00507

Table 31. Caffeine concentration as a function of time using Zeolite as the filtering bed with a depth of 18 cm.

Range of time taken from samples [s]	Represented Time [s]	Absorbance				% Standard Deviation	Concentration [ppm]	Absolute Uncertainty	C/C0	Absolute Uncertainty
		Test 1	Test 2	Test 3	Average					
0-15	7	0.907	0.921	0.888	0.905	1.829	18.327	0.335	0.368	0.00673
15-30	22	1.576	1.584	1.569	1.576	0.476	32.021	0.152	0.642	0.00306
50-70	60	1.951	1.962	1.944	1.952	0.465	39.695	0.184	0.796	0.00370
110-130	120	2.149	2.155	2.139	2.148	0.376	43.681	0.164	0.876	0.00330
170-180	180	2.238	2.242	2.229	2.236	0.298	45.490	0.135	0.913	0.00272
230-250	240	2.275	2.281	2.271	2.276	0.221	46.293	0.102	0.929	0.00205
290-310	300	2.29	2.322	2.291	2.301	0.791	46.810	0.370	0.939	0.00742
350-370	360	2.326	2.327	2.321	2.325	0.138	47.293	0.065	0.949	0.00131

Table 32. Caffeine concentration as a function of time using Zeolite as the filtering bed with a depth of 13 cm.

Range of time taken from samples [s]	Represented Time [s]	Absorbance				% Standard Deviation	Concentration [ppm]	Absolute Uncertainty	C/C0	Absolute Uncertainty
		Test 1	Test 2	Test 3	Average					
0-15	7	1.281	1.314	1.402	1.332	4.695	27.041	1.270	0.542	0.02547
15-30	22	1.897	1.911	1.924	1.911	0.707	38.844	0.275	0.779	0.00551
50-70	60	2.097	2.165	2.185	2.149	2.147	43.708	0.938	0.877	0.01882
110-130	120	2.255	2.262	2.276	2.264	0.472	46.062	0.218	0.924	0.00436
170-180	180	2.286	2.293	2.301	2.293	0.327	46.654	0.153	0.936	0.00306
230-250	240	2.291	2.301	2.314	2.302	0.501	46.831	0.235	0.939	0.00471
290-310	300	2.317	2.323	2.33	2.323	0.280	47.266	0.132	0.948	0.00266
350-370	360	2.401	2.408	2.411	2.407	0.213	48.967	0.104	0.982	0.00209

Table 33. Caffeine concentration as a function of time using Gravel as the filtering bed with a depth of 54 cm.

Range of time taken from samples [s]	Represented Time [s]	Absorbance				% Standard Deviation	Concentration [ppm]	Absolute Uncertainty	C/C0	Absolute Uncertainty
		Test 1	Test 2	Test 3	Average					
0-15	7	0.233	0.276	0.205	0.238	15.027	4.708	0.707	0.094	0.01419
15-30	22	0.962	0.988	0.951	0.967	1.965	19.586	0.385	0.393	0.00772
50-70	60	1.799	1.803	1.797	1.800	0.170	36.579	0.062	0.734	0.00125
110-130	120	2.127	2.134	2.124	2.128	0.241	43.286	0.104	0.868	0.00209
170-180	180	2.208	2.212	2.206	2.209	0.138	44.926	0.062	0.901	0.00125
230-250	240	2.267	2.271	2.265	2.268	0.135	46.130	0.062	0.925	0.00125
290-310	300	2.282	2.285	2.281	2.283	0.091	46.436	0.042	0.931	0.00085
350-370	360	2.292	2.296	2.289	2.292	0.153	46.633	0.071	0.935	0.00143

Table 34. Caffeine concentration as a function of time using Gravel as the filtering bed with a depth of 37 cm.

Range of time taken from samples [s]	Represented Time [s]	Absorbance				% Standard Deviation	Concentration [ppm]	Absolute Uncertainty	C/C0	Absolute Uncertainty
		Test 1	Test 2	Test 3	Average					
0-15	7	0.616	0.522	0.689	0.609	13.747	12.280	1.688	0.246	0.03386
15-30	22	1.488	1.475	1.492	1.485	0.599	30.157	0.181	0.605	0.00362
50-70	60	2.085	2.003	2.101	2.063	2.548	41.953	1.069	0.842	0.02145
110-130	120	2.213	2.189	2.225	2.209	0.830	44.933	0.373	0.901	0.00748
170-180	180	2.309	2.294	2.313	2.305	0.434	46.899	0.204	0.941	0.00409
230-250	240	2.282	2.277	2.289	2.283	0.264	46.436	0.123	0.931	0.00246
290-310	300	2.309	2.300	2.311	2.307	0.254	46.926	0.119	0.941	0.00239
350-370	360	2.389	2.386	2.391	2.389	0.105	48.599	0.051	0.975	0.00103

Table 35. Caffeine concentration as a function of time using Gravel as the filtering bed with a depth of 27 cm.

Range of time taken from samples [s]	Represented Time [s]	Absorbance				% Standard Deviation	Concentration [ppm]	Absolute Uncertainty	C/C0	Absolute Uncertainty
		Test 1	Test 2	Test 3	Average					
0-15	7	0.899	0.941	0.976	0.939	4.107	19.007	0.781	0.381	0.01566
15-30	22	1.882	1.895	1.945	1.907	1.744	38.776	0.676	0.778	0.01356
50-70	60	2.221	2.236	2.243	2.233	0.503	45.429	0.229	0.911	0.00459
110-130	120	2.315	2.323	2.338	2.325	0.502	47.307	0.238	0.949	0.00477
170-180	180	2.309	2.318	2.326	2.318	0.367	47.150	0.173	0.946	0.00347
230-250	240	2.348	2.356	2.368	2.357	0.427	47.960	0.205	0.962	0.00411
290-310	300	2.376	2.388	2.397	2.387	0.441	48.565	0.214	0.974	0.00430
350-370	360	2.391	2.399	2.402	2.397	0.237	48.776	0.116	0.978	0.00232

Table 36. Caffeine concentration as a function of time using Gravel as the filtering bed with a depth of 18 cm.

Range of time taken from samples [s]	Represented Time [s]	Absorbance				% Standard Deviation	Concentration [ppm]	Absolute Uncertainty	C/C0	Absolute Uncertainty
		Test 1	Test 2	Test 3	Average					
0-15	7	1.536	1.505	1.551	1.531	1.533	31.089	0.476	0.624	0.00956
15-30	22	2.200	2.189	2.212	2.200	0.523	44.756	0.234	0.898	0.00469
50-70	60	2.335	2.318	2.349	2.334	0.665	47.484	0.316	0.953	0.00634
110-130	120	2.353	2.344	2.369	2.355	0.538	47.919	0.258	0.961	0.00517
170-180	180	2.388	2.377	2.398	2.388	0.440	48.579	0.214	0.974	0.00429
230-250	240	2.339	2.322	2.343	2.335	0.478	47.497	0.227	0.953	0.00455
290-310	300	2.426	2.421	2.429	2.425	0.167	49.348	0.082	0.990	0.00165
350-370	360	2.431	2.428	2.434	2.431	0.123	49.463	0.061	0.992	0.00122

Table 37. Caffeine concentration as a function of time using *Moringa oleifera* Lam. Husk as the filtering bed with a depth of 46 cm.

Range of time taken from samples [s]	Represented Time [s]	Absorbance				% Standard Deviation	Concentration [ppm]	Absolute Uncertainty	C/C0	Absolute Uncertainty
		Test 1	Test 2	Test 3	Average					
0-15	7	0.224	0.381	0.301	0.302	25.995	6.014	1.563	0.121	0.0314
15-30	22	1.010	1.340	1.107	1.152	14.719	23.368	3.439	0.469	0.0690
50-70	60	1.749	1.843	1.896	1.829	4.070	37.184	1.513	0.746	0.0304
110-130	120	2.008	2.043	2.139	2.063	3.287	41.960	1.379	0.842	0.0277
170-180	180	2.069	2.117	2.196	2.127	3.014	43.266	1.304	0.868	0.0262
230-250	240	2.152	2.136	2.256	2.181	2.987	44.368	1.325	0.890	0.0266
290-310	300	2.230	2..211	2.290	2.260	1.877	45.973	0.863	0.922	0.0173
350-370	360	2.250	2.270	2.334	2.285	1.921	46.477	0.893	0.932	0.0179

Table 38. Caffeine concentration as a function of time using *Moringa oleifera* Lam. Husk as the filtering bed with a depth of 35 cm.

Range of time taken from samples [s]	Represented Time [s]	Absorbance				% Standard Deviation	Concentration [ppm]	Absolute Uncertainty	C/C0	Absolute Uncertainty
		Test 1	Test 2	Test 3	Average					
0-15	7	0.349	0.281	0.409	0.346	18.491	6.919	1.279	0.139	0.0257
15-30	22	1.366	1.332	1.388	1.362	2.071	27.647	0.573	0.555	0.0115
50-70	60	1.949	1.850	2.041	1.947	4.907	39.579	1.942	0.794	0.0390
110-130	120	2.181	2.159	2.201	2.180	0.964	44.348	0.427	0.890	0.0086
170-180	180	2.249	2.233	2.261	2.248	0.625	45.722	0.286	0.917	0.0057
230-250	240	2.285	2.282	2.293	2.287	0.249	46.518	0.116	0.933	0.0023
290-310	300	2.313	2.304	2.324	2.314	0.433	47.069	0.204	0.944	0.0041
350-370	360	2.333	2.328	2.339	2.333	0.236	47.470	0.112	0.952	0.0022

Table 39. Caffeine concentration as a function of time using *Moringa oleifera* Lam. Husk as the filtering bed with a depth of 27 cm

Range of time taken from samples [s]	Represented Time [s]	Absorbance				% Standard Deviation	Concentration [ppm]	Absolute Uncertainty	C/C0	Absolute Uncertainty
		Test 1	Test 2	Test 3	Average					
0-15	7	0.405	0.678	0.955	0.679	40.481	13.715	5.552	0.275	0.1114
15-30	22	1.517	1.632	1.751	1.633	7.164	33.184	2.377	0.666	0.0477
50-70	60	2.031	2.104	2.179	2.105	3.516	42.803	1.505	0.859	0.0302
110-130	120	2.231	2.256	2.284	2.257	1.175	45.912	0.539	0.921	0.0108
170-180	180	2.299	2.305	2.315	2.306	0.350	46.919	0.164	0.941	0.0033
230-250	240	2.311	2.326	2.342	2.326	0.666	47.327	0.315	0.949	0.0063
290-310	300	2.336	2.341	2.35	2.342	0.303	47.654	0.144	0.956	0.0029
350-370	360	2.339	2.345	2.355	2.346	0.344	47.735	0.164	0.958	0.0033

Table 40. Caffeine concentration as a function of time using *Moringa oleifera* Lam. Husk as the filtering bed with a depth of 15 cm

Range of time taken from samples [s]	Represented Time [s]	Absorbance				% Standard Deviation	Concentration [ppm]	Absolute Uncertainty	C/C0	Absolute Uncertainty
		Test 1	Test 2	Test 3	Average					
0-15	7	1.361	1.114	1.236	1.237	9.984	25.096	2.506	0.503	0.0503
15-30	22	2.004	1.882	1.979	1.955	3.296	39.749	1.310	0.797	0.0263
50-70	60	2.321	2.107	2.215	2.214	4.832	45.041	2.177	0.904	0.0437
110-130	120	2.338	2.278	2.306	2.307	1.301	46.939	0.611	0.942	0.0123
170-180	180	2.366	2.311	2.337	2.338	1.177	47.565	0.560	0.954	0.0112
230-250	240	2.368	2.342	2.351	2.354	0.561	47.885	0.269	0.961	0.0054
290-310	300	2.371	2.359	2.364	2.365	0.255	48.110	0.123	0.965	0.0025
350-370	360	2.372	2.361	2.365	2.366	0.235	48.137	0.113	0.966	0.0023

APPENDIX J:
CONCENTRATION OF THE DIFFERENT FILTERING BEDS (ACTIVATED CARBON, ZEOLITE, GRAVEL, AND *Moringa oleifera* HUSK) AS A FUNCTION OF DEPTH

Table 41. Caffeine concentration as a function of depth using Activated Carbon as filtering bed at an operation time of 15 seconds.

Filter Depth [cm]	Absorbance				% Standard Deviation	Concentration [ppm]	Absolute Uncertainty	C/C0	Absolute Uncertainty
	Test 1	Test 2	Test 3	Average					
13	1.573	1.569	1.578	1.573	0.2866	31.9599	0.0916	0.6411	0.001837
18	1.31	1.2	1.367	1.292	6.5687	26.2252	1.7227	0.5261	0.034556
22	1.037	1.041	0.899	0.992	8.1478	20.1027	1.6379	0.4033	0.032857
27	0.843	0.743	0.831	0.806	6.7772	16.2932	1.1042	0.3268	0.022150
0	2.450	2.450	2.450	2.450	0.0000	49.8510	0.0000	1.0000	0.000000

Table 42. Caffeine concentration as a function of depth using Activated Carbon as filtering bed at an operation time of 30 seconds.

Filter Depth [cm]	Absorbance				% Standard Deviation	Concentration [ppm]	Absolute Uncertainty	C/C0	Absolute Uncertainty
	Test 1	Test 2	Test 3	Average					
13	2.159	2.158	2.164	2.160	0.1488	43.9395	0.0654	0.8814	0.001312
18	2.071	2.001	2.084	2.052	2.1756	41.7286	0.9078	0.8371	0.018211
22.5	1.864	1.809	1.766	1.813	2.7094	36.8510	0.9985	0.7392	0.020029
27	1.64	1.954	1.877	1.824	8.9738	37.0687	3.3265	0.7436	0.066729
0	2.450	2.450	2.450	2.450	0.0000	49.8510	0.0000	1.0000	0.000000

Table 43. Caffeine concentration as a function of depth using Activated Carbon as filtering bed at an operation time of 1 min.

Filter Depth [cm]	Absorbance				% Standard Deviation	Concentration [ppm]	Absolute Uncertainty	C/C0	Absolute Uncertainty
	Test 1	Test 2	Test 3	Average					
13	2.329	2.333	2.337	2.333	0.1715	47.4633	0.0814	0.9521	0.001632
18	2.252	2.261	2.291	2.268	0.9004	46.1367	0.4154	0.9255	0.008333
22.5	2.179	2.169	2.143	2.164	0.8589	44.0075	0.3780	0.8828	0.007582
27	2.003	2.159	2.132	2.098	3.9739	42.6673	1.6956	0.8559	0.034013
0	2.450	2.450	2.450	2.450	0.0000	49.8510	0.0000	1.0000	0.000000

Table 44. Caffeine concentration as a function of depth using Activated Carbon as filtering bed at an operation time of 2 min.

Filter Depth [cm]	Absorbance				% Standard Deviation	Concentration [ppm]	Absolute Uncertainty	C/C0	Absolute Uncertainty
	Test 1	Test 2	Test 3	Average					
13	2.381	2.379	2.384	2.381	0.1057	48.4497	0.0512	0.9719	0.001027
18	2.362	2.351	2.364	2.359	0.2967	47.9939	0.1424	0.9627	0.002857
22.5	2.307	2.305	2.304	2.305	0.0663	46.8986	0.0311	0.9408	0.000623
27	2.177	2.213	2.199	2.196	0.8263	44.6741	0.3691	0.8962	0.007405
0	2.450	2.450	2.450	2.450	0.0000	49.8510	0.0000	1.0000	0.000000

Table 45. Caffeine concentration as a function of depth using Activated Carbon as filtering bed at an operation time of 3 min.

Filter Depth [cm]	Absorbance				% Standard Deviation	Concentration [ppm]	Absolute Uncertainty	C/C0	Absolute Uncertainty
	Test 1	Test 2	Test 3	Average					
13	2.381	2.379	2.384	2.381	0.1057	48.4497	0.0512	0.9719	0.001027
18	2.362	2.351	2.364	2.359	0.2967	47.9939	0.1424	0.9627	0.002857
22.5	2.307	2.305	2.304	2.305	0.0663	46.8986	0.0311	0.9408	0.000623
27	2.177	2.213	2.199	2.196	0.8263	44.6741	0.3691	0.8962	0.007405
0	2.450	2.450	2.450	2.450	0.0000	49.8510	0.0000	1.0000	0.000000

Table 46. Caffeine concentration as a function of depth using Activated Carbon as filtering bed at an operation time of 4 min.

Filter Depth [cm]	Absorbance				% Standard Deviation	Concentration [ppm]	Absolute Uncertainty	C/C0	Absolute Uncertainty
	Test 1	Test 2	Test 3	Average					
13	2.388	2.39	2.392	2.390	0.0837	48.6265	0.0407	0.9754	0.000816
18	2.362	2.37	2.371	2.368	0.2083	48.1707	0.1004	0.9663	0.002013
22.5	2.301	2.317	2.307	2.308	0.3502	46.9599	0.1644	0.9420	0.003299
27	2.175	2.27	2.243	2.229	2.1958	45.3476	0.9958	0.9097	0.019975
0	2.450	2.450	2.450	2.450	0.0000	49.8510	0.0000	1.0000	0.000000

Table 47. Caffeine concentration as a function of depth using Activated Carbon as filtering bed at an operation time of 5 min.

Filter Depth [cm]	Absorbance				% Standard Deviation	Concentration [ppm]	Absolute Uncertainty	C/C0	Absolute Uncertainty
	Test 1	Test 2	Test 3	Average					
13	2.391	2.394	2.395	2.393	0.0870	48.6946	0.0424	0.9768	0.000850
18	2.383	2.388	2.39	2.387	0.1510	48.5653	0.0734	0.9742	0.001472
22.5	2.322	2.333	2.329	2.328	0.2392	47.3612	0.1133	0.9501	0.002272
27	2.227	2.235	2.236	2.233	0.2209	45.4156	0.1003	0.9110	0.002013
0	2.450	2.450	2.450	2.450	0.0000	49.8510	0.0000	1.0000	0.000000

Table 48. Caffeine concentration as a function of depth using Zeolite as filtering bed at an operation time of 15 seconds.

Filter Depth [cm]	Absorbance				% Standard Deviation	Concentration [ppm]	Absolute Uncertainty	C/C0	Absolute Uncertainty
	Test 1	Test 2	Test 3	Average					
13	1.281	1.314	1.402	1.332	4.695	27.041	1.270	0.542	0.02547
18	0.907	0.921	0.888	0.905	1.829	18.327	0.335	0.368	0.00673
23	0.398	0.561	0.49	0.483	16.920	9.708	1.643	0.195	0.03295
26	0.491	0.474	0.455	0.473	3.805	9.511	0.362	0.191	0.00726
0	2.450	2.450	2.450	2.450	0.000	49.851	0.000	1.000	0.00000

Table 49. Caffeine concentration as a function of depth using Zeolite as filtering bed at an operation time of 30 seconds.

Filter Depth [cm]	Absorbance				% Standard Deviation	Concentration [ppm]	Absolute Uncertainty	C/C0	Absolute Uncertainty
	Test 1	Test 2	Test 3	Average					
13	1.897	1.911	1.924	1.910	0.707	38.844	0.275	0.779	0.00551
18	1.576	1.584	1.569	1.576	0.476	32.021	0.152	0.642	0.00306
23	0.951	1.002	0.971	0.974	2.636	19.742	0.520	0.396	0.01044
26	0.934	0.908	0.876	0.906	3.207	18.341	0.588	0.368	0.01180
0	2.450	2.450	2.450	2.450	0.000	49.851	0.000	1.000	0.00000

Table 50. Caffeine concentration as a function of depth using Zeolite as filtering bed at an operation time of 1 min.

Filter Depth [cm]	Absorbance				% Standard Deviation	Concentration [ppm]	Absolute Uncertainty	C/C0	Absolute Uncertainty
	Test 1	Test 2	Test 3	Average					
13	2.097	2.165	2.185	2.149	2.147	43.708	0.938	0.877	0.01882
18	1.951	1.962	1.944	1.952	0.465	39.695	0.184	0.796	0.00370
23	1.529	1.545	1.538	1.537	0.522	31.225	0.163	0.626	0.00327
26	1.471	1.461	1.456	1.463	0.522	29.701	0.155	0.596	0.00311
0	2.450	2.450	2.450	2.450	0.000	49.851	0.000	1.000	0.00000

Table 51. Caffeine concentration as a function of depth using Zeolite as filtering bed at an operation time of 2 min.

Filter Depth [cm]	Absorbance				% Standard Deviation	Concentration [ppm]	Absolute Uncertainty	C/C0	Absolute Uncertainty
	Test 1	Test 2	Test 3	Average					
13	2.255	2.262	2.276	2.264	0.472	46.062	0.218	0.924	0.00436
18	2.149	2.155	2.139	2.148	0.376	43.681	0.164	0.876	0.00330
23	1.901	1.943	1.913	1.919	1.127	39.014	0.440	0.783	0.00882
26	1.891	1.883	1.874	1.883	0.452	38.273	0.173	0.768	0.00347
0	2.450	2.450	2.450	2.450	0.000	49.851	0.000	1.000	0.00000

Table 52. Caffeine concentration as a function of depth using Zeolite as filtering bed at an operation time of 3 min.

Filter Depth [cm]	Absorbance				% Standard Deviation	Concentration [ppm]	Absolute Uncertainty	C/C0	Absolute Uncertainty
	Test 1	Test 2	Test 3	Average					
13	2.286	2.293	2.301	2.293	0.327	46.654	0.153	0.936	0.00306
18	2.238	2.242	2.229	2.236	0.298	45.490	0.135	0.913	0.00272
23	2.041	2.066	2.05	2.052	0.617	41.735	0.257	0.837	0.00517
26	2.121	2.118	2.111	2.117	0.242	43.048	0.104	0.864	0.00209
0	2.450	2.450	2.450	2.450	0.000	49.851	0.000	1.000	0.00000

Table 53. Caffeine concentration as a function of depth using Zeolite as filtering bed at an operation time of 4 min.

Filter Depth [cm]	Absorbance				% Standard Deviation	Concentration [ppm]	Absolute Uncertainty	C/C0	Absolute Uncertainty
	Test 1	Test 2	Test 3	Average					
13	2.291	2.301	2.314	2.302	0.501	46.831	0.235	0.939	0.00471
18	2.275	2.281	2.271	2.276	0.221	46.293	0.102	0.929	0.00205
23	2.108	2.138	2.125	2.124	0.708	43.191	0.306	0.866	0.00614
26	2.223	2.202	2.189	2.205	0.778	44.844	0.349	0.900	0.00700
0	2.450	2.450	2.450	2.450	0.000	49.851	0.000	1.000	0.00000

Table 54. Caffeine concentration as a function of depth using Zeolite as filtering bed at an operation time of 5 min.

Filter Depth [cm]	Absorbance				% Standard Deviation	Concentration [ppm]	Absolute Uncertainty	C/C0	Absolute Uncertainty
	Test 1	Test 2	Test 3	Average					
13	2.317	2.323	2.33	2.323	0.280	47.266	0.132	0.948	0.00266
18	2.290	2.322	2.291	2.301	0.791	46.810	0.370	0.939	0.00742
23	2.153	2.182	2.165	2.167	0.673	44.069	0.296	0.884	0.00595
26	2.251	2.243	2.236	2.243	0.335	45.633	0.153	0.915	0.00306
0	2.450	2.450	2.450	2.450	0.000	49.851	0.000	1.000	0.00000

Table 55. Caffeine concentration as a function of depth using Gravel as filtering bed at an operation time of 15 seconds.

Filter Depth [cm]	Absorbance				% Standard Deviation	Concentration [ppm]	Absolute Uncertainty	C/C0	Absolute Uncertainty
	Test 1	Test 2	Test 3	Average					
18	1.536	1.505	1.551	1.531	1.5326	31.0891	0.4765	0.6236	0.00956
27	0.899	0.941	0.976	0.939	4.1072	19.0075	0.7807	0.3813	0.01566
37	0.616	0.522	0.689	0.609	13.7471	12.2796	1.6881	0.2463	0.03386
54	0.233	0.276	0.205	0.238	15.0265	4.7082	0.7075	0.0944	0.01419
0	2.45	2.45	2.45	2.450	0.0000	49.8510	0.0000	1.0000	0.00000

Table 56. Caffeine concentration as a function of depth using Gravel as filtering bed at an operation time of 30 seconds.

Filter Depth [cm]	Absorbance				% Standard Deviation	Concentration [ppm]	Absolute Uncertainty	C/C0	Absolute Uncertainty
	Test 1	Test 2	Test 3	Average					
18	2.2	2.189	2.212	2.200	0.5228	44.7558	0.2340	0.8978	0.00469
27	1.882	1.895	1.945	1.907	1.7439	38.7762	0.6762	0.7778	0.01356
37	1.488	1.475	1.492	1.485	0.5985	30.1571	0.1805	0.6049	0.00362
54	0.962	0.988	0.951	0.967	1.9648	19.5857	0.3848	0.3929	0.00772
0	2.45	2.45	2.45	2.450	0.0000	49.8510	0.0000	1.0000	0.00000

Table 57. Caffeine concentration as a function of depth using Gravel as filtering bed at an operation time of 1 min.

Filter Depth [cm]	Absorbance				% Standard Deviation	Concentration [ppm]	Absolute Uncertainty	C/C0	Absolute Uncertainty
	Test 1	Test 2	Test 3	Average					
18	2.335	2.318	2.349	2.334	0.6651	47.4837	0.3158	0.9525	0.00634
27	2.221	2.236	2.243	2.23333333	0.5033	45.4293	0.2286	0.9113	0.00459
37	2.085	2.003	2.101	1.90733333	2.7564	38.7762	1.0688	0.7778	0.02144
54	1.799	1.803	1.797	1.800	0.1698	36.5789	0.0621	0.7338	0.00125
0	2.45	2.45	2.45	2.450	0.0000	49.8510	0.0000	1.0000	0.00000

Table 58. Caffeine concentration as a function of depth using Gravel as filtering bed at an operation time of 2 min.

Filter Depth [cm]	Absorbance				% Standard Deviation	Concentration [ppm]	Absolute Uncertainty	C/C0	Absolute Uncertainty
	Test 1	Test 2	Test 3	Average					
18	2.353	2.344	2.369	2.355	0.5376	47.9190	0.2576	0.9612	0.00517
27	2.315	2.323	2.338	2.355	0.4957	47.9190	0.2376	0.9612	0.00477
37	2.213	2.189	2.225	2.334	0.7854	47.4837	0.3729	0.9525	0.00748
54	2.127	2.134	2.124	2.128	0.2411	43.2864	0.1044	0.8683	0.00209
0	2.45	2.45	2.45	2.450	0.0000	49.8510	0.0000	1.0000	0.00000

Table 59. Caffeine concentration as a function of depth using Gravel as filtering bed at an operation time of 3 min.

Filter Depth [cm]	Absorbance				% Standard Deviation	Concentration [ppm]	Absolute Uncertainty	C/C0	Absolute Uncertainty
	Test 1	Test 2	Test 3	Average					
18	2.388	2.377	2.398	2.388	0.4399	48.5789	0.2137	0.9745	0.00429
27	2.309	2.318	2.326	2.318	0.3670	47.1503	0.1730	0.9458	0.00347
37	2.309	2.294	2.313	2.305	0.4345	46.8986	0.2038	0.9408	0.00409
54	2.208	2.212	2.206	2.209	0.1383	44.9259	0.0621	0.9012	0.00125
0	2.450	2.450	2.450	2.450	0.0000	49.8510	0.0000	1.0000	0.00000

Table 60. Caffeine concentration as a function of depth using Gravel as filtering bed at an operation time of 4 min.

Filter Depth [cm]	Absorbance				% Standard Deviation	Concentration [ppm]	Absolute Uncertainty	C/C0	Absolute Uncertainty
	Test 1	Test 2	Test 3	Average					
18	2.339	2.322	2.343	2.335	0.4776	47.4973	0.2268	0.9528	0.00455
27	2.348	2.356	2.368	2.357	0.4270	47.9599	0.2048	0.9621	0.00411
37	2.282	2.277	2.289	2.283	0.2641	46.4361	0.1226	0.9315	0.00246
54	2.267	2.271	2.265	2.268	0.1347	46.1299	0.0621	0.9254	0.00125
0	2.45	2.45	2.45	2.450	0.0000	49.8510	0.0000	1.0000	0.00000

Table 61. Caffeine concentration as a function of depth using Gravel as filtering bed at an operation time of 5 min.

Filter Depth [cm]	Absorbance				% Standard Deviation	Concentration [ppm]	Absolute Uncertainty	C/C0	Absolute Uncertainty
	Test 1	Test 2	Test 3	Average					
18	2.426	2.421	2.429	2.425	0.1666	49.3476	0.0822	0.9899	0.00165
27	2.376	2.388	2.397	2.387	0.4414	48.5653	0.2144	0.9742	0.00430
37	2.309	2.300	2.311	2.307	0.2540	46.9259	0.1192	0.9413	0.00239
54	2.282	2.285	2.281	2.283	0.0912	46.4361	0.0423	0.9315	0.00085
0	2.45	2.45	2.45	2.450	0.0000	49.8510	0.0000	1.0000	0.00000

Table 62. Caffeine concentration as a function of depth using *Moringa oleifera* Lam. Husk as filtering bed at an operation time of 15 seconds.

Filter Depth [cm]	Absorbance				% Standard Deviation	Concentration [ppm]	Absolute Uncertainty	C/C0	Absolute Uncertainty
	Test 1	Test 2	Test 3	Average					
15	1.361	1.114	1.236	1.237	9.9841	25.0959	2.5056	0.5034	0.0503
27	0.405	0.678	0.955	0.679	40.4812	13.7150	5.5520	0.2751	0.1114
35	0.349	0.281	0.409	0.346	18.4913	6.9190	1.2794	0.1388	0.0257
46	0.224	0.381	0.301	0.302	25.9950	6.0143	1.5634	0.1206	0.0314
0	2.45	2.45	2.45	2.450	0.0000	49.8510	0.0000	1.0000	0.0000

Table 63. Caffeine concentration as a function of depth using *Moringa oleifera* Lam. Husk as filtering bed at an operation time of 30 seconds.

Filter Depth [cm]	Absorbance				% Standard Deviation	Concentration [ppm]	Absolute Uncertainty	C/C0	Absolute Uncertainty
	Test 1	Test 2	Test 3	Average					
15	2.004	1.882	1.979	1.955	3.2964	39.7490	1.3103	0.7974	0.0263
27	1.517	1.632	1.751	1.633	7.1636	33.1844	2.3772	0.6657	0.0477
35	1.366	1.332	1.388	1.362	2.0715	27.6469	0.5727	0.5546	0.0115
46	1.01	1.34	1.107	1.152	14.7185	23.3680	3.4394	0.4688	0.0690
0	2.45	2.45	2.45	2.450	0.0000	49.8510	0.0000	1.0000	0.0000

Table 64. Caffeine concentration as a function of depth using *Moringa oleifera* Lam. Husk as filtering bed at an operation time of 1 min.

Filter Depth [cm]	Absorbance				% Standard Deviation	Concentration [ppm]	Absolute Uncertainty	C/C0	Absolute Uncertainty
	Test 1	Test 2	Test 3	Average					
15	2.321	2.107	2.215	2.214	4.8322	45.0415	2.1765	0.9035	0.0437
27	2.031	2.104	2.179	2.105	3.5161	42.8034	1.5050	0.8586	0.0302
35	1.949	1.85	2.041	1.947	4.9069	39.5789	1.9421	0.7939	0.0390
46	1.749	1.843	1.896	1.829	4.0696	37.1844	1.5133	0.7459	0.0304
0	2.45	2.45	2.45	2.450	0.0000	49.8510	0.0000	1.0000	0.0000

Table 65. Caffeine concentration as a function of depth using *Moringa oleifera* Lam. Husk as filtering bed at an operation time of 2 min.

Filter Depth [cm]	Absorbance				% Standard Deviation	Concentration [ppm]	Absolute Uncertainty	C/C0	Absolute Uncertainty
	Test 1	Test 2	Test 3	Average					
15	2.338	2.278	2.306	2.307	1.3012	46.9395	0.6108	0.9416	0.0123
27	2.231	2.256	2.284	2.257	1.1748	45.9122	0.5394	0.9210	0.0108
35	2.181	2.159	2.201	2.180	0.9635	44.3476	0.4273	0.8896	0.0086
46	2.008	2.043	2.139	2.063	3.2872	41.9599	1.3793	0.8417	0.0277
0	2.45	2.45	2.45	2.450	0.0000	49.8510	0.0000	1.0000	0.0000

Table 66. Caffeine concentration as a function of depth using *Moringa oleifera* Lam. Husk as filtering bed at an operation time of 3 min.

Filter Depth [cm]	Absorbance				% Standard Deviation	Concentration [ppm]	Absolute Uncertainty	C/C0	Absolute Uncertainty
	Test 1	Test 2	Test 3	Average					
15	2.366	2.311	2.337	2.338	1.1768	47.5653	0.5597	0.9541	0.0112
27	2.299	2.305	2.315	2.306	0.3505	46.9190	0.1644	0.9412	0.0033
35	2.249	2.233	2.261	2.248	0.6250	45.7218	0.2858	0.9172	0.0057
46	2.069	2.117	2.196	2.127	3.0145	43.2660	1.3042	0.8679	0.0262
0	2.45	2.45	2.450	2.450	0.0000	49.8510	0.0000	1.0000	0.0000

Table 67. Caffeine concentration as a function of depth using *Moringa oleifera* Lam. Husk as filtering bed at an operation time of 4 min.

Filter Depth [cm]	Absorbance				% Standard Deviation	Concentration [ppm]	Absolute Uncertainty	C/C0	Absolute Uncertainty
	Test 1	Test 2	Test 3	Average					
15	2.368	2.342	2.351	2.353	0.5610	47.8850	0.2686	0.9606	0.0054
27	2.311	2.326	2.342	2.326	0.6664	47.3272	0.3154	0.9494	0.0063
35	2.285	2.282	2.293	2.287	0.2487	46.5177	0.1157	0.9331	0.0023
46	2.152	2.136	2.256	2.181	2.9870	44.3680	1.3253	0.8900	0.0266
0	2.45	2.45	2.45	2.450	0.0000	49.8510	0.0000	1.0000	0.0000

Table 68. Caffeine concentration as a function of depth using *Moringa oleifera* Lam. Husk as filtering bed at an operation time of 5 min.

Filter Depth [cm]	Absorbance				% Standard Deviation	Concentration [ppm]	Absolute Uncertainty	C/C0	Absolute Uncertainty
	Test 1	Test 2	Test 3	Average					
15	2.371	2.359	2.364	2.365	0.2549	48.1095	0.1226	0.9651	0.0025
27	2.336	2.341	2.35	2.342	0.3029	47.6537	0.1443	0.9559	0.0029
35	2.313	2.304	2.324	2.314	0.4329	47.0687	0.2038	0.9442	0.0041
46	2.23	2..211	2.29	2.260	1.8773	45.9735	0.8630	0.9222	0.0173
0	2.45	2.45	2.45	2.450	0.0000	49.8510	0.0000	1.0000	0.0000